Positron Annihilation Spectroscopy on Defects in Semiconductors

R. Krause-Rehberg

Universität Halle, Inst. für Physik

Aalto University

ICDS 2015

28th International Conference on Defects in Semiconductors, July 27 – 31, 2015

Martin-Luther-Universität
Halle-Wittenberg

- Some historical remarks
- Techniques of Positron Annihilation
- Study of Defects in Semiconductors
- User-dedicated Positron Facilities

Discovery of the Positron

- Positron was predicted in 1928 by Paul A.M. Dirac
- Discovery in 1932 in cloud chamber pictures by C.D. Anderson

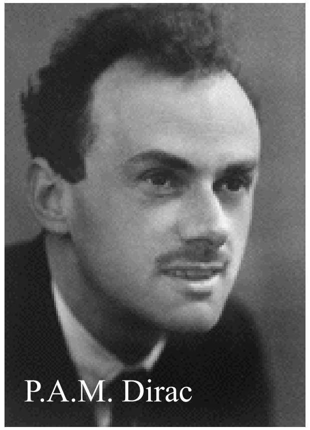

C.D. Anderson

- Positronium as bound state of e^- and e^+ lightest atom was predicted (1934) and discovered (1951)
- Annihilation in matter was studied beginning in the 40^s
- Positrons can be obtained by
  - pair production from gamma radiation (E_γ > 1022 keV)
  - β^+ decay from isotopes (mostly ^{22}Na)

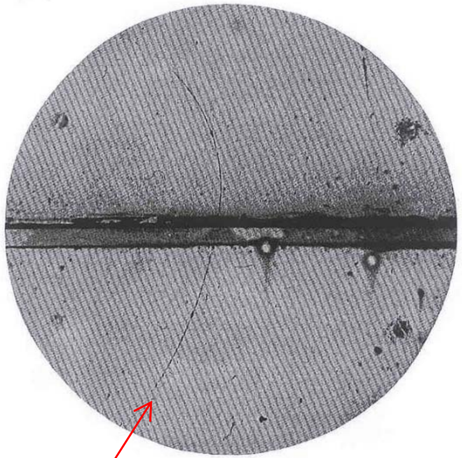

- first Identification of a positron in a cloud chamber
- 5 mm lead plate
- photo taken by C.D. Anderson

Electron structure of solids can be discovered

- during annihilation: conservation laws must be fulfilled (energy, momentum)
- positron cools down to thermal energies ->
- energy of annihilating electron-positron pair = energy of electron
- electron momentum distribution can directly be measured

MARCH 1 AND 15, 1942 PHYSICAL REVIEW VOLUME 61

The Angular Distribution of Positron Annihilation Radiation

Robert Beringer* and C. G. Montgomery
Sloane Physics Laboratory, Yale University, New Haven, Connecticut
(Received January 7, 1942)

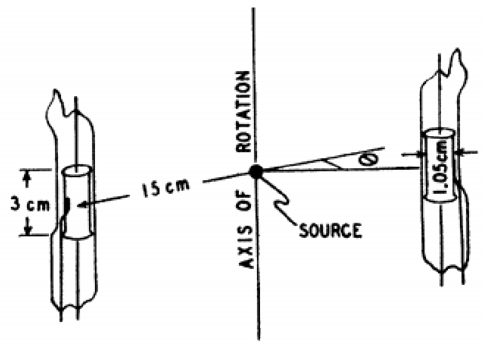

Fig. 1. Schematic arrangement of counters for observing coincidences from annihilation radiation.

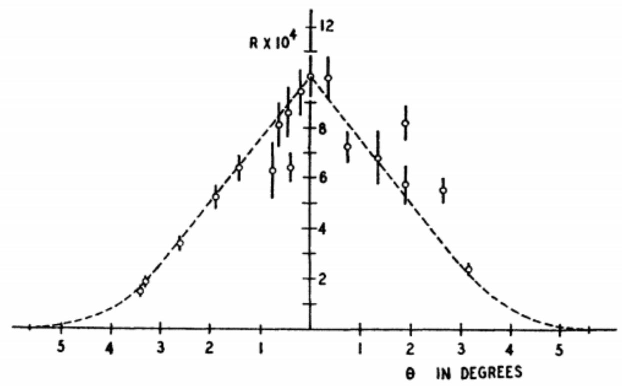

2D – ACAR (Angular Correlation of Annihilation Radiation)

- now: two-dimensional (position-sensitive) detectors
- measurement of single crystals in different directions:
- reconstruction of Fermi surface possible

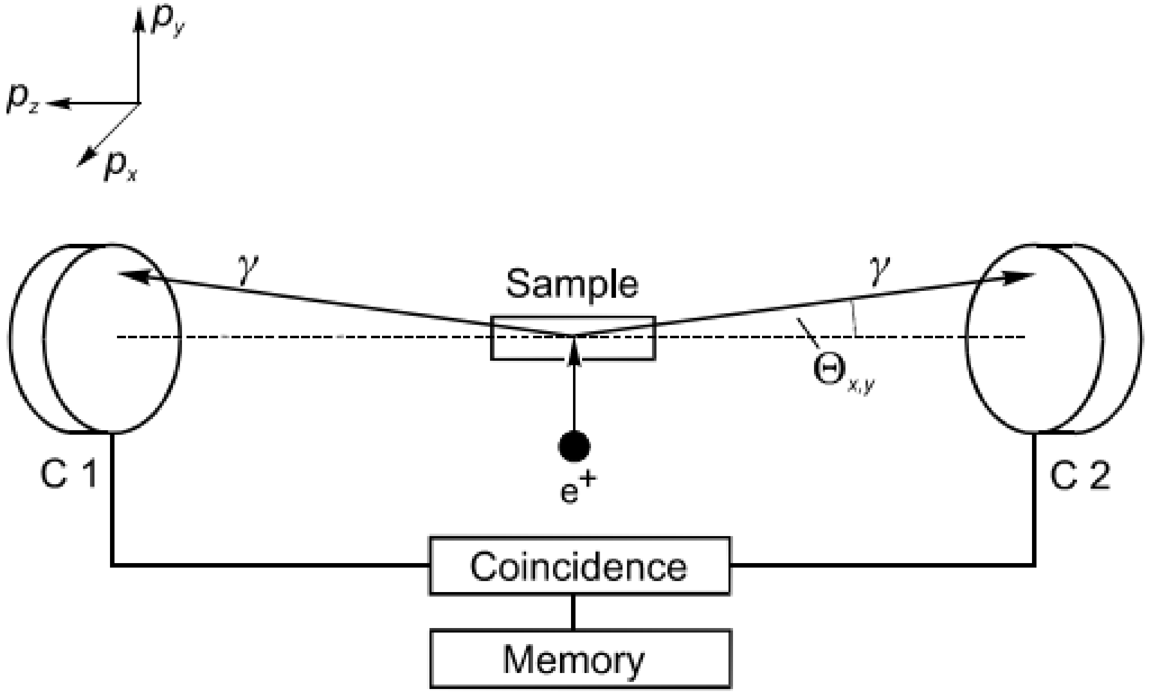

$$N_c(\Theta_x, \Theta_y) = A_c \int_{-\infty}^{\infty} \sigma(\Theta_x m_0 c, \Theta_y m_0 c, p_z) \mathrm{d}p_z$$

2D-ACAR of Copper

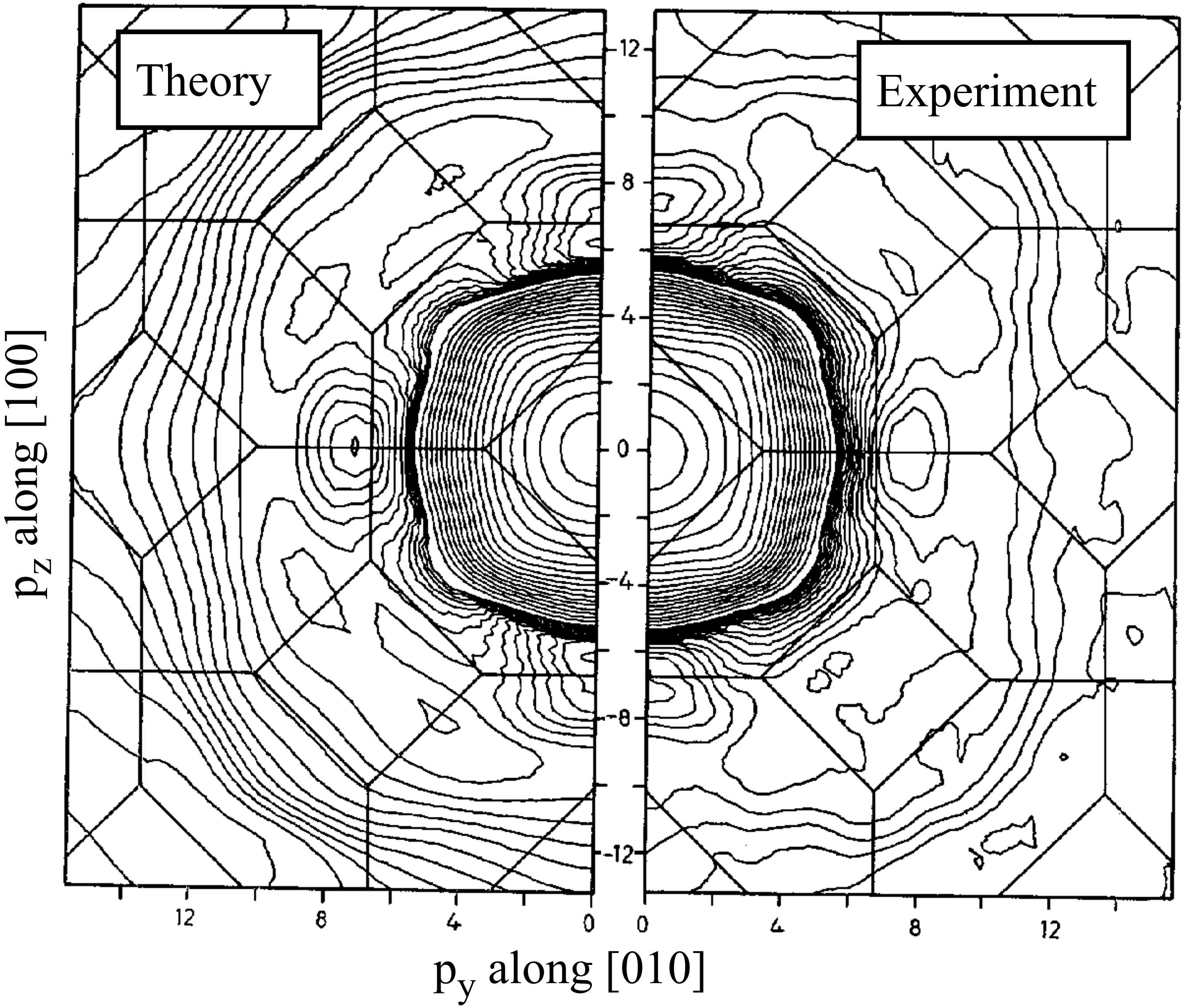

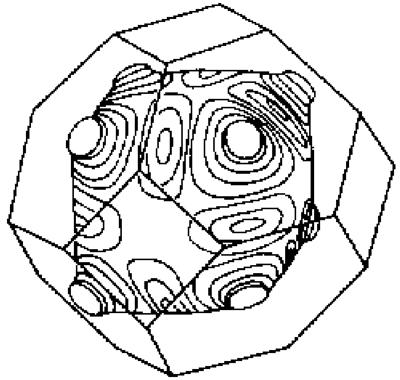

Fermi surface of copper

(Berko, 1979)

Positrons are sensitive for Crystal Lattice Defects

- 1950…1960: in addition to ACAR -> different experimental techniques were developed
- Positron lifetime spectroscopy and Doppler broadening spectroscopy
- end of 60s: lifetime is sensitive to lattice imperfections
  - Brandt et al. (1968): **vacancies in ionic crystals**
  - Dekhtyar et al. (1969): **plastically deformed semiconductors**
  - MacKenzie et al. (1967): **vacancies in thermal equilibrium** in metals
- Positrons are localized (trapped) by open-volume defects

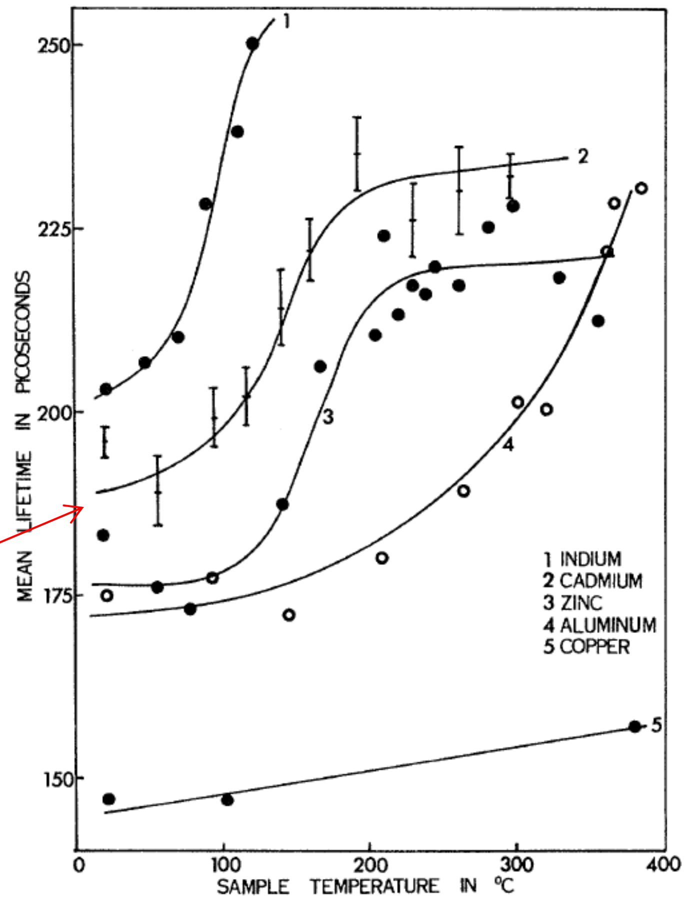

FIG. 1. Positron mean lifetimes in several metals as a function of temperature.

Vacancies in thermal Equilibrium

- Vacancy concentration in thermal equilibrium:
- in metals $H^F \approx 1...4$ eV $\Rightarrow$ at T_m [1v] $\approx 10^{-4...-3}$ /atom
- fits well to the sensitivity range of positron annihilation

$$C_{1v}(T) = \exp\left(\frac{S_{1v}^F}{k}\right)\exp\left(\frac{H_{1v}^F}{kT}\right)$$

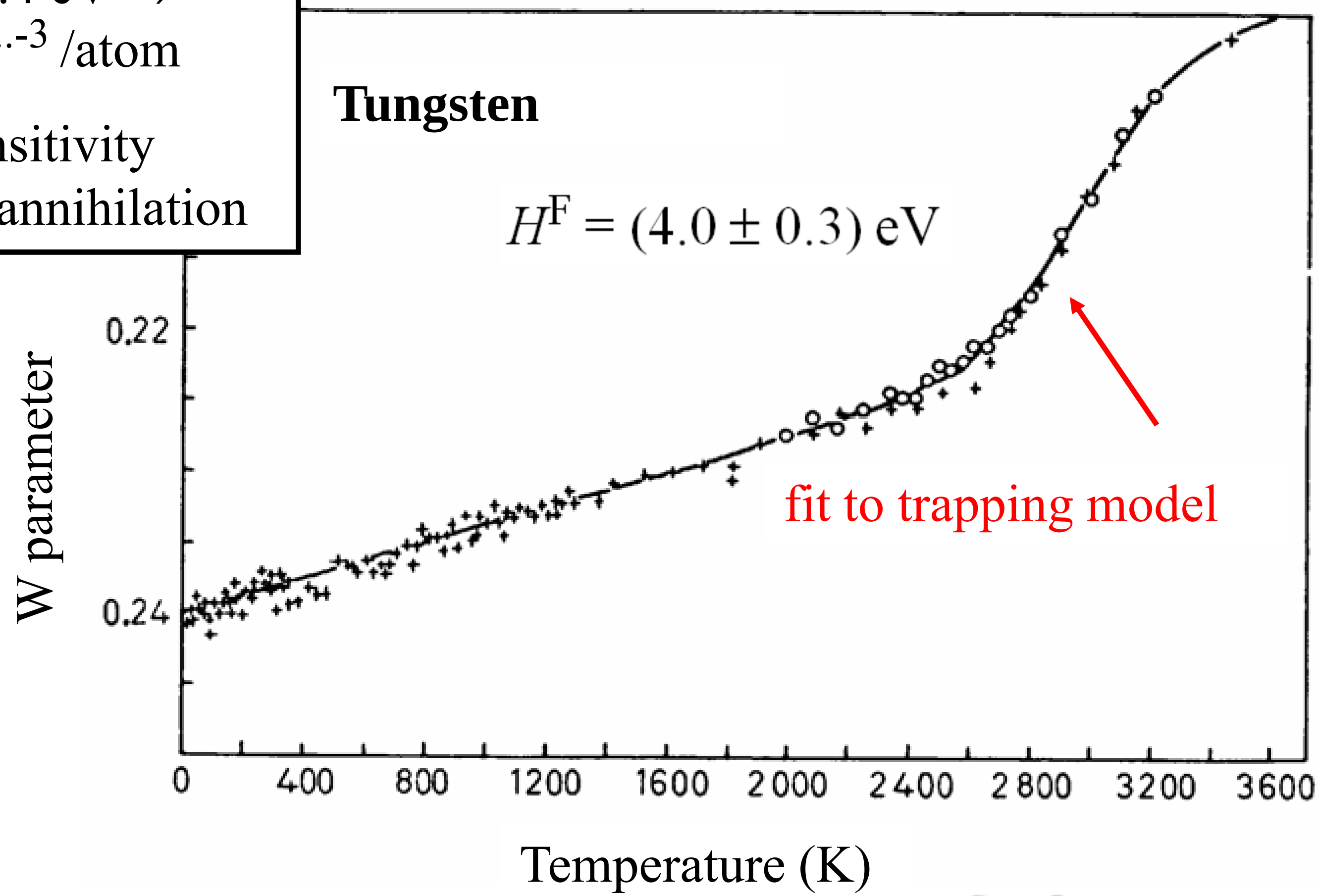

(Ziegler, 1979)

The positron lifetime spectroscopy

^{22}Na

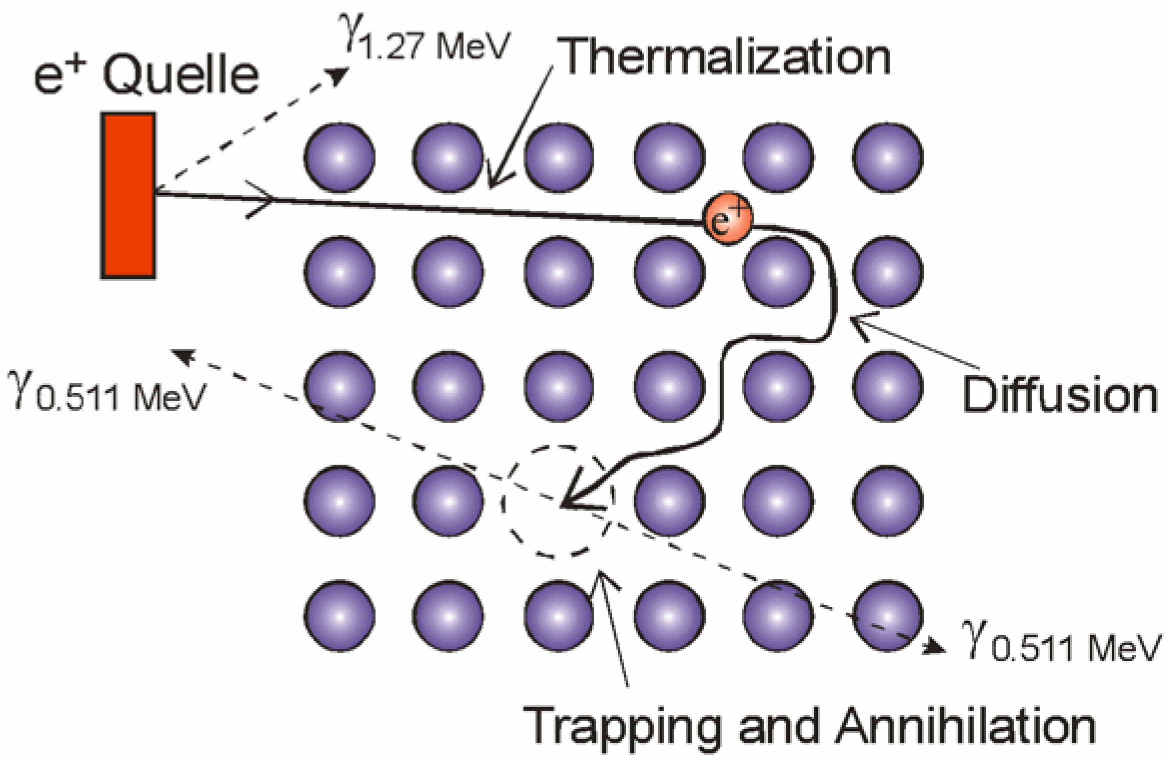

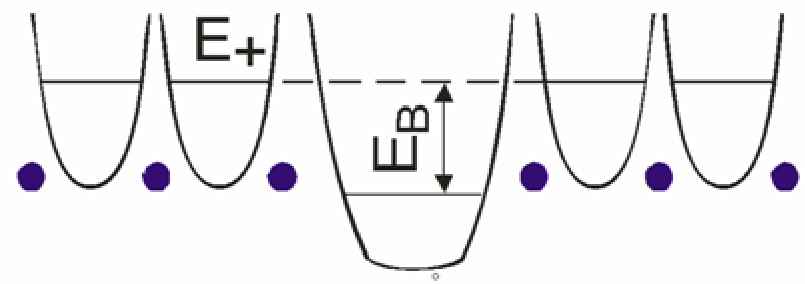

- positron wave-function can be localized in the attractive potential of a defect
- annihilation parameters change in the localized state
- e.g. positron lifetime increases in a vacancy
- lifetime is measured as time difference between appearance of 1.27 (start) and 0.51 MeV (stop) quanta
- defect identification and quantification possible

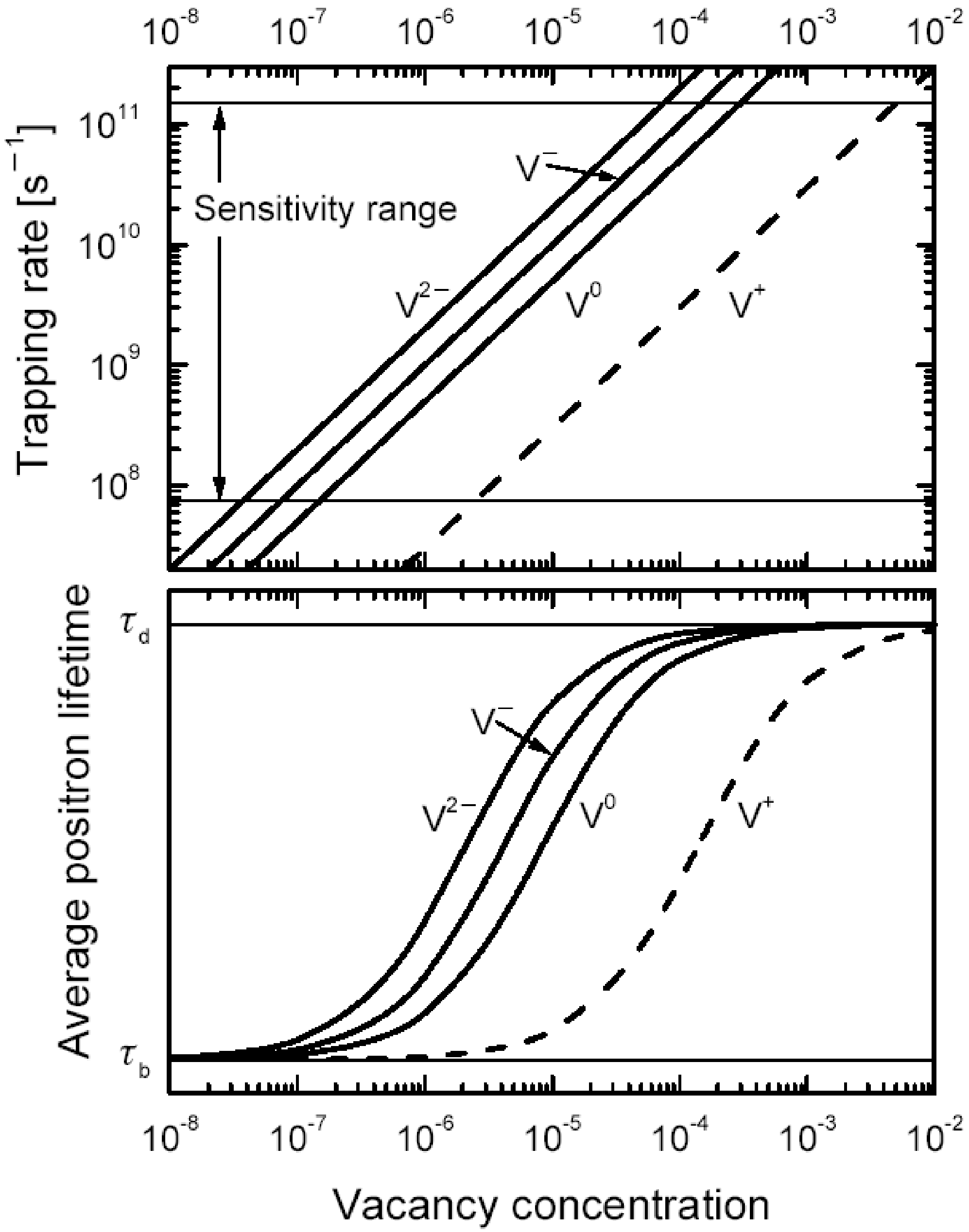

Sensitivity limits of PAS for vacancy detection

- **lower sensitivity limit** e.g. for negatively charged divacancies in Si starts at about 10^{15} cm^{-3}
- **upper limit**: saturated positron trapping
- defect identification still possible
- Then: only lower limit for defect density can be given

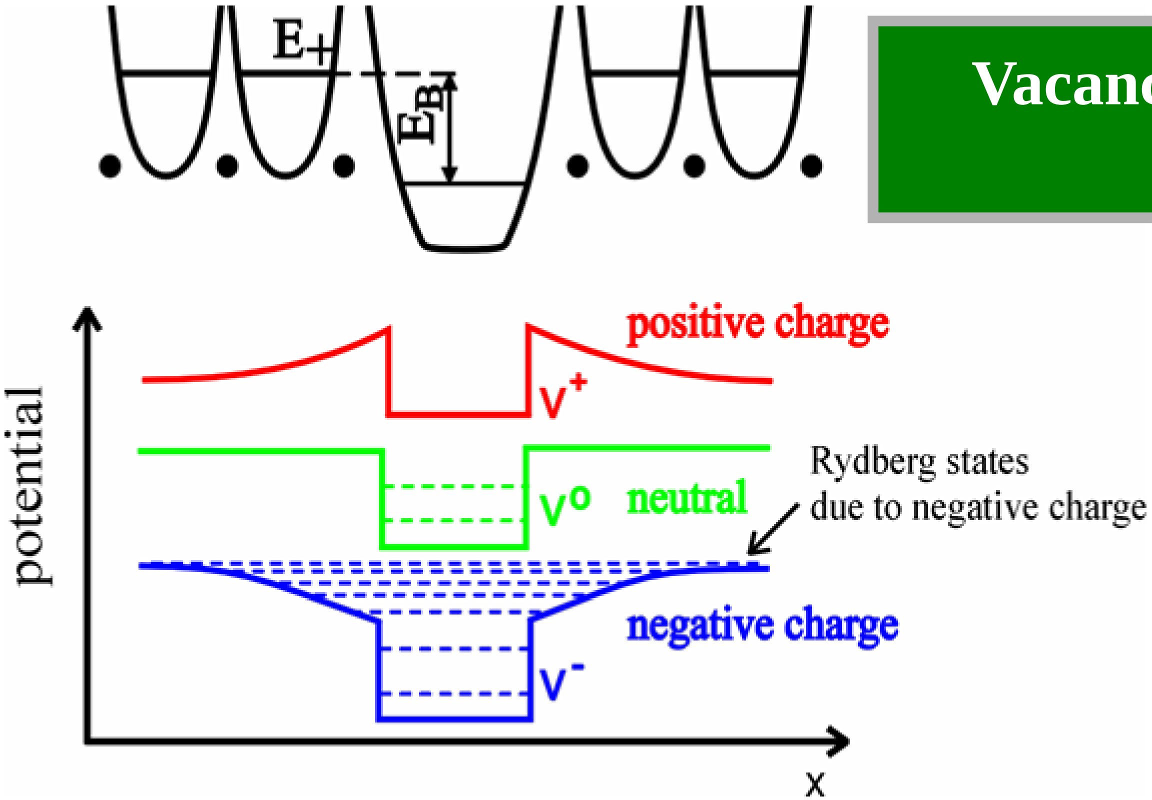

Vacancies in a semiconductor may be charged

- in a metal: charge of a vacancy is effectively screened by free electrons
- they are not available in semiconductors
- thus, long-range Coulomb potential added
- positrons may be attracted or repelled
- trapping coefficient μ is function of charge state

Digital positron lifetime measurement

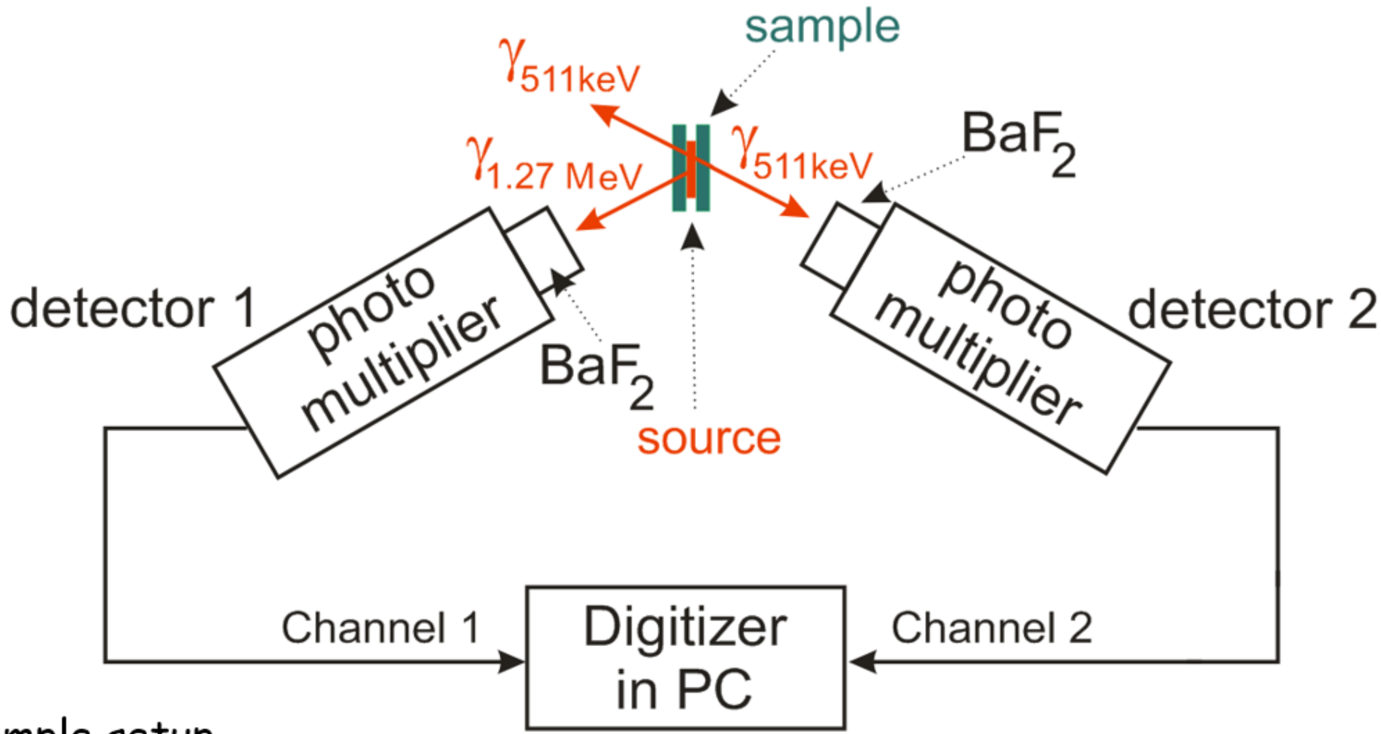

- simple setup
- timing very accurate
- each detector for start & stop (double statistics)

Screenshot of two digitized anode pulses

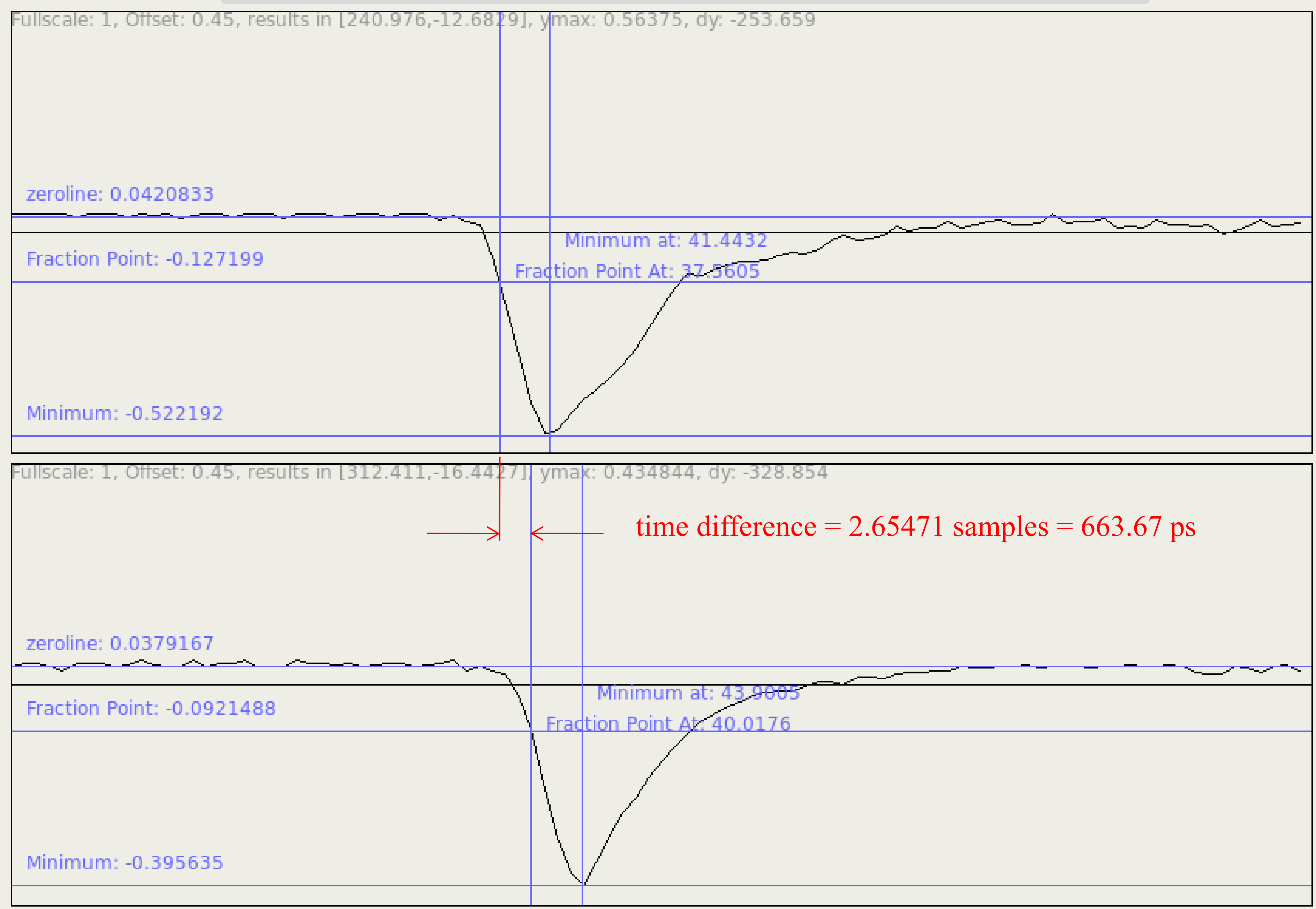

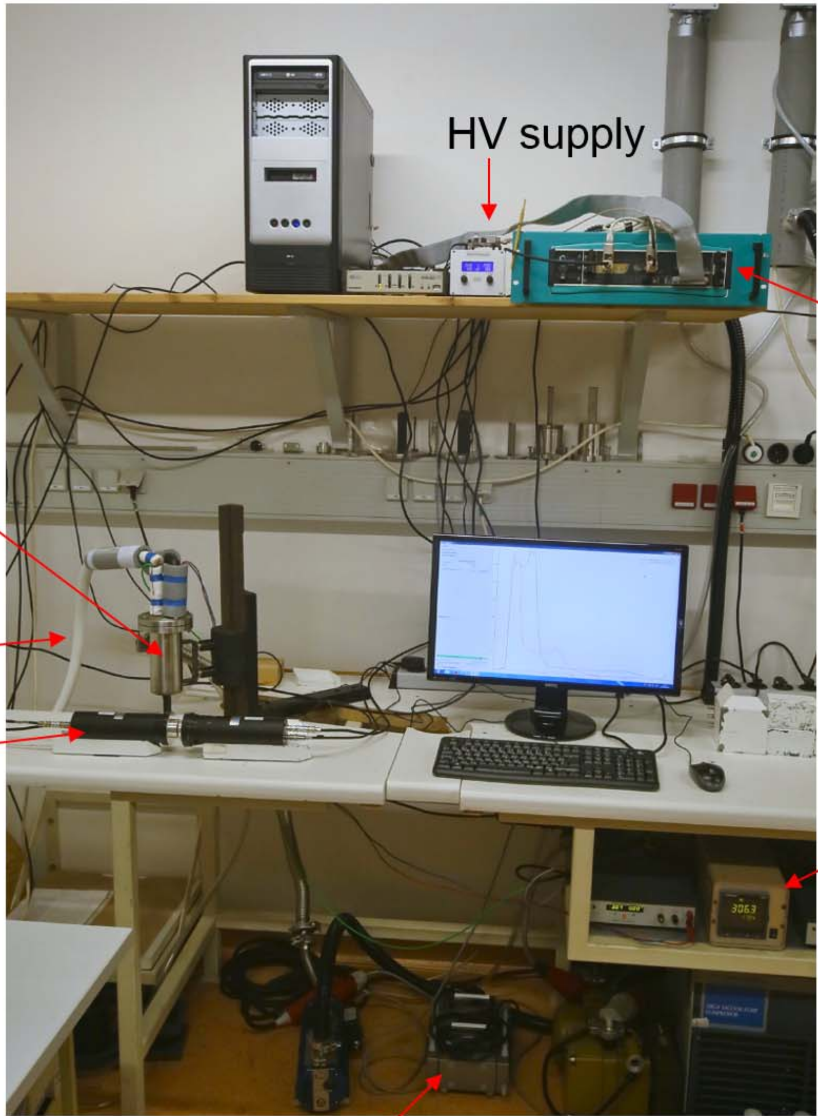
HV supply
Digitizer
Cryostat
LN2 supply
for sample cooling
PMTs
PID controller for
sample heating
Vacuum pumps

Positron lifetime spectroscopy

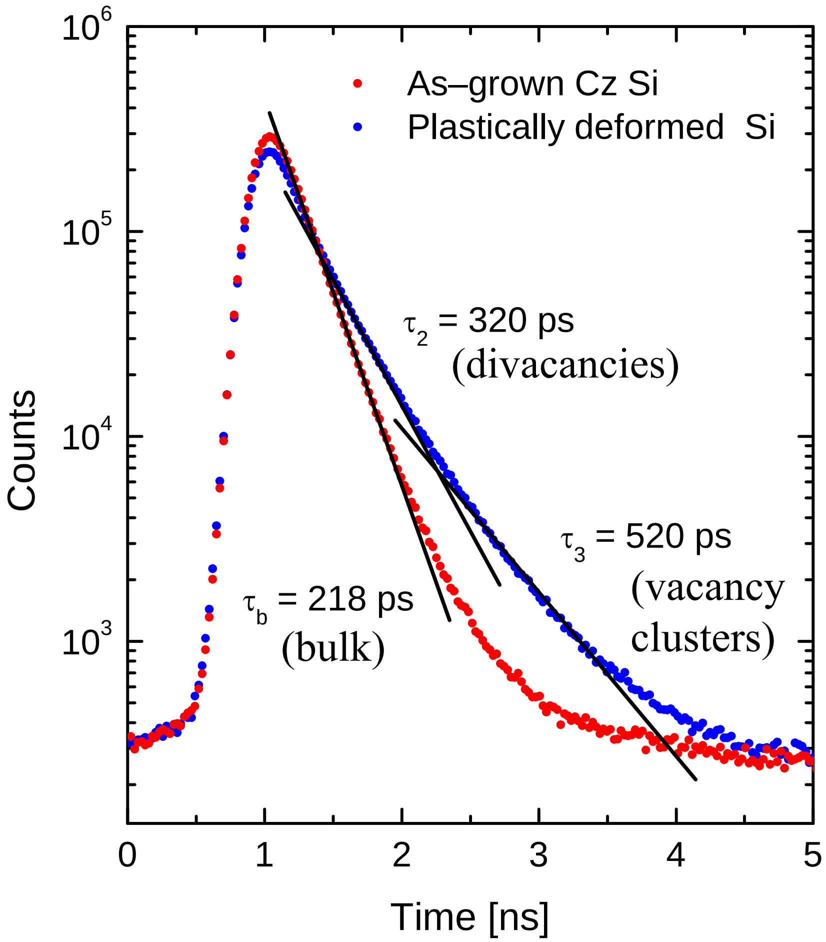

- positron lifetime spectra consist of exponential decay components
- positron trapping in open-volume defects leads to long-lived components
- longer lifetime due to lower electron density
- analysis by non-linear fitting: lifetimes τ_i and intensities I_i

positron lifetime spectrum:

$$N(t) = \sum_{i=1}^{k+1} \frac{I_i}{\tau_i} \exp\left(-\frac{t}{\tau_i} \right)$$

trapping coefficient

$$\boxed{\kappa_d = \mu C_d} = \frac{I_2}{I_1}\left(\frac{1}{\tau_b} - \frac{1}{\tau_d} \right)$$

trapping rate

defect concentration

Doppler Broadening Spectroscopy

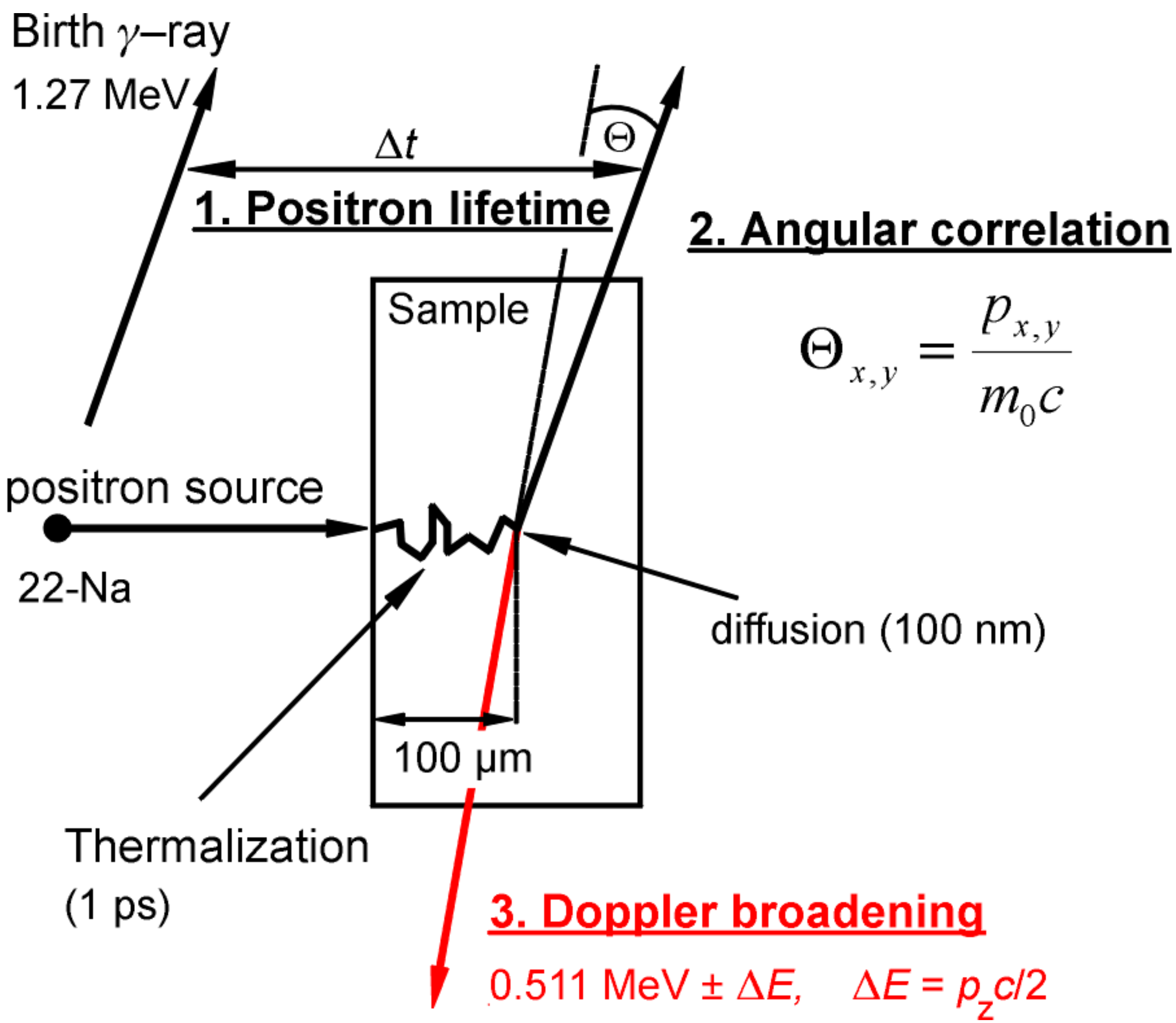

Measurement of Doppler Broadening

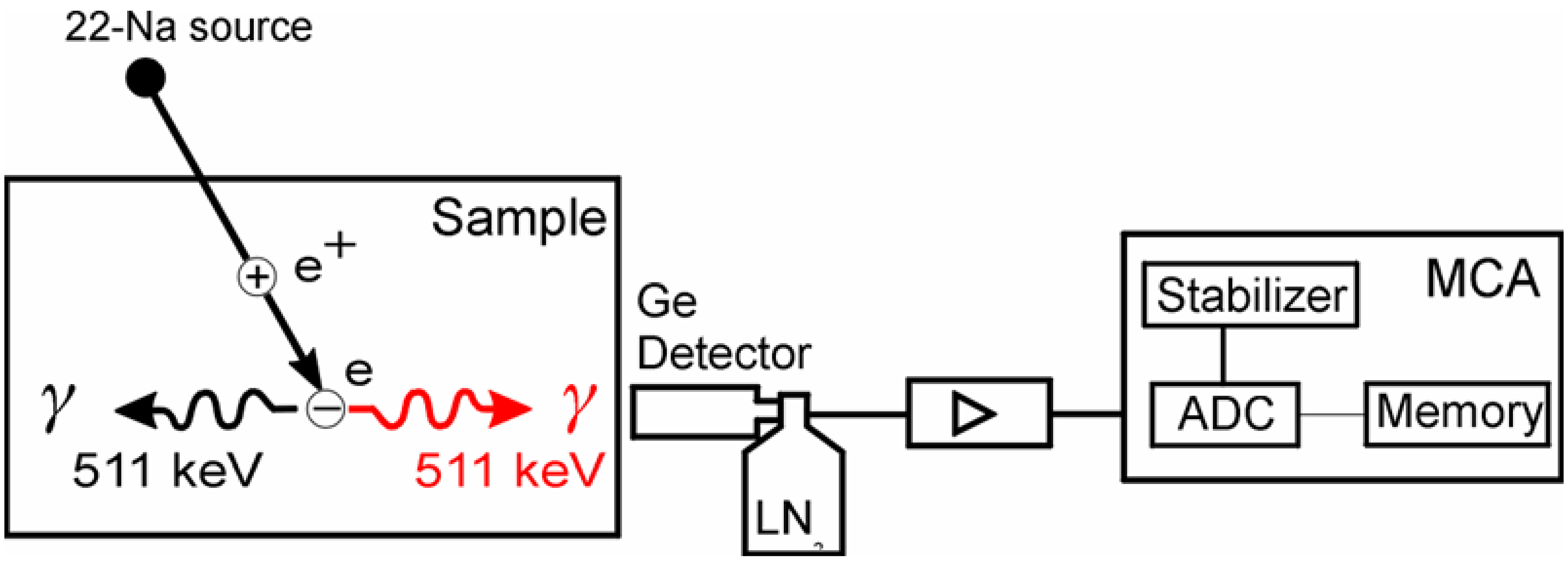

- electron momentum in propagation direction of 511 keV γ-ray leads to Doppler broadening of annihilation line
- can be detected by conventional energy-dispersive Ge detectors and standard electronics

Line Shape Parameters

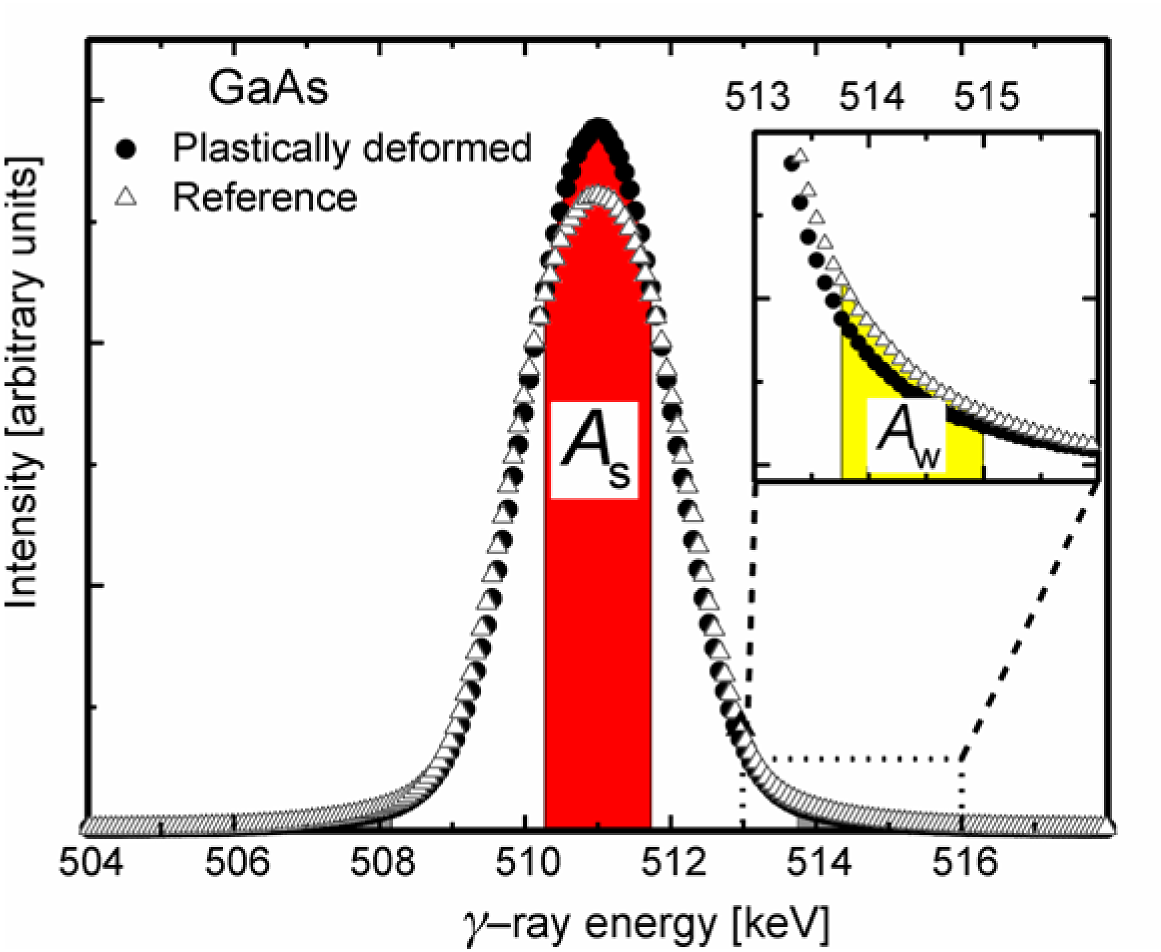

S parameter:

$S = A_S/A_0$

W parameter:

$W = A_W/A_0$

W parameter mainly determined by annihilations of core electrons (chemical information)

Doppler Coincidence Spectroscopy

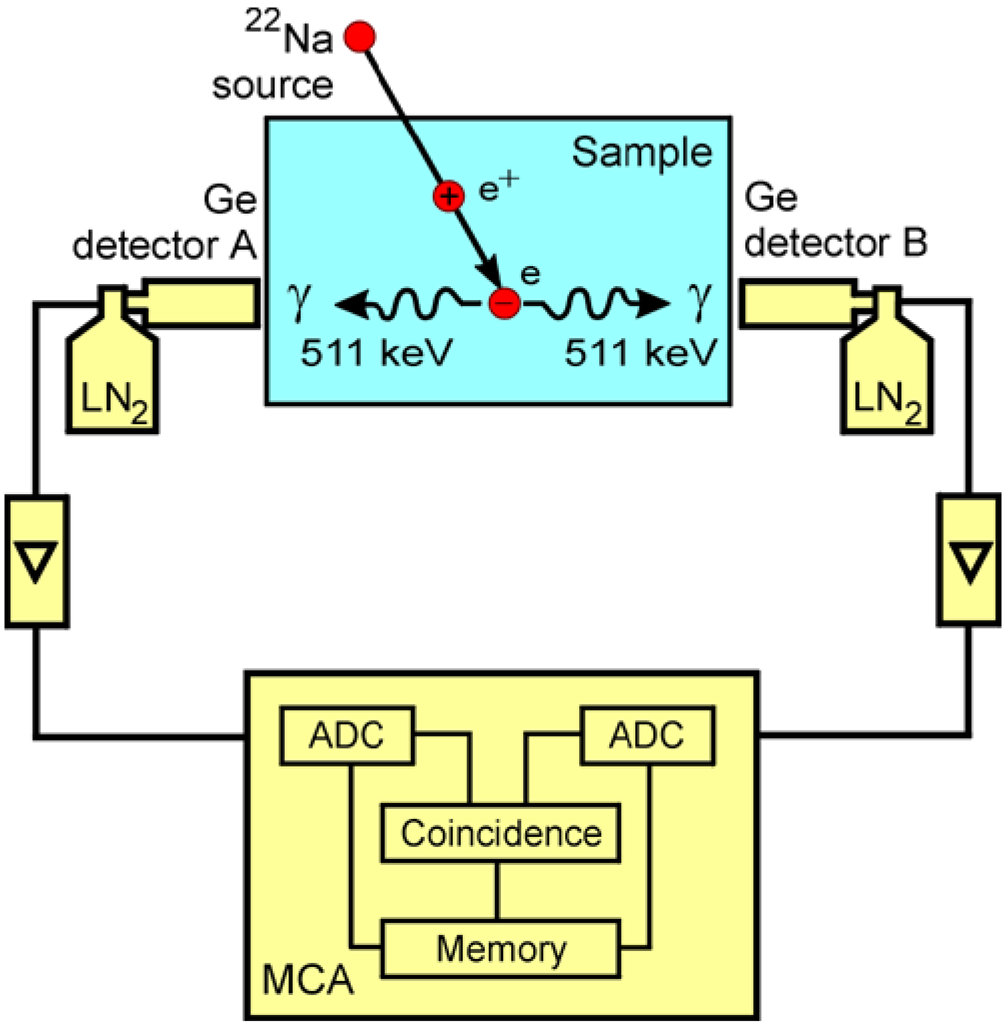

- coincident detection of second annihilation γ reduces background
- use of a second Ge detector improves energy resolution of system

Doppler Coincidence Spectra

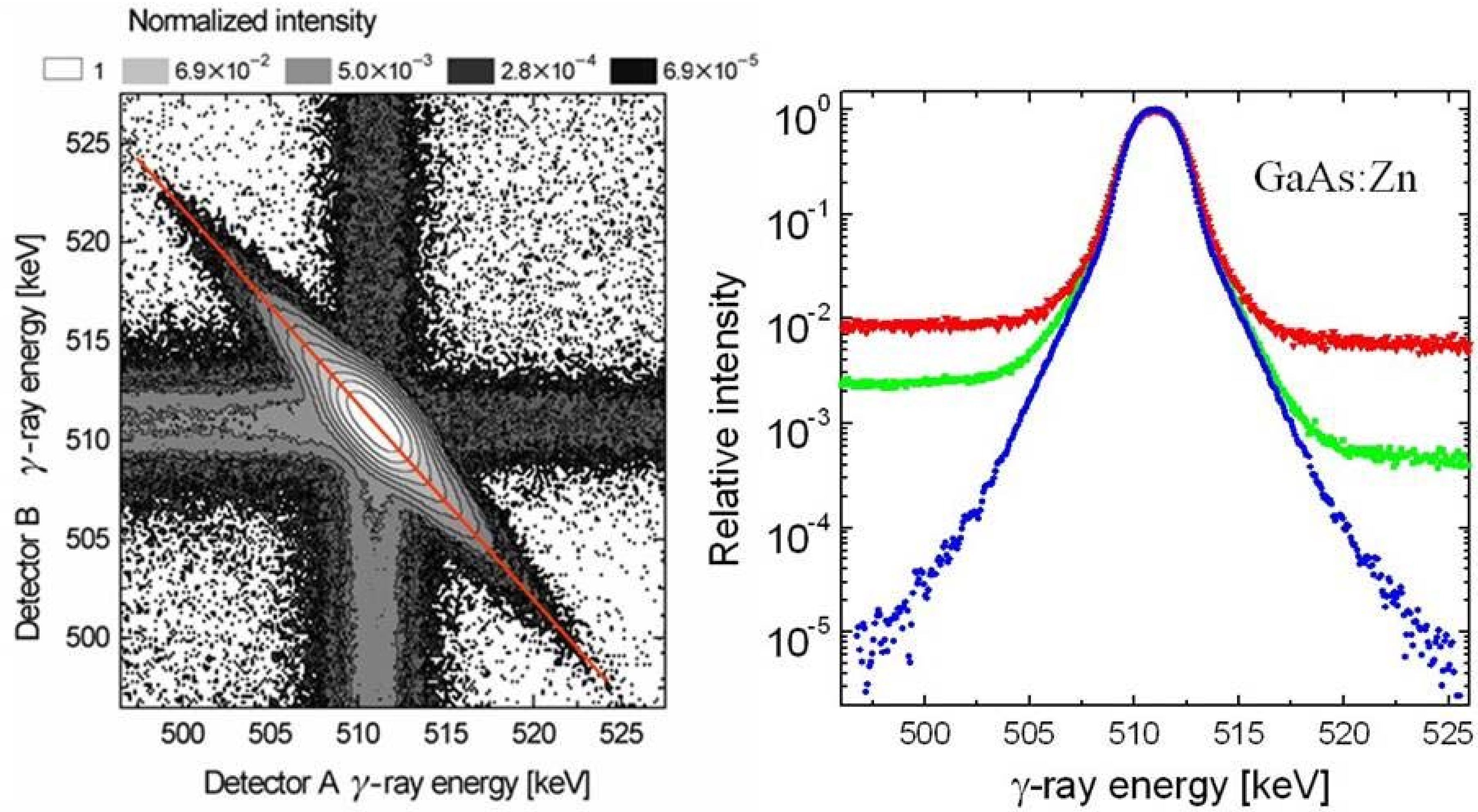

$$E_1+E_2= 2\ m_0\ c^2 =1022\ \mathrm{keV}$$

Doppler-Coincidence-Spectroscopy in GaAs

- Chemical sensitivity due to electrons at high momentum (core electrons)
- a single impurity atom aside a vacancy is detectable
- examples: V_{Ga}-Te_{As} in GaAs:Te

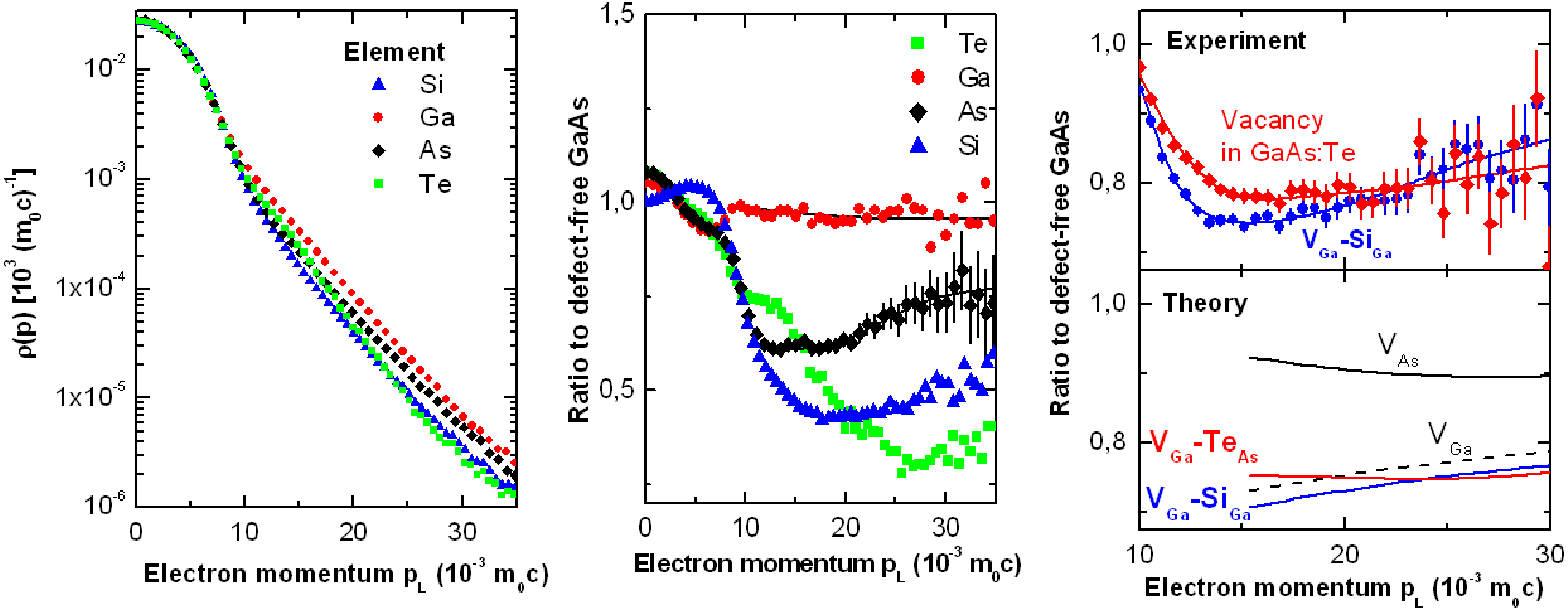

J. Gebauer et al., Phys. Rev. B **60** (1999) 1464

Moderation of Positrons

Mean implantation depth of un-moderated positrons from a 22-Na source (1/e) in Si: 50μm

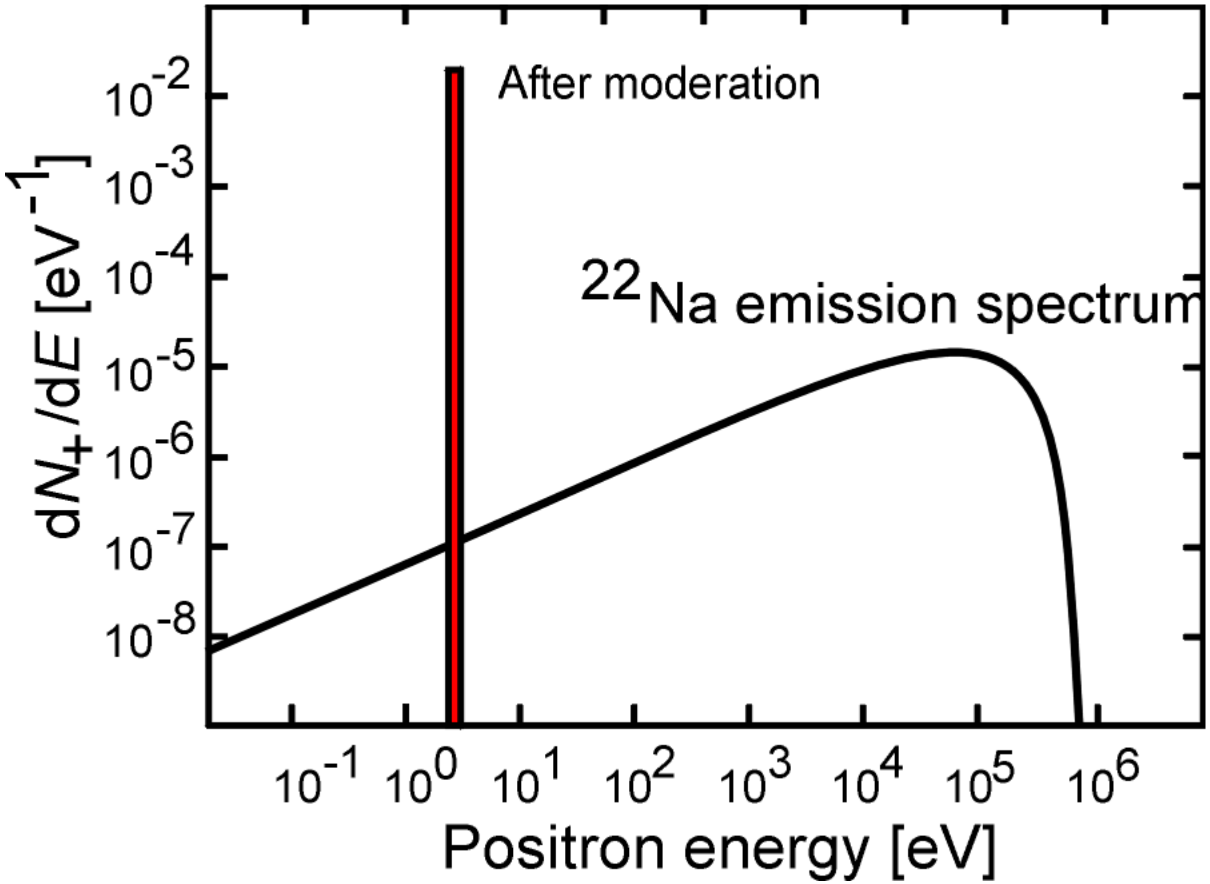

- broad β^+ positron emission spectrum
- deep implantation into solids
- not useful for study of defects in thin layers
- for defect depth profiling: moderation necessary
- monoenergetic positrons can be implanted to different depth

Moderation of Positrons

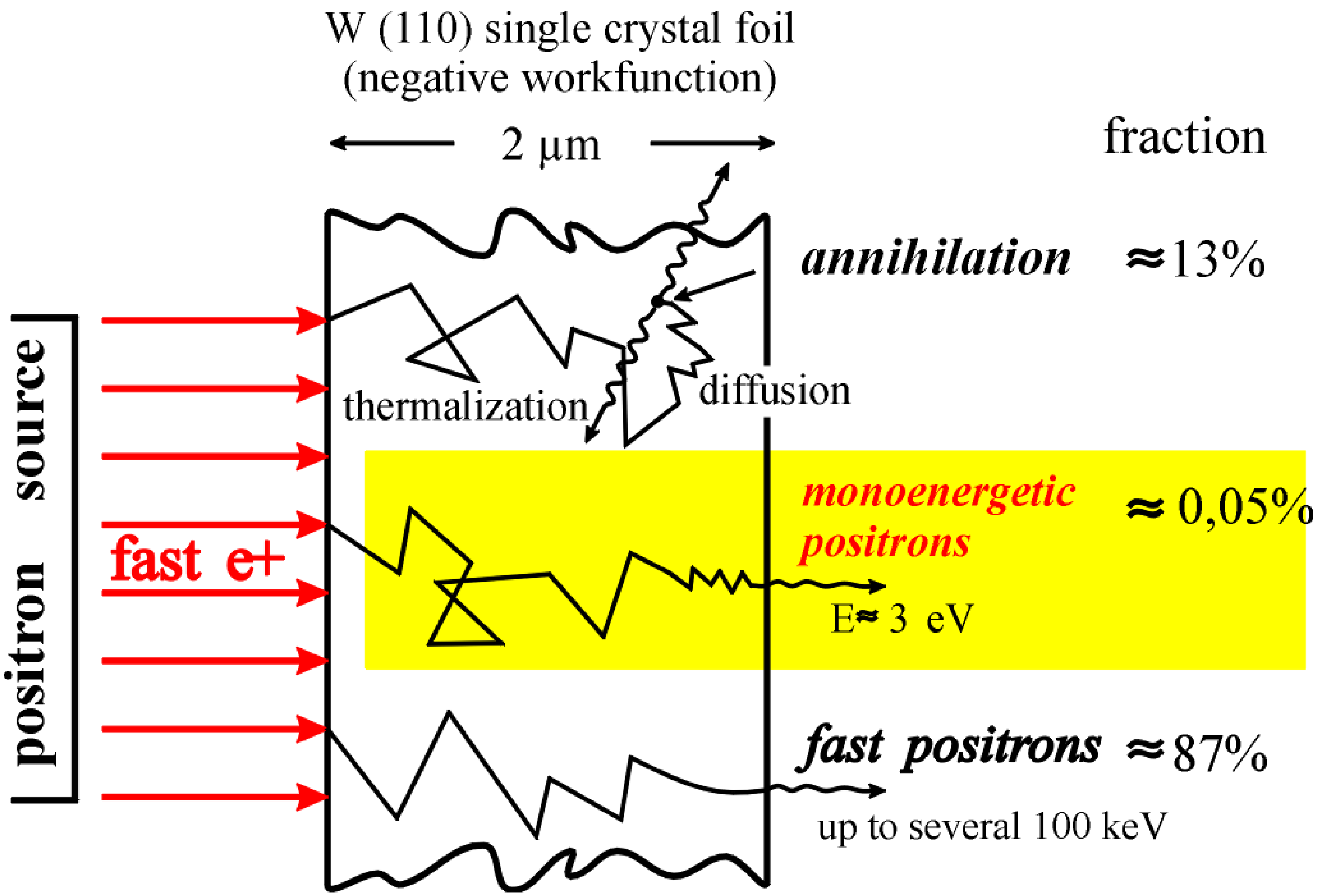

moderation efficiency: $\approx 10^{-4}$

The Positron Beam System at Halle University

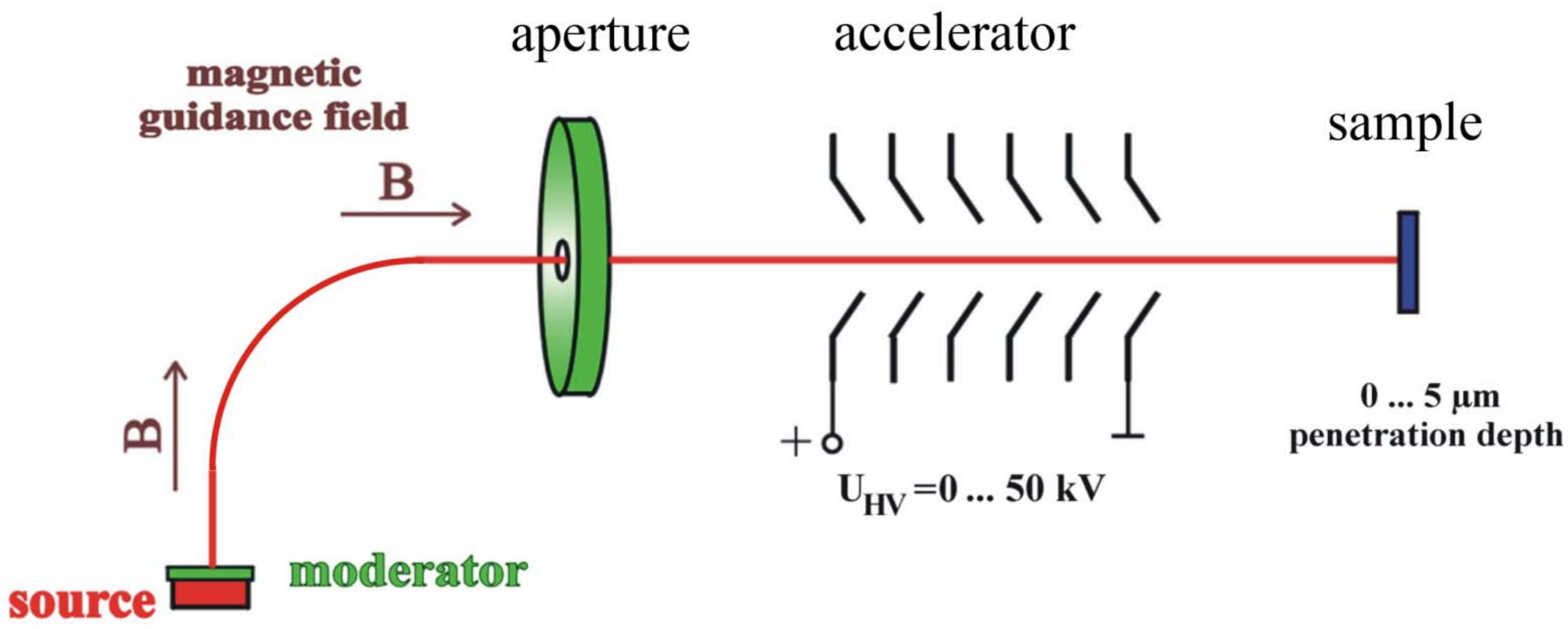

- spot diameter: 4 mm
- time per single Doppler measurement: 20 min
- time per depth scan: 8 hours
- no lifetime measurements


Hochspannung!

Defects in Si induced by Ion Implantation

- ion implantation is most important doping technique in planar technology
- main problem: generation of defects ⇒ positron beam measurements

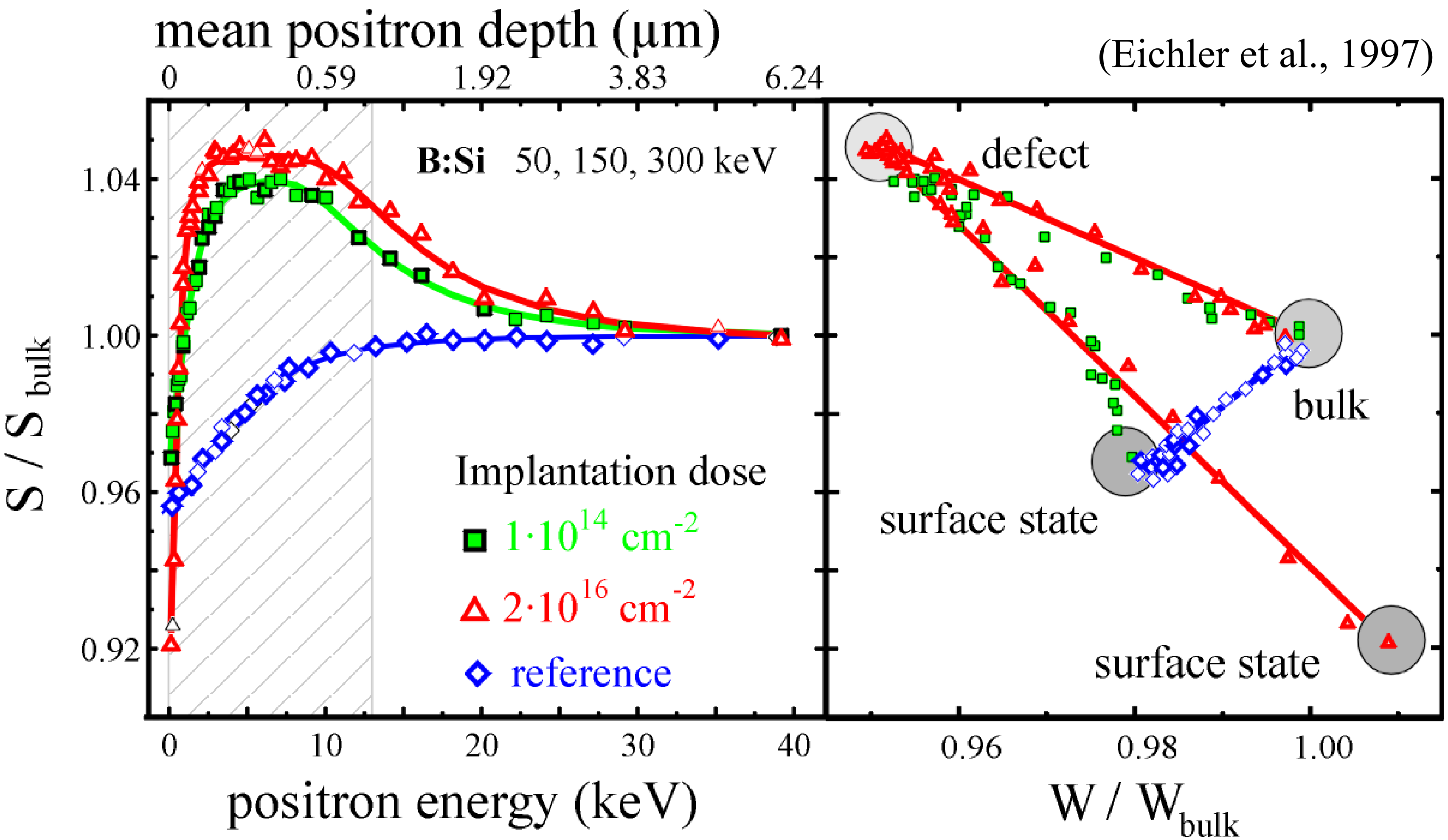

Point defects determine properties of materials

Galliumphosphide

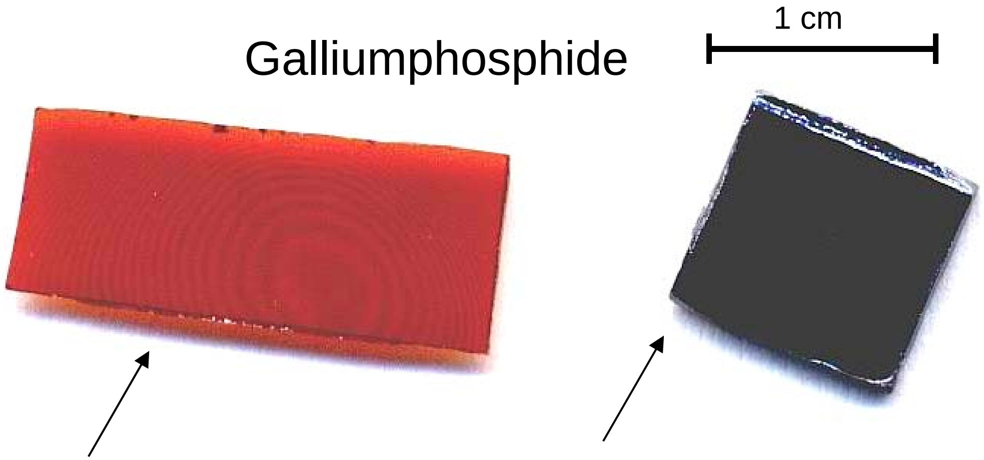

without vacancies
transparent

with 0.001% vacancies
opaque
1 vacancy in 100000 atoms

- Point defects determine electronic and optical properties

- Point defects are generated by crystal growth, irradiation, by plastic deformation, by diffusion, …
- Metals in high radiation environment -> formation of voids -> embrittlement

Defects in electron-irradiated Ge

- Electron irradiation (2 MeV @ 4K) induces Frenkel pairs (vacancy - interstitial pairs)
- steep annealing stage at 200 K
- at high irradiation dose: divacancies are formed (thermally more stable)

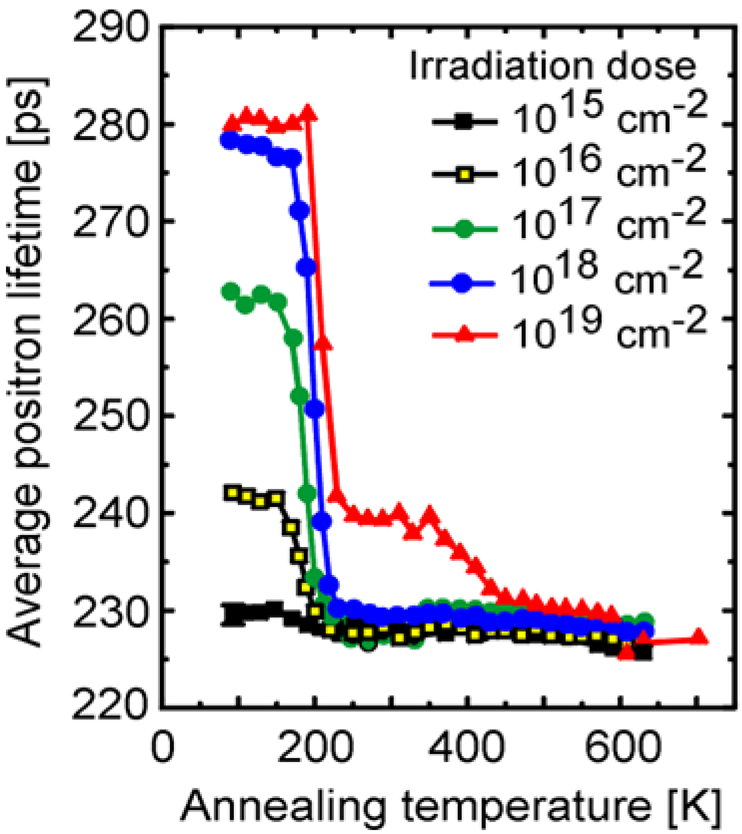

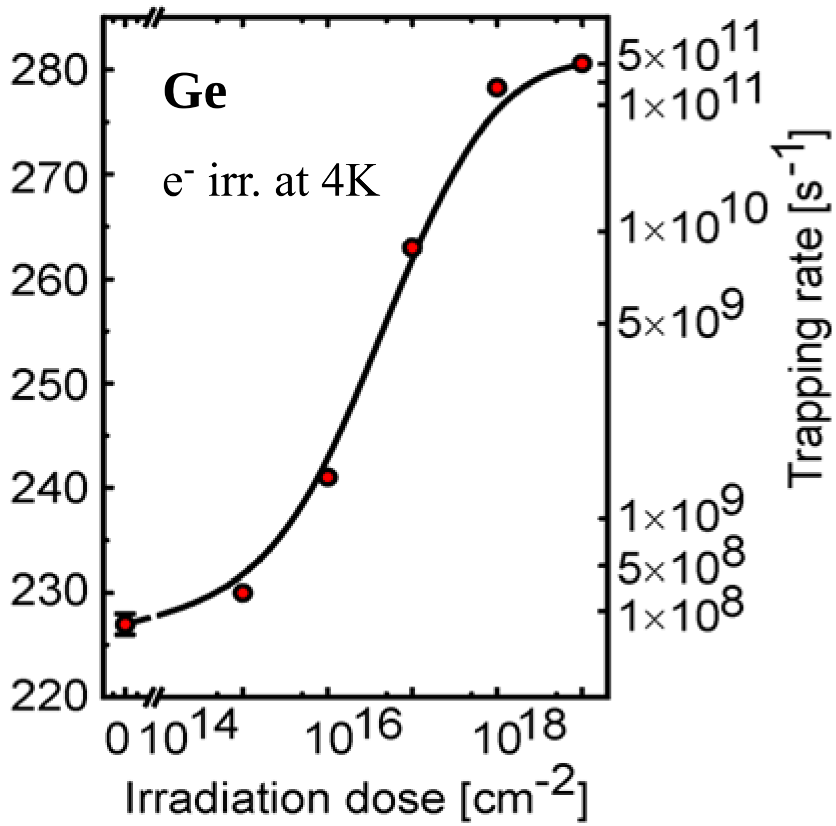

(Polity et al., 1997)

GaAs: annealing under defined As-partial pressure

- two-zone-furnace: Control of sample temperature **and** As partial pressure allows
- T_{As}: determines As-partial pressure
- navigate freely in phase diagram (existence area of compound)

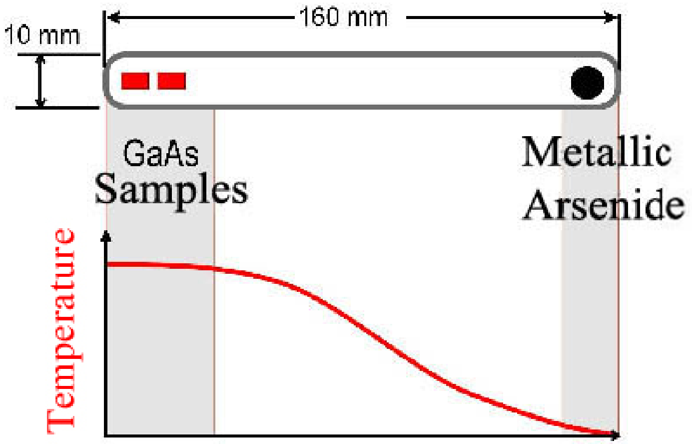

T_{sample}: 1100° C

Equilibrium Phase Diagram of GaAs

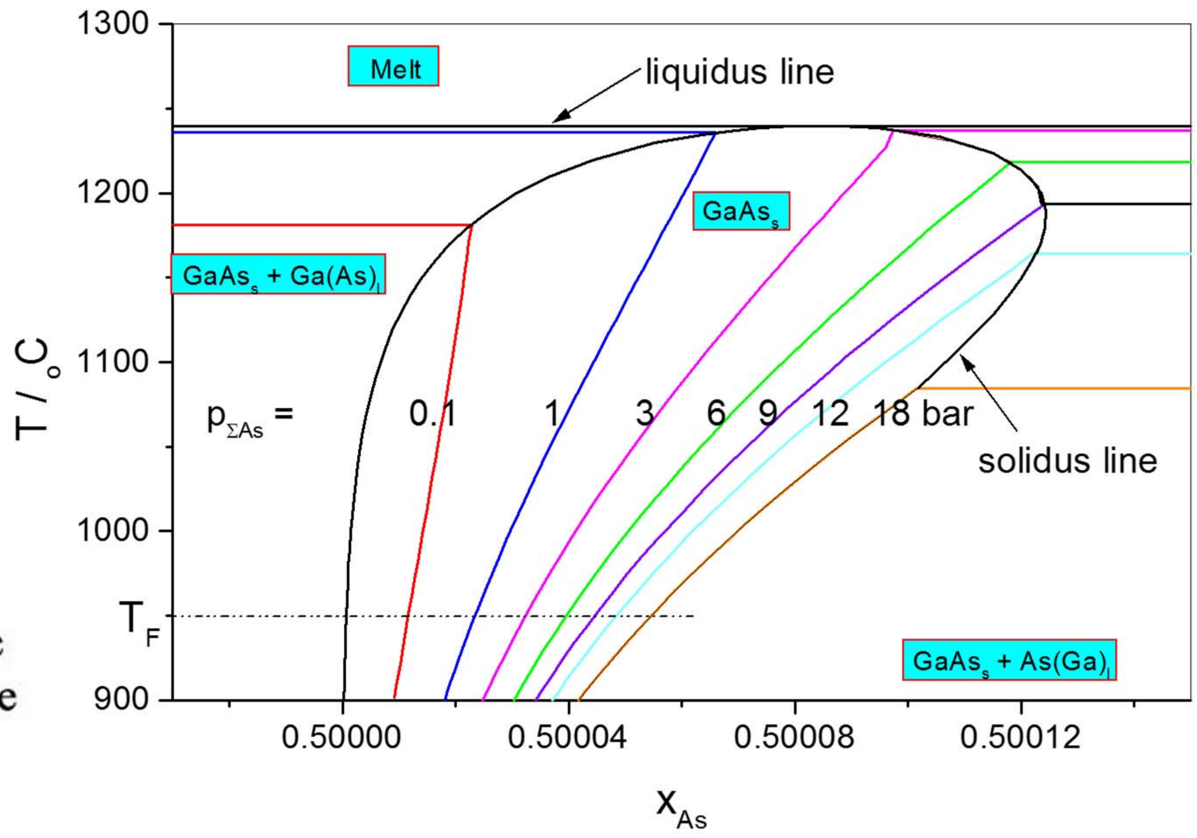

Jurisch, Wenzl; 2002

GaAs: Annealing under defined As pressure

Si_{Ga}-V_{Ga}

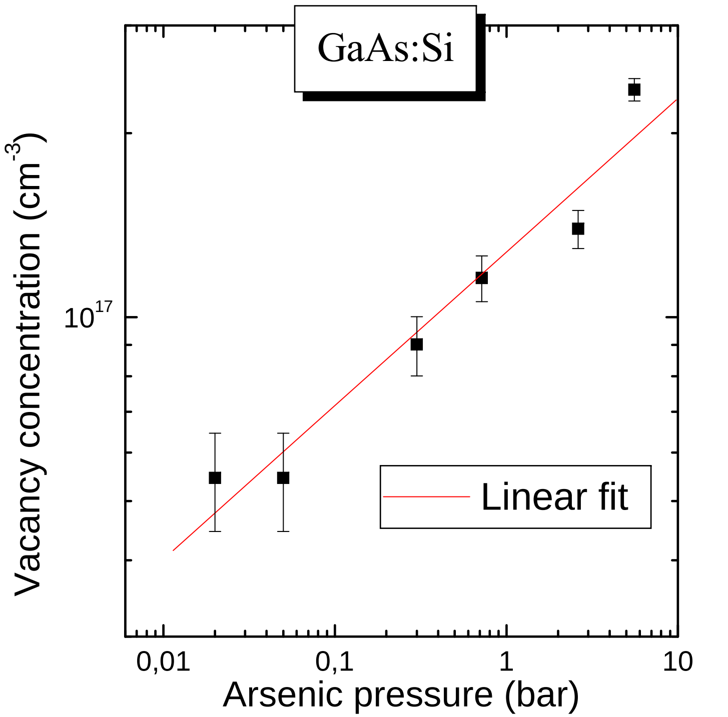

Te_{As}-V_{Ga}

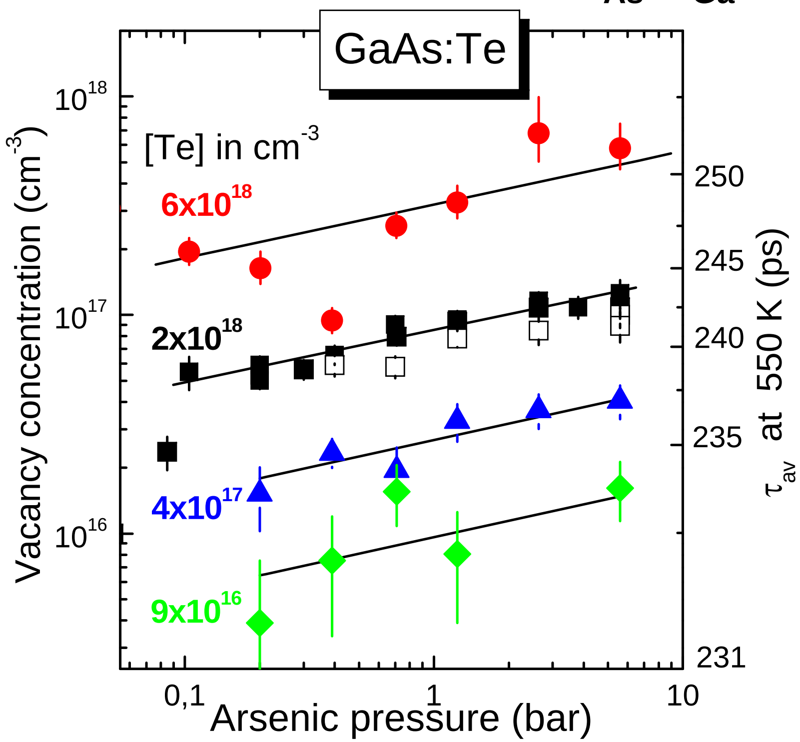

J. Gebauer et al., Physica B 273-274, 705 (1999)

Thermodynamic reaction:

$1/4\ As_4^{gas} \leftrightarrow As_{As} + V_{Ga}$

Mass action law:

$[V_{Ga}] = K_{VG} \times p_{As}^{1/4}$

Fit: $[V_{Ga}\text{-Dopant}] \sim p_{As}^{n}$

$\rightarrow n = 1/4$

Comparison of doped and undoped GaAs

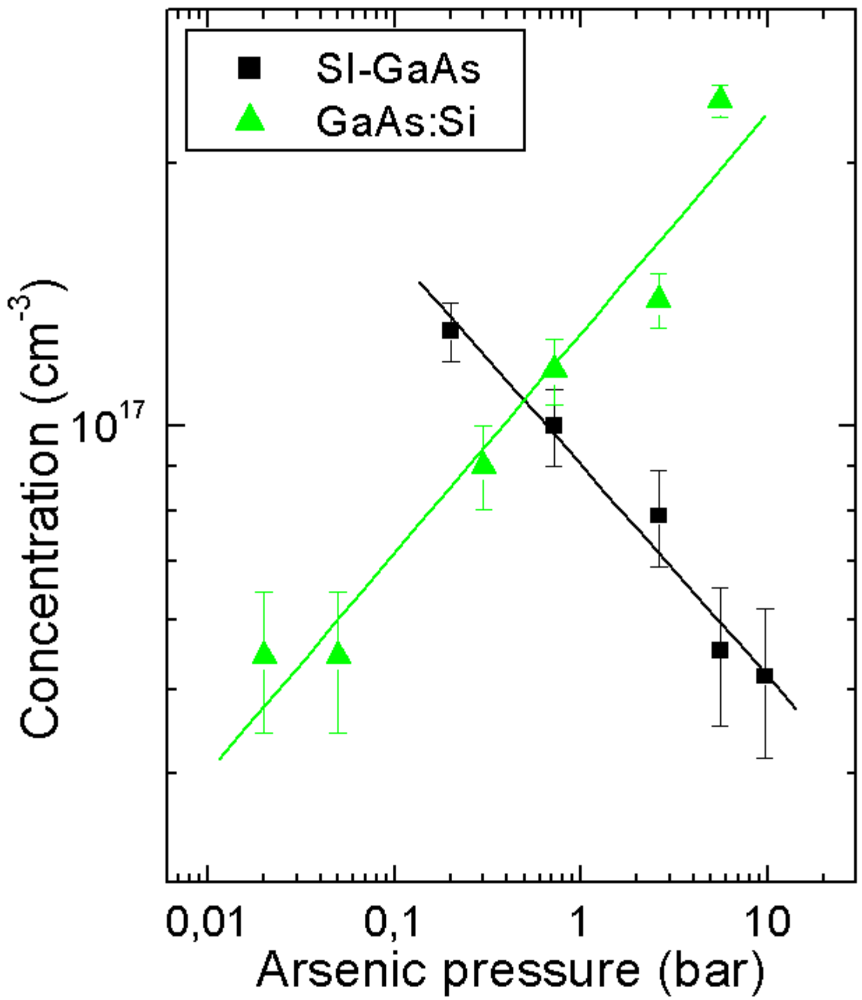

Thermodynamic reaction:

$$As_{As} \leftrightarrow V_{As} + 1/4 As_4^{gas}$$

Mass action law:

$$[V_{As}] = K_{VAs} \times p_{As}^{-1/4}$$

Fit: $[\text{V-complex}] \sim p_{As}^{n}$

$\rightarrow n = -1/4$

undoped GaAs: As vacancy

Bondarenko et al., 2003

EL2 in GaAs: important Antisite Defect

- interesting feature: EL2 exhibits metastability
- illumination at low temperature → properties changes (e.g. no IR absorption any more)
- many structural models were discussed
- Dabrowski/Scheffler and Chadi/Chang: EL2 is isolated As_{Ga} and in metastable state the antisite atom moves outward and leaves a V_{Ga}
- Metastability is lost during warming-up to 115 K

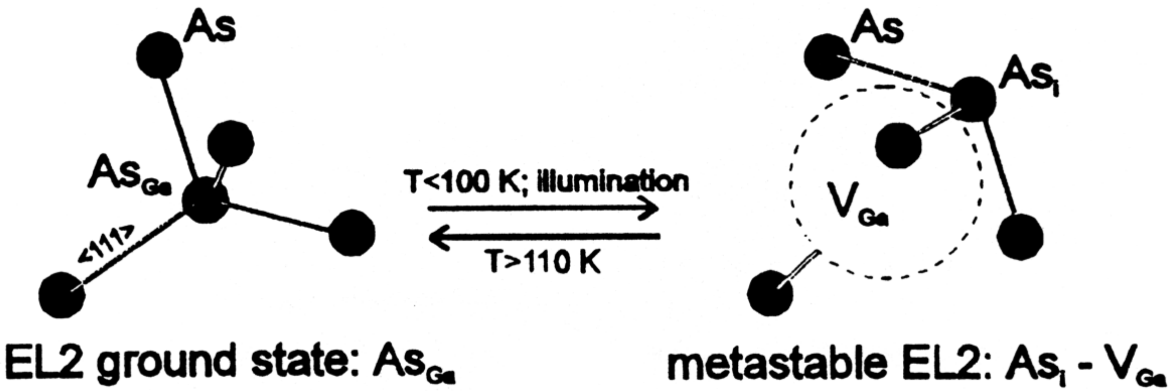

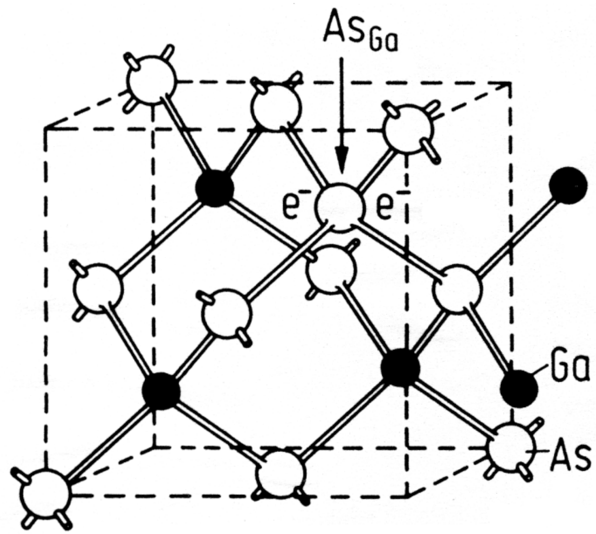

EL2 in GaAs: important antisite Defect

- before annihilation, diffusing positrons can be trapped by such defects
- as a consequence: positron lifetime increases due to the reduced electron density in the vacancy
- experiment shows the existence of a Ga vacancy in the metastable state of GaAs, which does not exist in stable ground state
- was prove of As_{Ga} model of EL2

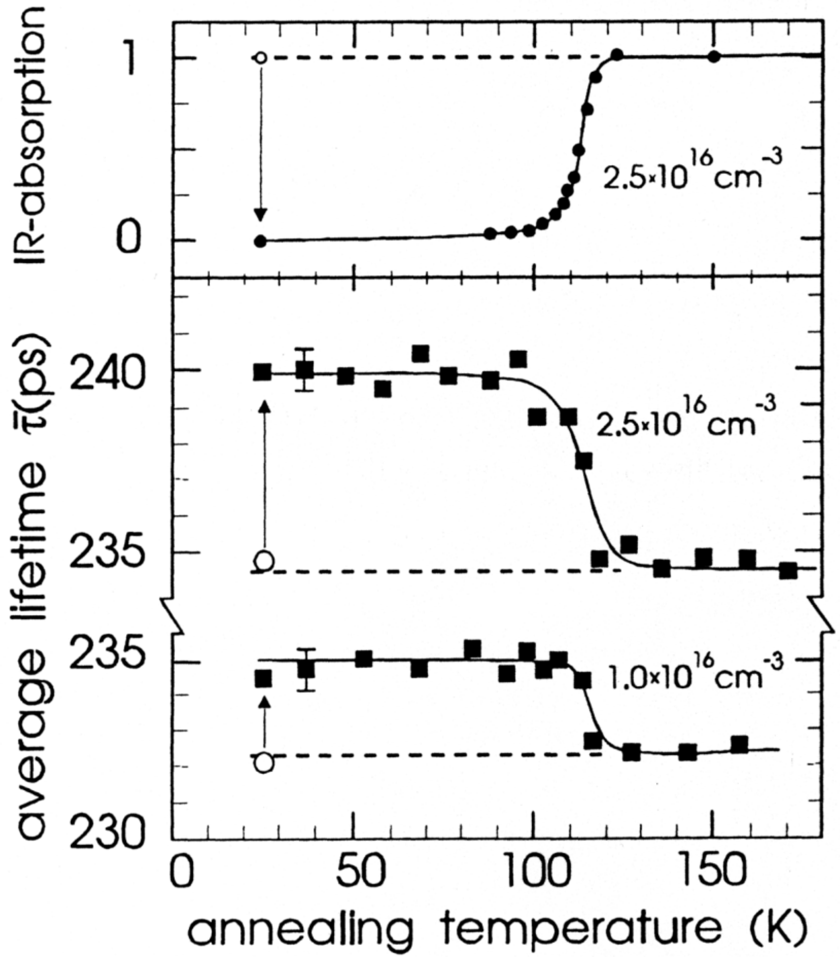

R. Krause et al.: **Observation of a monovacancy in the metastable state of the EL2 defect in GaAs by positron annihilation**
Phys. Rev. Lett. **65** (26), 3329-32 (1990).

DX Center in GaAlSb

- defect appears in doped quasi-ternary III-V compound semiconductors (e.g. $Al_xGa_{1-x}As$, $Al_xGa_{1-x}Sb$)
- is complex: donor-? (so-called DX center)
- also shows metastable state at low temperatures
- model of Dabrowski/Scheffler predicted vacancy in stable state and the disappearance of this vacancy in metastable state
- also proved by positron annihilation

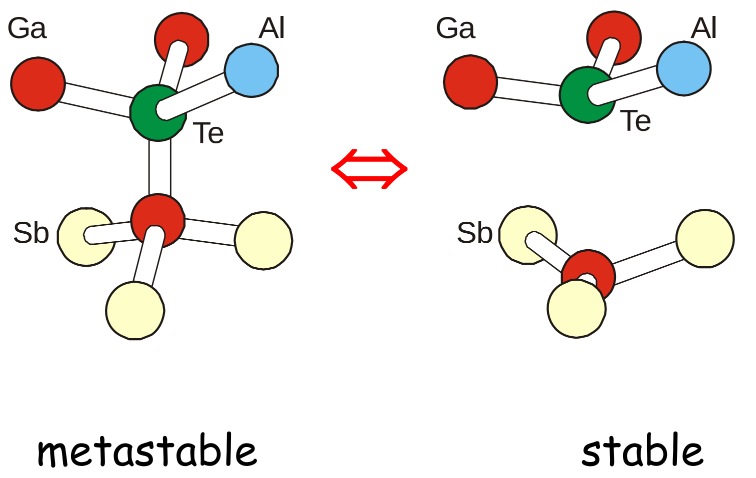

GaAlSb:Te

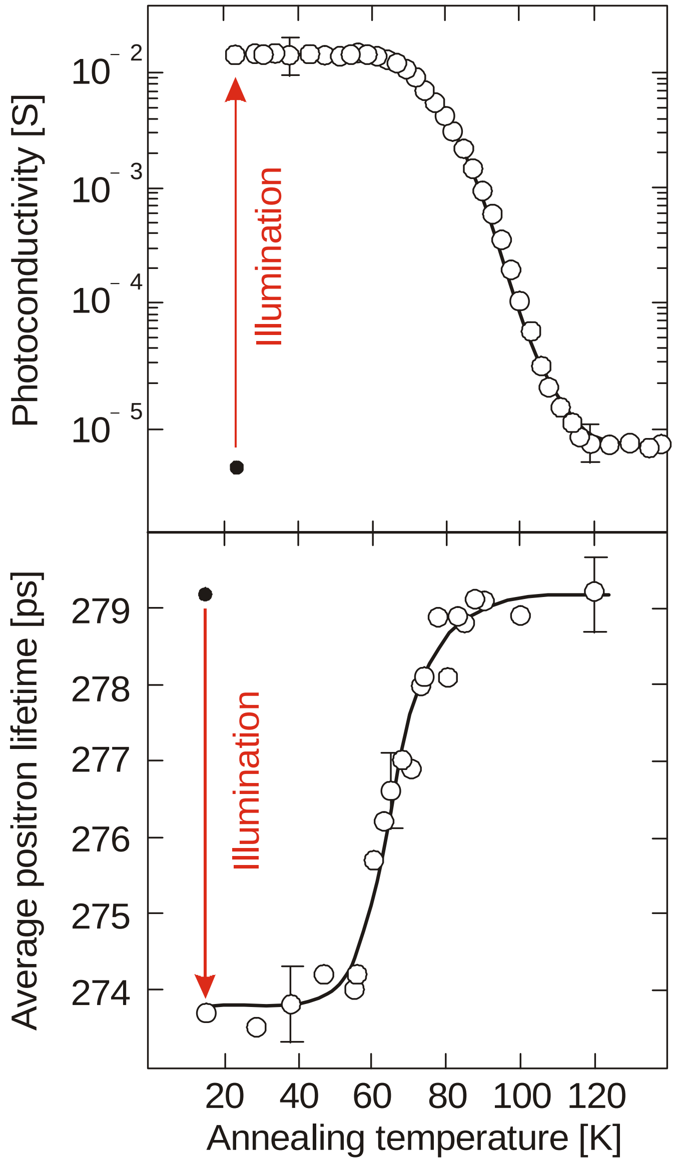

R. Krause-Rehberg et al., Phys. Rev. B <u>48</u> (1993) 11723

Compensating Defects in GaAs:Si

- Si is also often used as donor in GaAs
- Si is built-in as Si_{Ga}^{+} and also as Si_{As}^{-} (amphoteric behavior)
- degree of compensation not constant, but growing with Si content
- result: doping only possible up to 10^{19} cm^{-3}
- at higher Si content: almost complete auto-compensation
- model for additional compensating center (acceptor): $V_{Ga}Si_{Ga}^{-}$

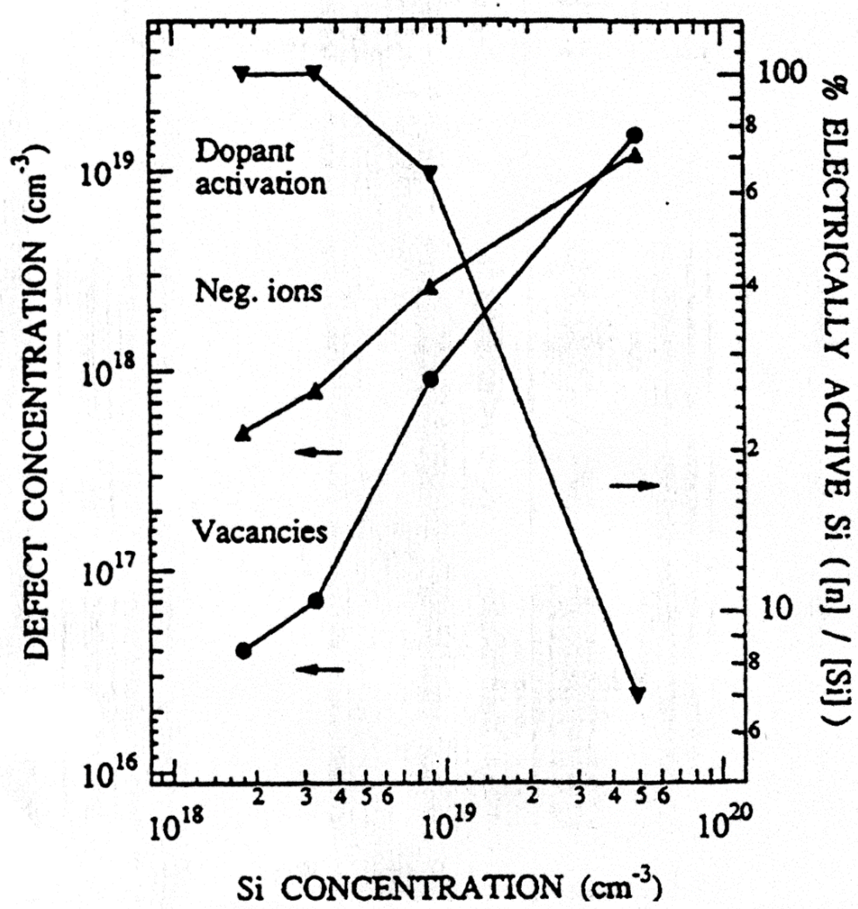

The dopant activation, expressed as the ratio of free carrier and Si concentrations (▼), the concentration of negative ions (▲), and the concentration of Ga vacancies (●) all as a function of Si concentration in four Si-doped GaAs samples.

(K. Saarinen et. al, Helsinki UT)

Identification of V_{Ga}-Si_{Ga}-Complexes in GaAs:Si

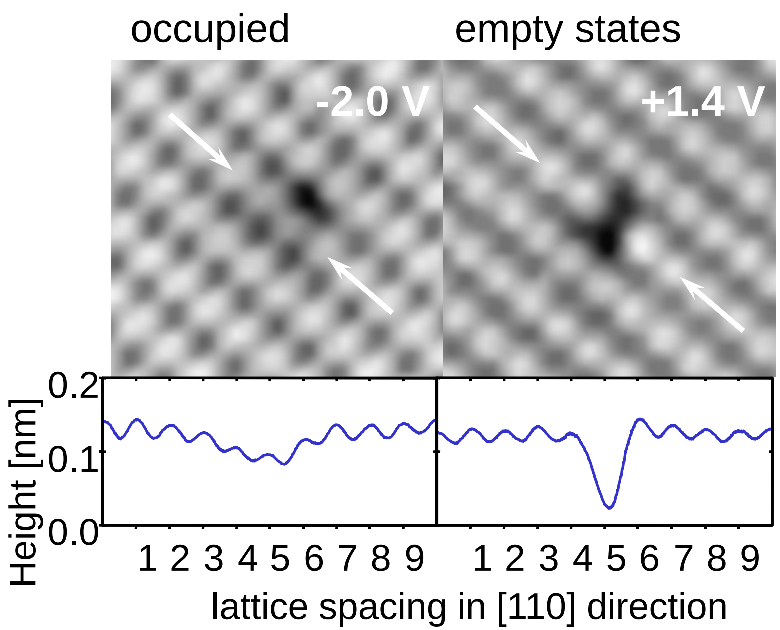

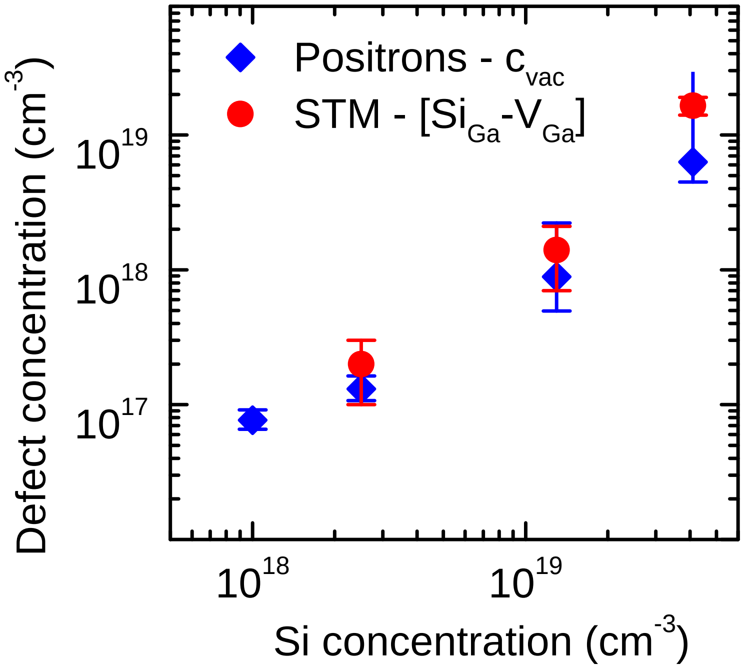

- Scanning tunneling microscopy at GaAs (110)-cleavages planes (by Ph. Ebert, Jülich)
- Defect complex identified as $\mathbf{V_{Ga}}$-$\mathbf{Si_{Ga}}$

- Quantification → Agreement

Mono-vacancies in GaAs:Si are V_{Ga}- Si_{Ga}-complexes

Gebauer et al., Phys. Rev. Lett. **78** (1997) 3334

Vacancy clusters in semiconductors

- vacancy clusters were observed after neutron irradiation, ion implantation and plastic deformation
- due to large open volume (low electron density) -> positron lifetime increases distinctly
- example: plastically deformed Ge
- lifetime: τ = 525 ps
- reason for void formation: jog dragging mechanism
- trapping rate of voids disappears during annealing experiment

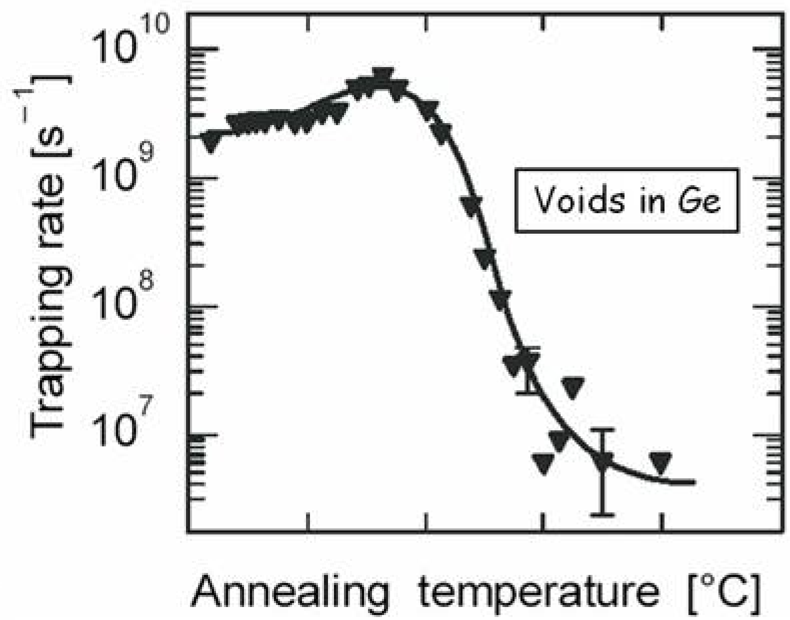

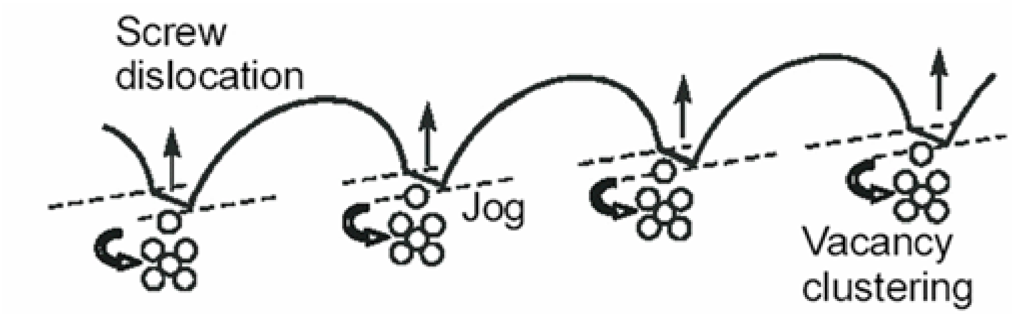

Krause-Rehberg et al., 1993

Theoretical calculation of vacancy clusters in Si

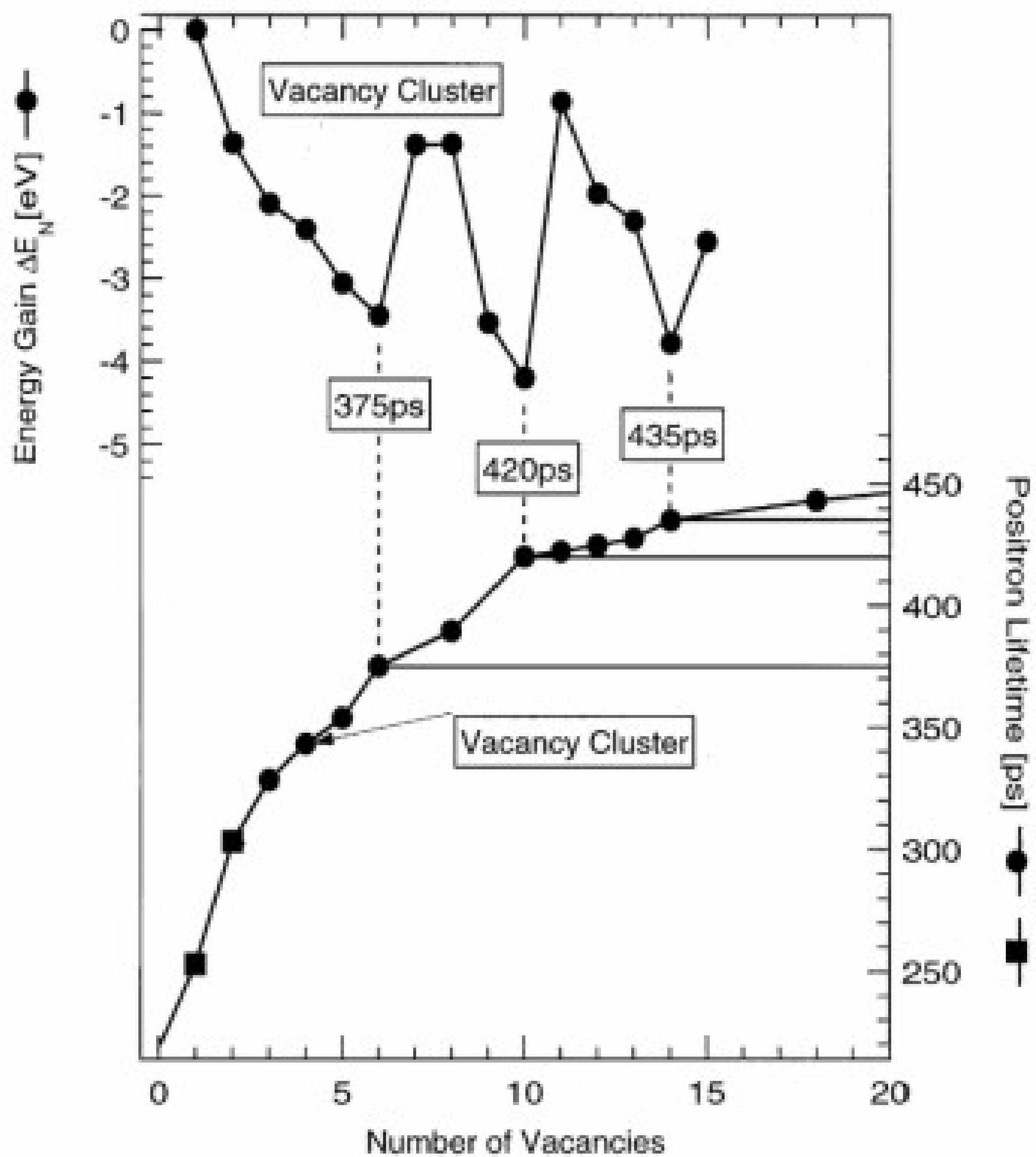

- there are cluster configurations with a large energy gain
- „Magic Numbers" with 6, 10 und 14 vacancies
- positron lifetime increases distinctly with cluster size
- for n > 10 saturation effect, i.e. size cannot be determined

T.E.M. Staab et al.,
Physica B 273-274 (1999) 501-504

Defect studies of GaN

- as-grown GaN (FCM GmbH) - 2012

Unterschied zwischen den 3 Proben ist die Wachstumstemperatur:

- 100387: 1050°C,
- 100430: 980°C sowie
- 100431: 950°C.

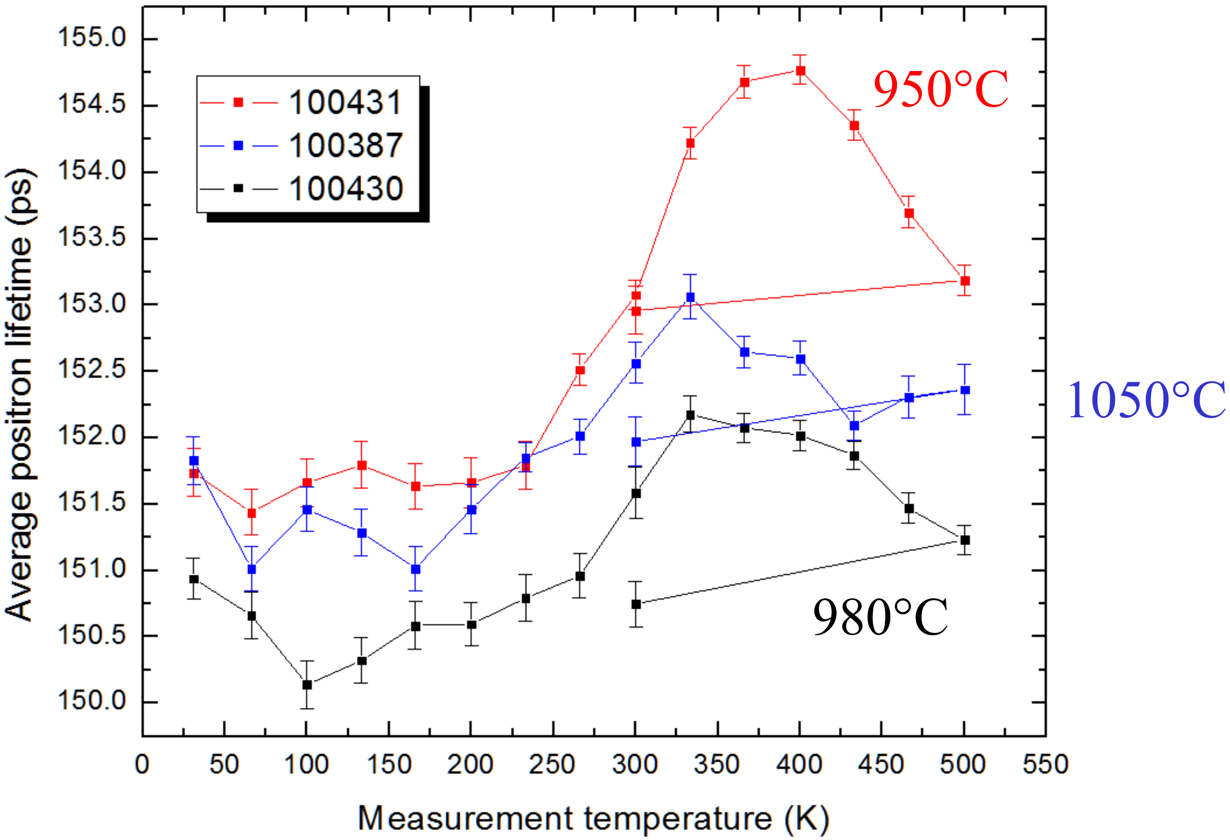

VOLUME 79, NUMBER 16 PHYSICAL REVIEW LETTERS 20 OCTOBER 1997

Observation of Native Ga Vacancies in GaN by Positron Annihilation

K. Saarinen,[1] T. Laine,[1] S. Kuisma,[1] J. Nissilä,[1] P. Hautojärvi,[1] L. Dobrzynski,[2] J. M. Baranowski,[3] K. Pakula,[3] R. Stepniewski,[3] M. Wojdak,[3] A. Wysmolek,[3] T. Suski,[4] M. Leszczynski,[4] I. Grzegory,[4] and S. Porowski[4]
[1]*Laboratory of Physics, Helsinki University of Technology, 02150 Espoo, Finland*
[2]*Institute of Physics, Warsaw University Branch, Lipowa 41, 15-424 Bialystok, Poland and Soltan Institute of Nuclear Studies, 05-400 Otwock-Swierk, Poland*
[3]*Institute of Experimental Physics, University of Warsaw, 00-681 Warsaw, Poland*
[4]*UNIPRESS, High Pressure Research Center, Polish Academy of Sciences, 01-142 Warsaw, Poland*

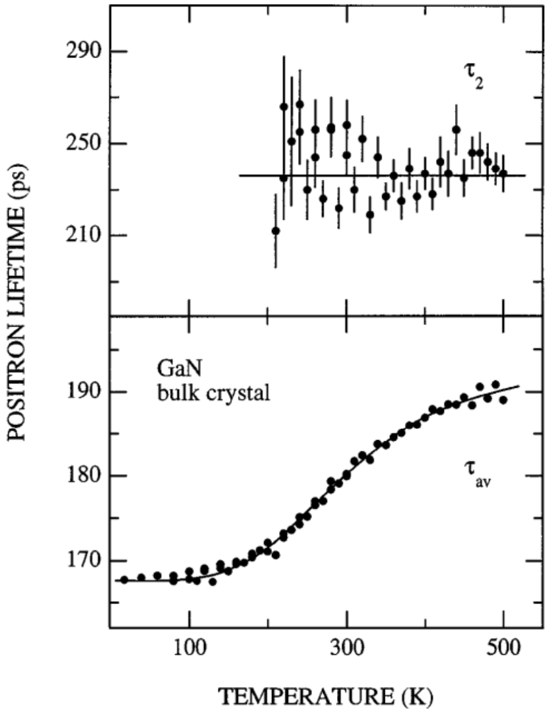

FIG. 1. The average positron lifetime τ_{av} and the lifetime component τ_2 vs measurement temperature GaN bulk crystal. The lifetime component τ_2 could be decomposed only at $T > 200$ K. The solid lines are drawn to guide the eye.

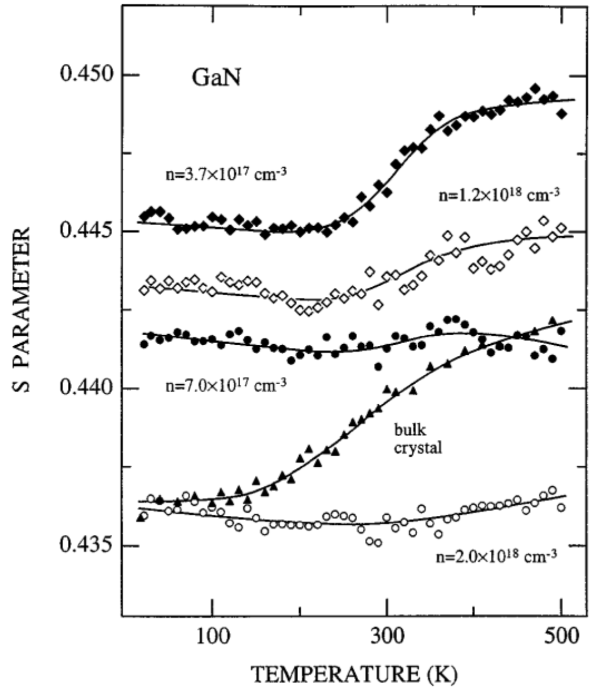

FIG. 2. The low electron-momentum parameter S vs measurement temperature in various GaN samples. The carrier concentrations of the GaN layers at 300 K are indicated in the figure. The solid lines are fits to the temperature dependent positron trapping model (Ref. [14]).

[Ga vacancies]≈10^{18} cm^{-3}

APPLIED PHYSICS LETTERS VOLUME 73, NUMBER 22 30 NOVEMBER 1998

Gallium vacancies and the growth stoichiometry of GaN studied by positron annihilation spectroscopy

K. Saarinen,[a] P. Seppälä, J. Oila, P. Hautojärvi, and C. Corbel
Laboratory of Physics, Helsinki University of Technology, P.O. Box 1100, 02015 HUT, Finland

O. Briot and R. L. Aulombard
Université Montpellier II, Groupe d'Etudes des Semiconducters, CC074, 34095 Montpellier Cedex 5, France

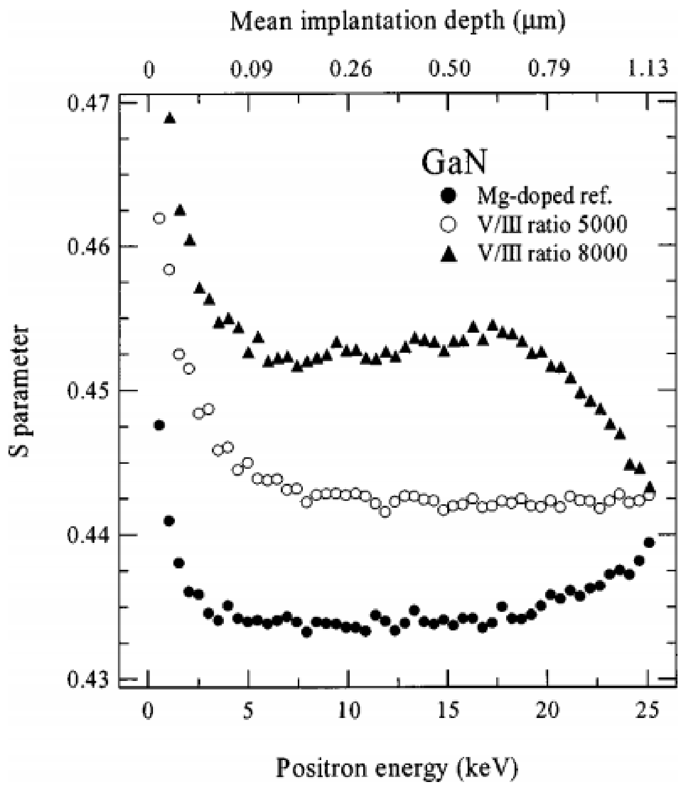

FIG. 1. The low electron-momentum parameter S as a function of the positron implantation energy in three GaN samples. The top axis shows the mean stopping depth corresponding to the positron implantation energy.

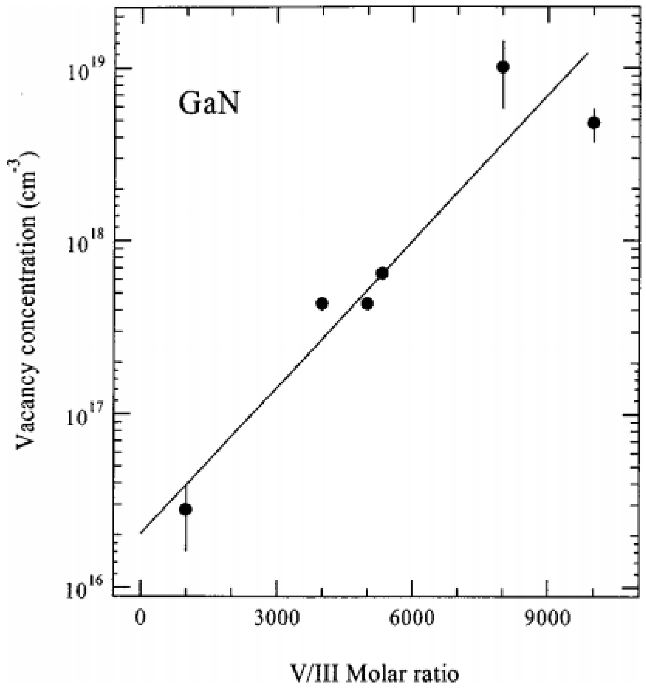

FIG. 3. The concentration of Ga vacancies vs the V/III molar ratio in undoped GaN samples. The straight line is drawn to emphasize the correlation.

APPLIED PHYSICS LETTERS VOLUME 75, NUMBER 16 18 OCTOBER 1999

The influence of Mg doping on the formation of Ga vacancies and negative ions in GaN bulk crystals

K. Saarinen,[a] J. Nissilä, and P. Hautojärvi
Laboratory of Physics, Helsinki University of Technology, FIN-02015 HUT, Finland

J. Likonen
Technical Research Centre of Finland, Chemical Technology, FIN-02044 VTT, Finland

T. Suski, I. Grzegory, B. Lucznik, and S. Porowski
UNIPRESS, High Pressure Research Center, Polish Academy of Sciences, 01-142 Warsaw, Poland

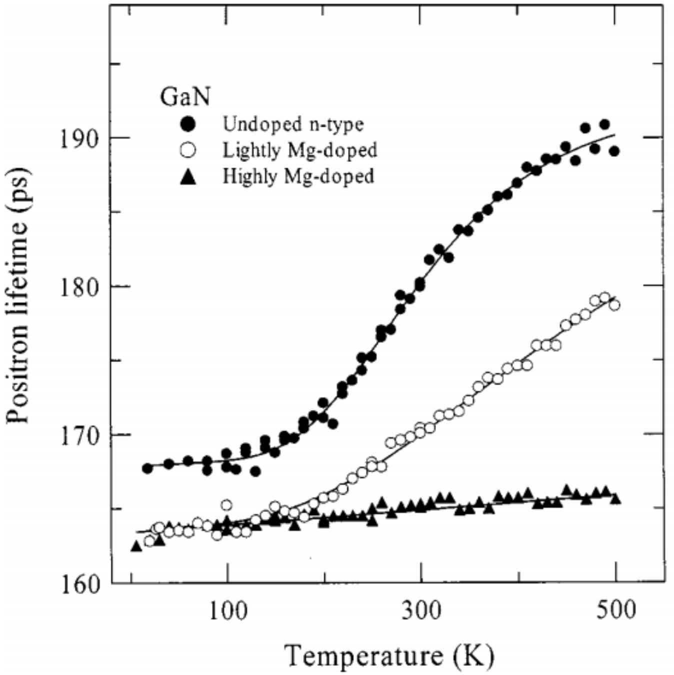

FIG. 2. Average positron lifetime vs measurement temperature in GaN bulk crystals. The solid lines correspond to the analyses with the temperature-dependent positron trapping model, where concentrations of Ga vacancies and negative ions (Table I) are determined as fitting parameters.

In conclusion, the positron experiments show the presence of Ga vacancies and negative ions in GaN crystals. The concentration of Ga vacancies decreases with increasing Mg doping, in good agreement with the trends expected for the V_{Ga} formation energy as a function of the Fermi level. The concentration of negative ions increases with Mg doping and correlates with the Mg concentration determined by SIMS. We thus associate the negative ions with Mg_{Ga}^-. The negative charge of Mg suggests that the loss of n-type conductivity in the Mg doping of GaN crystals is mainly due to compensation of O_N^+ donors by Mg_{Ga}^- acceptors.

ELSEVIER
Physica B 308–310 (2001) 77–80
PHYSICA B
www.elsevier.com/locate/physb

Ga vacancies in electron irradiated GaN: introduction, stability and temperature dependence of positron trapping

K. Saarinen[a,*], T. Suski[b], I. Grzegory[b], D.C. Look[c]

[a] Laboratory of Physics, Helsinki University of Technology, P.O. Box 1100, 02150 HUT, Finland
[b] UNIPRESS, High Pressure Research Center, Polish Academy of Sciences, 01-142 Warsaw, Poland
[c] Semiconductor Research Center, Wright State University, Dayton, OH, USA

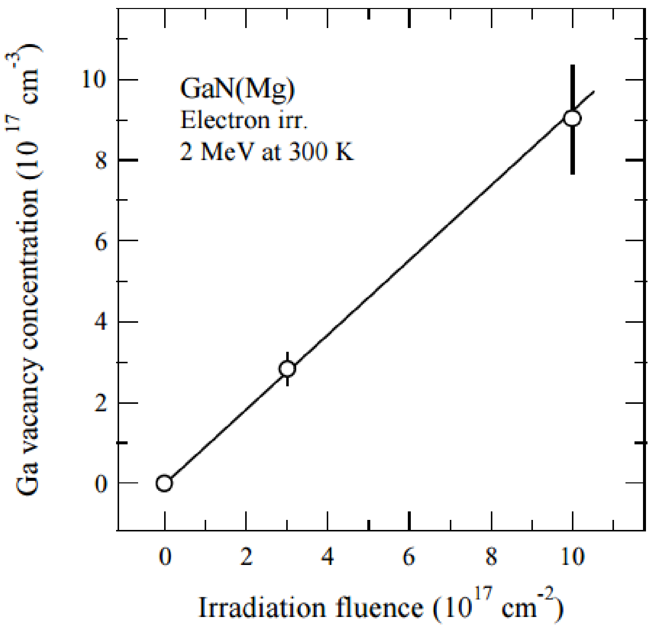

Fig. 3. The concentration of Ga vacancies as a function of 2 MeV electron irradiation fluence at 300 K. The solid line corresponds to the introduction rate of $\Sigma_V = 1\,\text{cm}^{-1}$ [3].

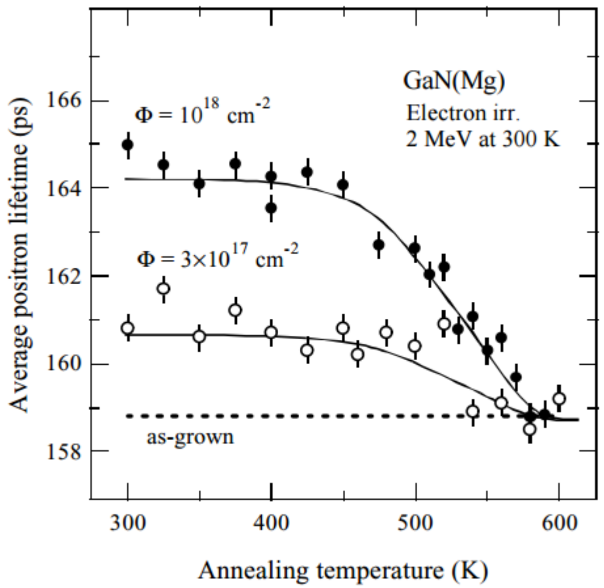

Fig. 1. Average positron lifetime as a function of annealing temperature T_{ann} in two GaN samples irradiated to fluences Φ. The measurement temperature was $T_{meas} = 300\,\text{K}$. The dashed line shows the level of the average positron lifetime in as-grown samples before irradiation [3].

Ga vacancies as dominant intrinsic acceptors in GaN grown by hydride vapor phase epitaxy

J. Oila, J. Kivioja, V. Ranki, and K. Saarinen[a)]
Laboratory of Physics, Helsinki University of Technology, P.O. Box 1100, FIN-02015 HUT, Finland

D. C. Look
Semiconductor Research Center, Wright State University, Dayton, Ohio

R. J. Molnar
Massachusetts Institute of Technology, Lincoln Laboratory, Lexington, Massachusetts 02420-9108

S. S. Park, S. K. Lee, and J. Y. Han
Samsung Advanced Institute of Technology, P.O. Box 111, Suwon, Korea 440-600

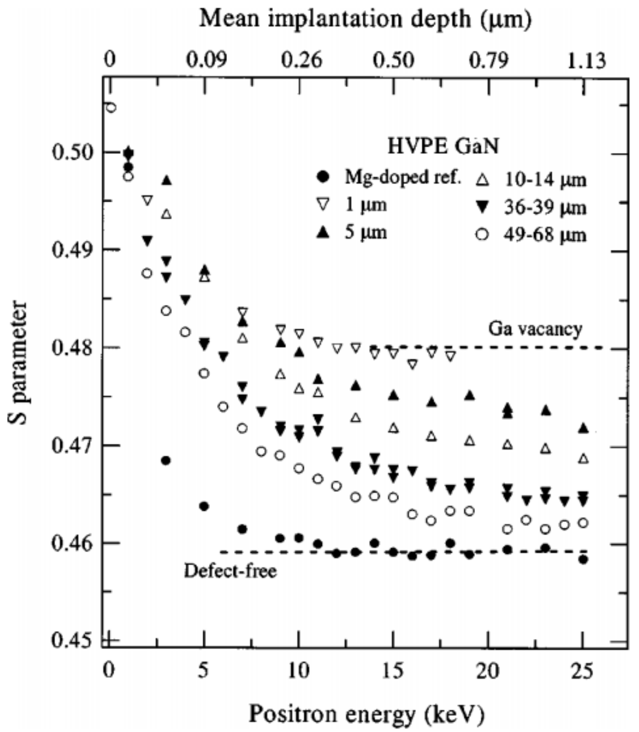

FIG. 2. The low electron-momentum parameter S as a function of the positron implantation energy. The dashed lines show the values of S parameter in defect-free GaN and at the Ga vacancy. The top axis indicates the mean stopping depth corresponding to the positron implantation energy.

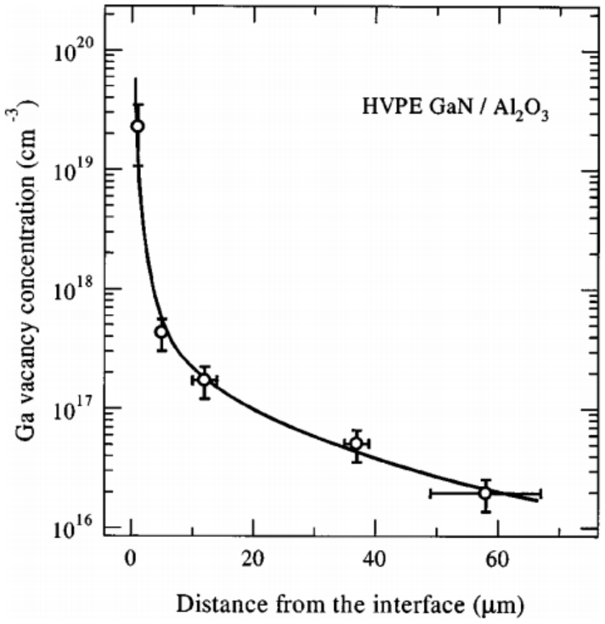

FIG. 3. The concentration of Ga vacancies as a function of the thickness of the GaN layers on sapphire.

In summary, our positron annihilation experiments show that Ga vacancies are the dominant acceptors *n*-type GaN grown by hydride vapor phase epitaxy on sapphire. The concentration of Ga vacancies decreases from almost 10^{20} cm^{-3} to less than 10^{16} cm^{-3} when the thickness of the GaN layers increases from 1 to more than 100 μm. Furthermore, the Ga vacancy concentration is equal to the total acceptor density determined by temperature-dependent Hall experiments. The depth profile of Ga vacancies is similar to that of O, suggesting that the Ga vacancies formed during the growth are bound to defect complexes with the oxygen impurities.

PHYSICAL REVIEW B **73**, 193301 (2006)

Direct evidence of impurity decoration of Ga vacancies in GaN from positron annihilation spectroscopy

S. Hautakangas, I. Makkonen, V. Ranki, M. J. Puska, and K. Saarinen*
Laboratory of Physics, Helsinki University of Technology, P.O.Box 1100, FIN-02150 Espoo, Finland

X. Xu
ATMI Inc., 7 Commerce Drive, Danbury, Connecticut 06810, USA

D. C. Look
Semiconductor Research Center, Wright State University, Dayton, Ohio 45435, USA
(Received 27 February 2006; published 3 May 2006)

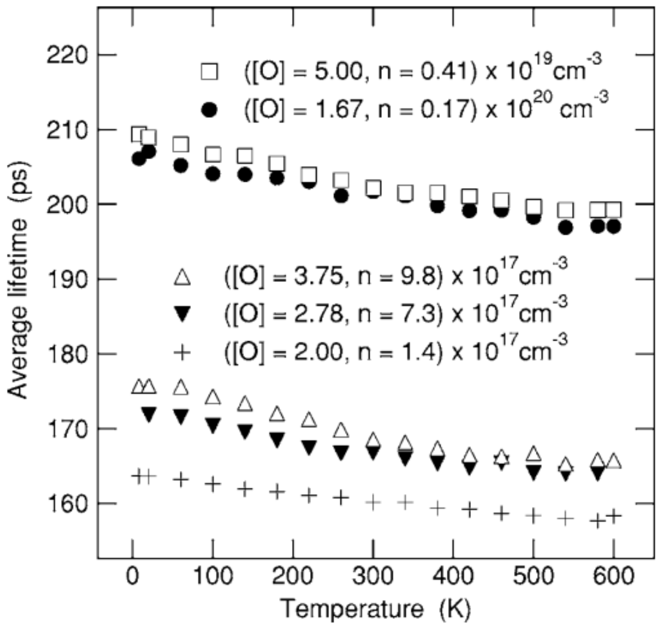

FIG. 1. The average positron lifetime as a function of measuring temperature. The first number in the parentheses stands for O concentration and the second one indicates the free carrier concentration.

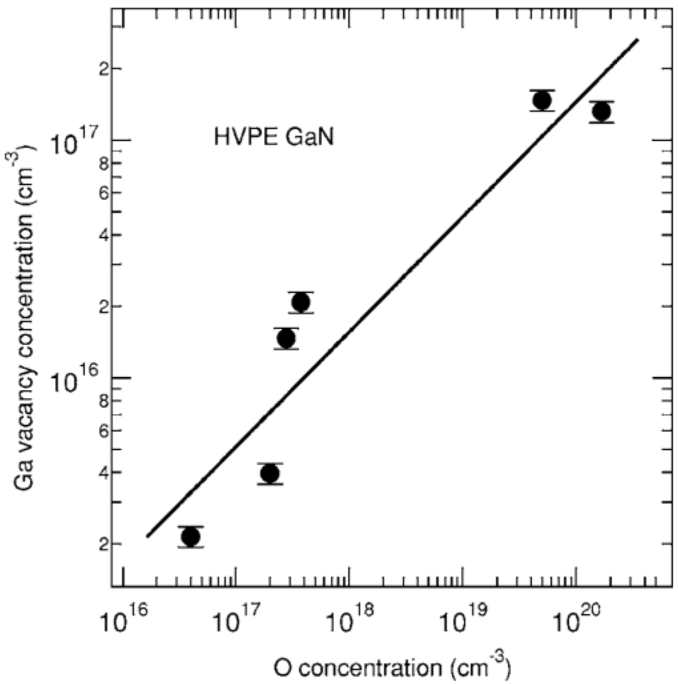

FIG. 2. Gallium vacancy concentration as a function of doping. The solid line is a guide to the eye. The results in the sample with the lowest O concentration have been taken from Ref. 18.

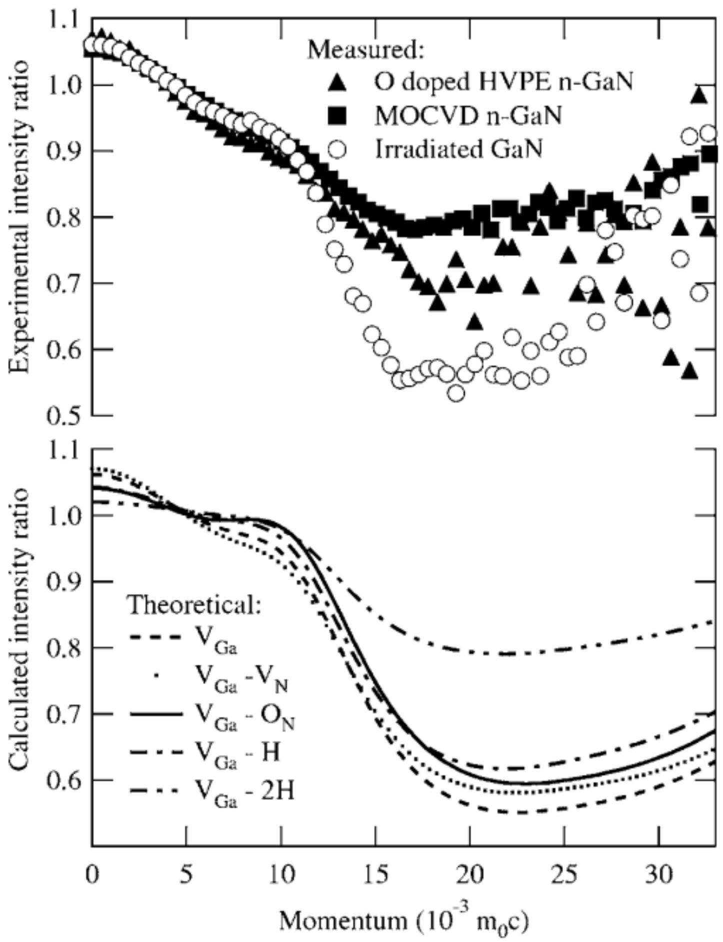

FIG. 4. Measured and calculated momentum distribution curves for different types of samples and defects, respectively. All these curves are shown as ratios to the data obtained in the GaN lattice.

We identify the isolated V_{Ga} in undoped electron irradiated GaN, and show that in O-doped HVPE GaN the Ga vacancy is complexed with the O atom forming V_{Ga}-O_N-pairs. In MOCVD material our data show that the Ga vacancy is likely to be decorated by both oxygen and hydrogen.

JOURNAL OF APPLIED PHYSICS **103**, 104505 (2008)

Vacancy-type defects in Er-doped GaN studied by a monoenergetic positron beam

A. Uedono,[1,a] C. Shaoqiang,[1] S. Jongwon,[1] K. Ito,[1] H. Nakamori,[1] N. Honda,[1] S. Tomita,[1] K. Akimoto,[1] H. Kudo,[1] and S. Ishibashi[2]
[1]*Institute of Applied Physics, University of Tsukuba, Tsukuba, Ibaraki, 305-8573, Japan*
[2]*Research Institute for Computational Sciences, National Institute of Advanced Industrial Science and Technology, Tsukuba, Ibaraki, 305-8568, Japan*

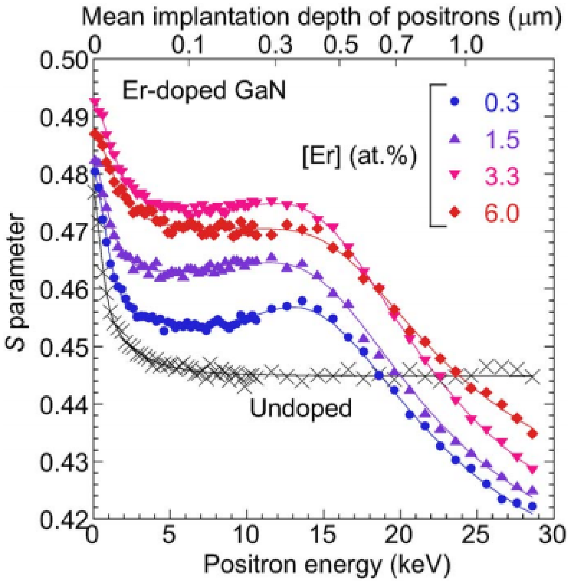

FIG. 1. (Color online) S as a function of incident positron energy E for Er-doped GaN with [Er]=0.3–6.0 at. %. The result for undoped GaN is also shown. The S values at $E \leq 14$ keV correspond to the annihilation of positrons in the GaN layers. The solid curves are fits to the experimental data. The derived depth distributions of S are shown in Fig. 3.

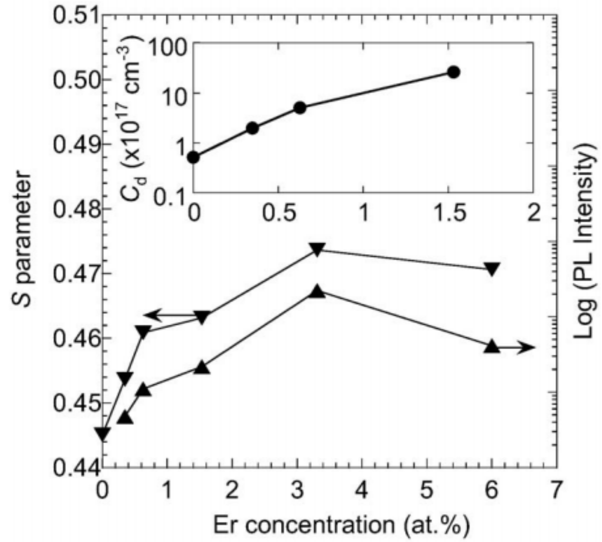

FIG. 2. S values corresponding to the annihilation of positrons in Er-doped GaN and the integrated intensities of a 551 nm PL line as a function of the Er concentration, where the PL intensity is shown in a logarithmic scale. The inset shows the concentration of Ga vacancies (V_{Ga}) derived from the positron trapping model.

APPLIED PHYSICS LETTERS **93**, 031916 (2008)

Microstructural evolution in H ion induced splitting of freestanding GaN

O. Moutanabbir,[1,a)] R. Scholz,[1] S. Senz,[1] U. Gösele,[1] M. Chicoine,[2] F. Schiettekatte,[2] F. Süßkraut,[3] and R. Krause-Rehberg[3]
[1]*Max Planck Institute of Microstructure Physics, Weinberg 2, D 06120 Halle, Germany*
[2]*Département de Physique, Université de Montréal, Succursale Centre Ville, Montréal, Québec, H3T 1J4, Canada*
[3]*Department of Physics, Martin-Luther-University Halle-Wittenberg, Friedemann-Bach-Platz 6, D 06108 Halle, Germany*

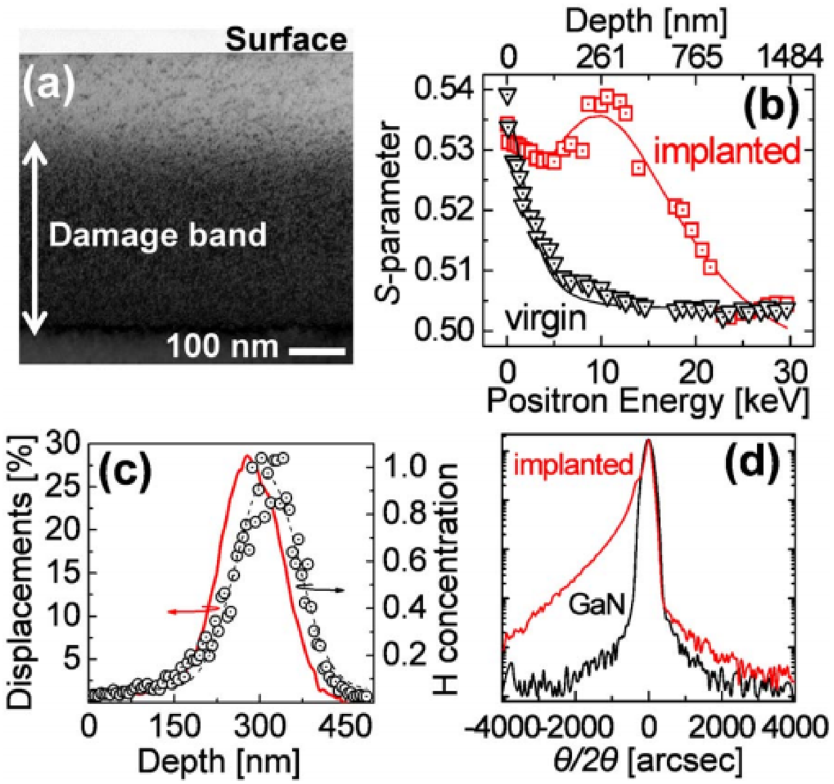

FIG. 1. (Color online) (a) XTEM image of damage induced in GaN by H ion implantation at 50 keV with a fluence of 2.6×10^{17} atom/cm^2. (b) S parameter depth profile measured before (triangles) and after (squares) H implantation. (c) H concentration/10^{22} cm^{-3} depth profile (circles) and implantation damage profile (line) as deduced from ERD and ion channeling, respectively. (d) X-ray $\theta/2\theta$ scans of (0002) GaN before and after H implantation.

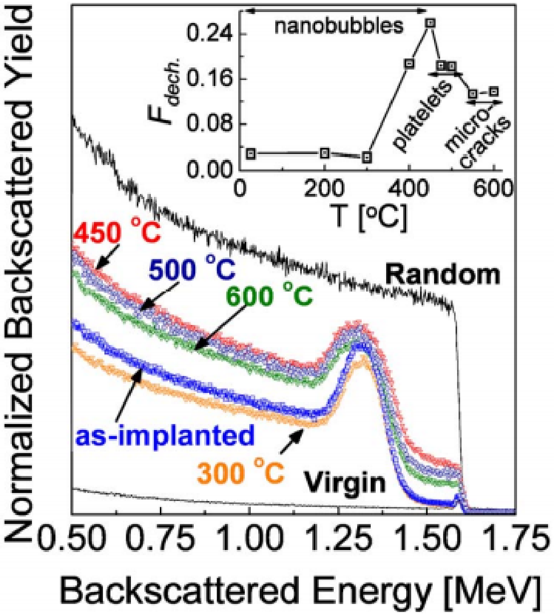

FIG. 2. (Color online) RBS/C yields as a function of annealing temperature for GaN substrates implanted with H at 2.6×10^{17} atom/cm^2. Inset: Evolution of dechanneling factor Fdech, as a function of temperature. The corresponding morphologies, as determined by XTEM, are also indicated.

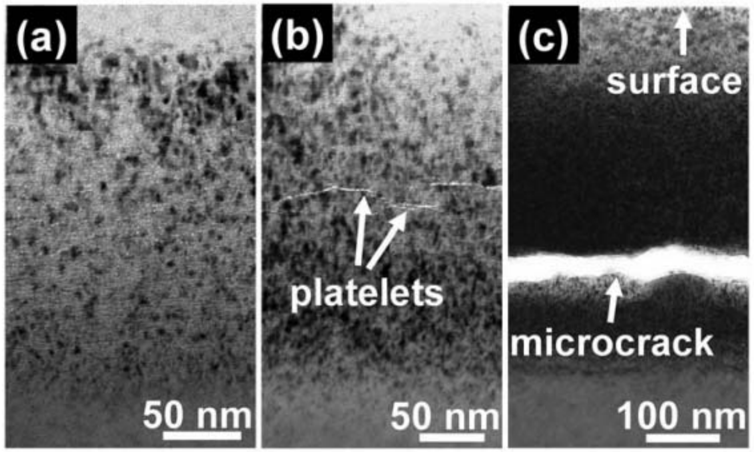

FIG. 3. XTEM micrographs of H-implanted GaN annealed at different temperatures: 450 °C (a), 500 °C (b), and 600 °C (c).

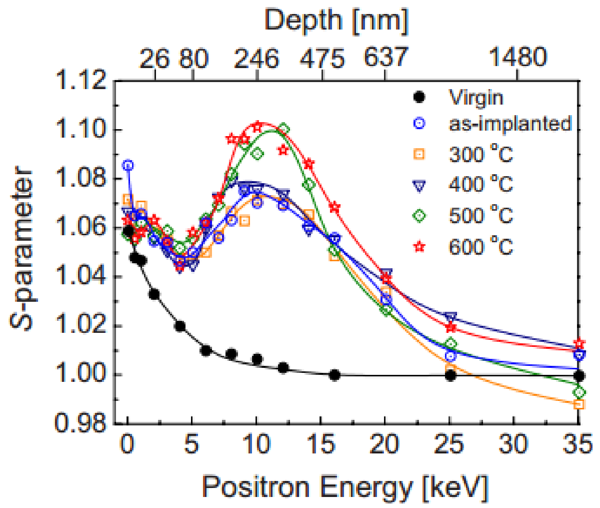

FIG. 3. (Color online) Thermoevolution of the normalized S parameter of H-implanted GaN samples as a function of incident positron energy. For comparison, the spectrum recorded from bulk GaN is also shown.

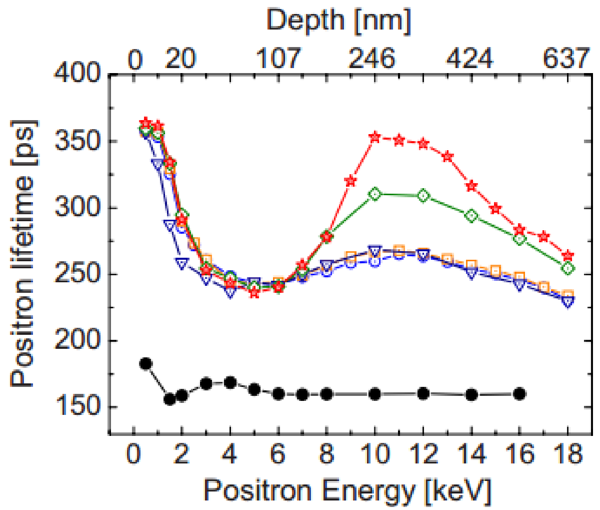

FIG. 4. (Color online) The evolution of the average positron lifetime as a function of the positron energy for the virgin, as-implanted, and annealed GaN samples. The symbols are the same as in Fig. 3.

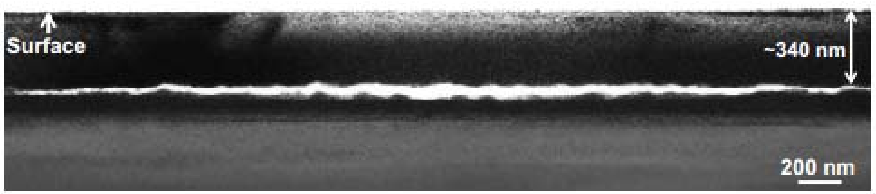

FIG. 2. XTEM image of H-implanted GaN substrate implanted under the conditions described in Fig. 1 and annealed at 600 °C for 5 min.

New Journal of Physics
The open-access journal for physics

New Journal of Physics **13** (2011) 013029
1367-2630/11/013029+12$33.00

Cu diffusion-induced vacancy-like defects in freestanding GaN

M Elsayed[1,6], R Krause-Rehberg[1], O Moutanabbir[2,6], W Anwand[3], S Richter[4] and C Hagendorf[5]
[1] Martin-Luther-University Halle-Wittenberg, von-Danckelmann-Platz 3, Halle (Saale) 06120, Germany

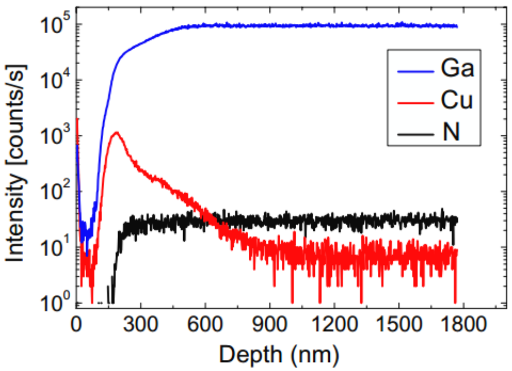

Figure 1. SIMS depth profiles of GaN sample after Cu diffusion induced by annealing for 96 h at 873 K. Note that surface peaks are artifacts of the SIMS measurements.

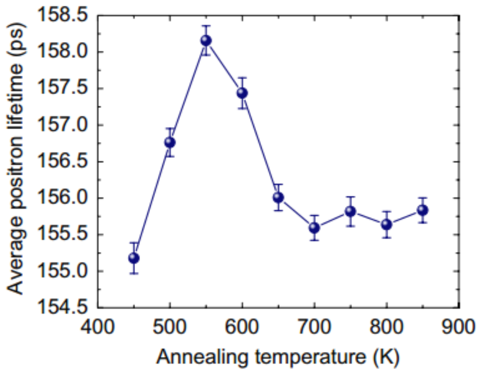

Figure 4. Average positron lifetime of Cu-diffused fs-GaN samples after the isochronal annealing. The spectra were measured at a sample temperature of 333 K.

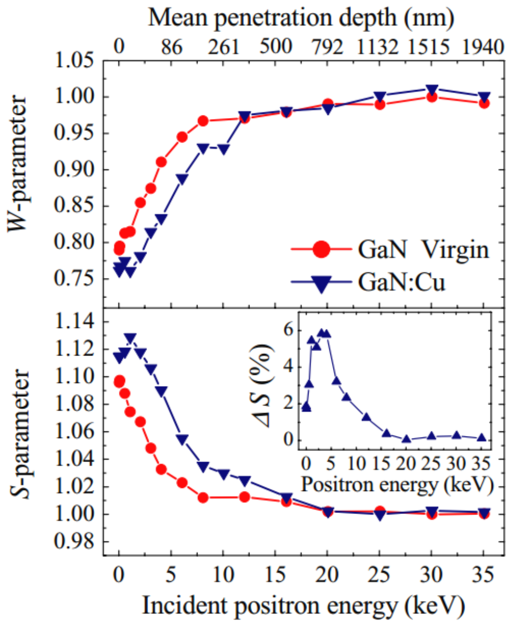

Figure 6. Normalized Doppler broadening parameters as a function of the incident positron energy measured for the virgin and Cu-diffused GaN samples annealed up to 550 K. The low momentum parameter *S* is shown in the lower panel and *W* in the upper panel. The positron mean penetration depth is shown in the top axis. The inset of the lower panel displays the difference in *S*

$$Cu_{Ga} \leftrightarrow V_{Ga} + Cu_{sink}$$

o-Positronium Lifetime allows Porosimetry

- In materials without free electrons Positronium may be formed (Polymers, glass, liquids, gases)
- p-Ps annihilates without interaction with host material
- o-Ps lifetime in vacuum 142 ns
- in matter: positron may pick off another electron with opposite spin -> fast annihilation with two gammas

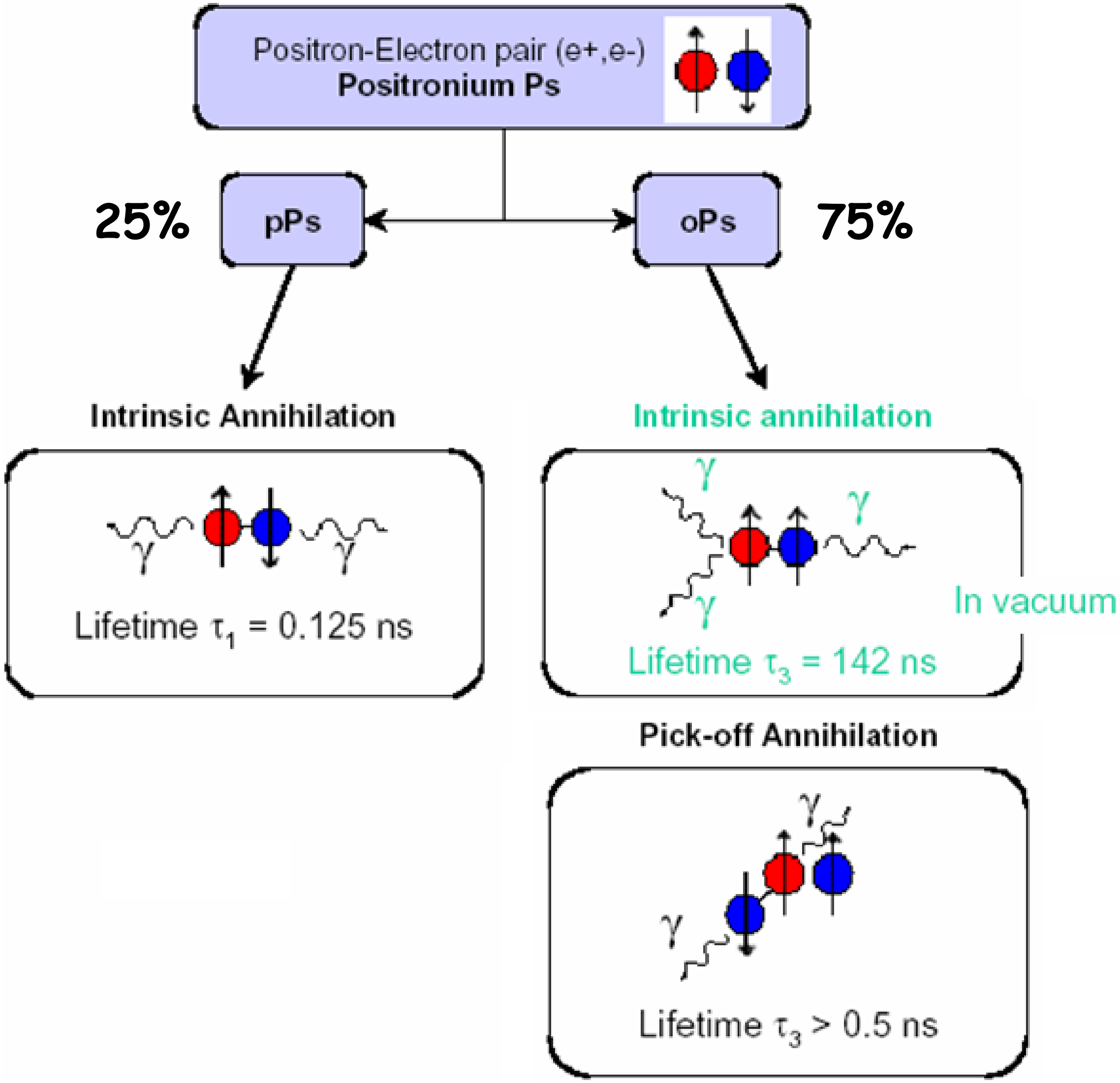

Pick-off Annihilation

pick-off annihilation:

- o-Ps is converted to p-Ps by capturing an electron with anti-parallel spin
- happens during collisions at walls of pore
- lifetime decreases rapidly
- lifetime is function of pore size 1.5 ns to 142 ns

positrons form Ps

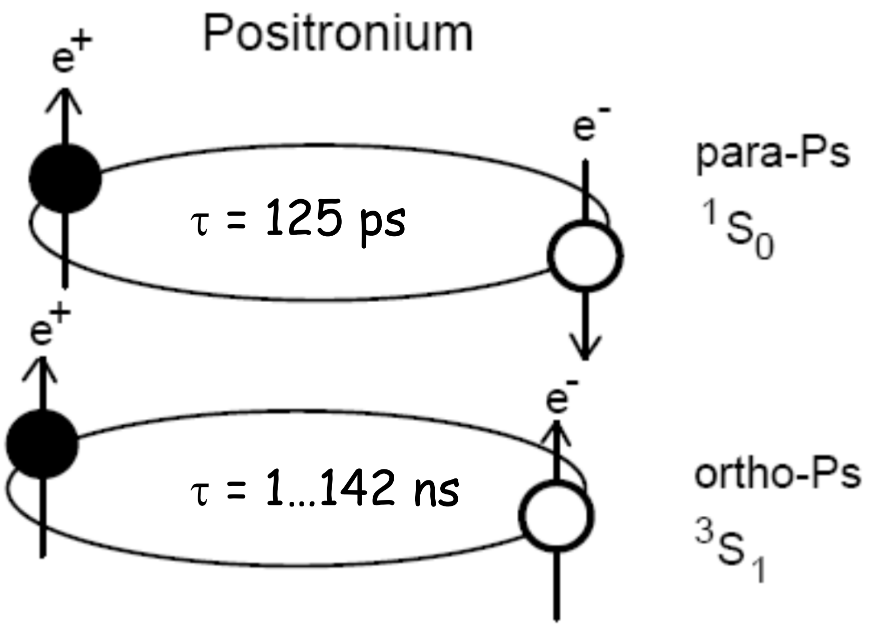

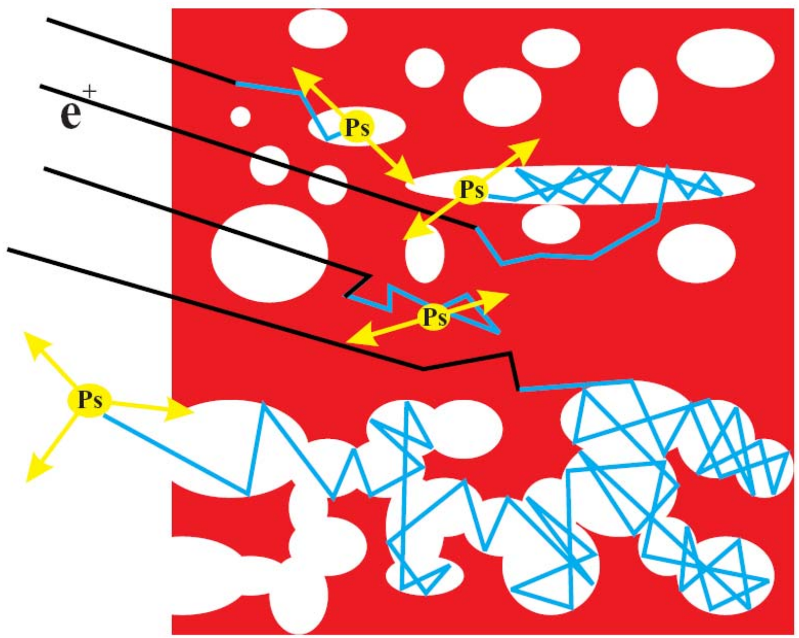

o-Ps lifetime τ_4 versus pore size in CPG Glass

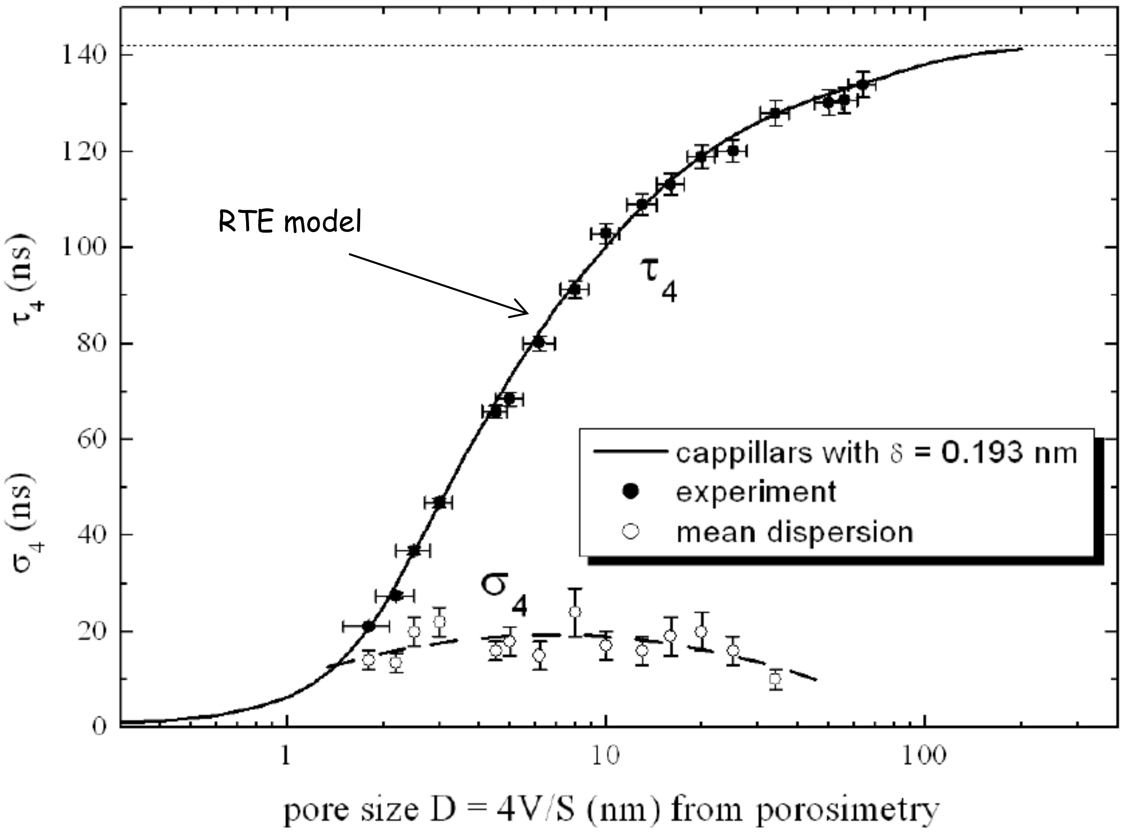

S.Thränert, Dissertation, MLU Halle 2008

- we measured porous CPG glass in a broad pore size range

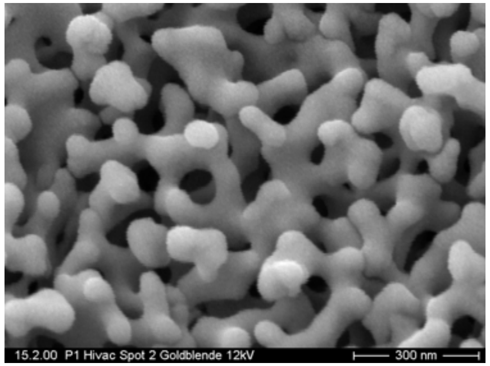

- given pore size obtained by N_2-adsorption and/or mercury intrusion technique
- for T=300 K fair agreement to the RTE model

User-dedicated intense Positron Sources in Germany

- Two intense positron sources available (positrons by pair production)
- **NEPOMUC** (NEutron induced POsitron Source MUniCh) at FRM-II
  - PLEPS (monoenergetic positron lifetime system)
  - PAES (Positron-induced Auger Electron Spectroscopy)
  - CDBS (Coincidence Doppler Broadening Spectroscopy)
  - SCM (Scanning Positron Microscope)
  - user beam line
- **EPOS** (ELBE Positron Source) at Helmholtz Center Dresden-Rossendorf
  - MePS (Mono-energetic Positron Spectroscopy)
  - GiPS (Gamma-induced Positron Spectroscopy)
  - CoPS (conventional setup using 22Na sources)

- at both sites: web-based application system for beam time

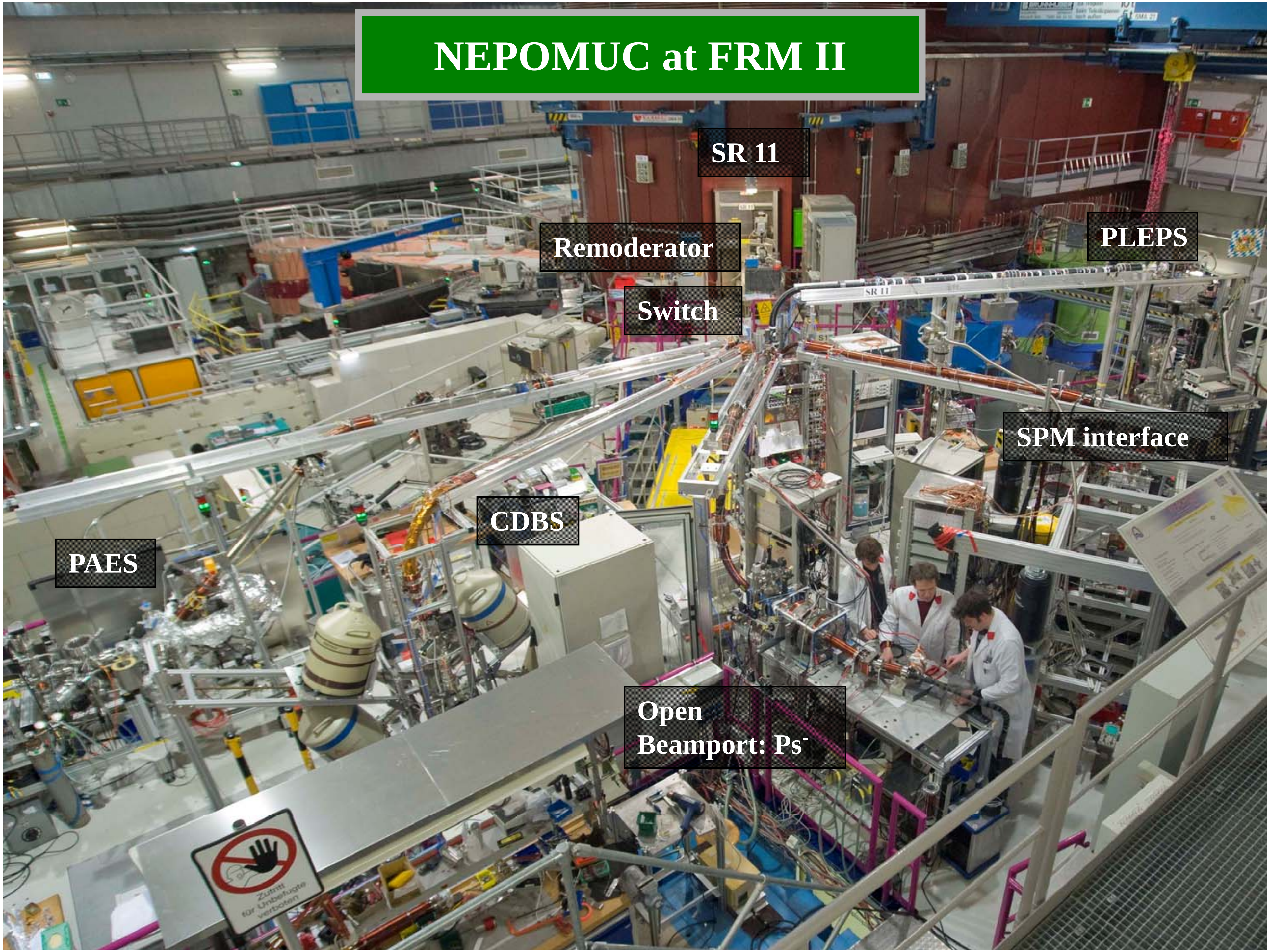
NEPOMUC at FRM II
SR 11
Remoderator
Switch
PLEPS
SPM interface
CDBS
PAES
Open
Beamport: Ps$^-$
Zutritt für Unbefugte verboten

Lateral Resolution with Scanning Positron Microscope

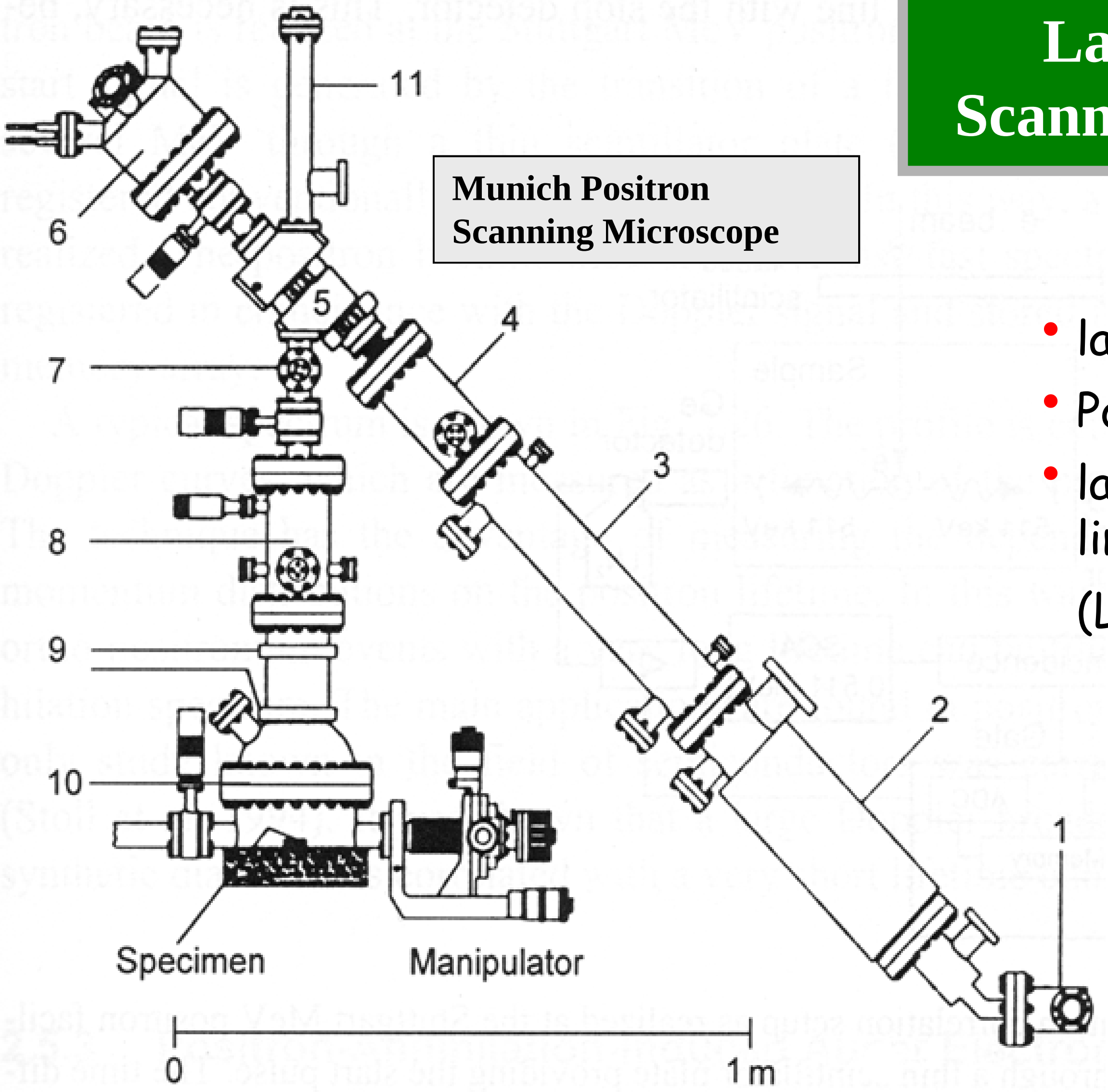

W. Triftshäuser et al., NIM B **130** (1997) 265

- lateral resolution 1…2 μm
- Positron lifetime spectroscopy
- lateral resolution principally limited by positron diffusion ($L_+ \approx$ 100nm)

Microhardness indentation in GaAs

- Comparison of SEM and Munich Positron Scanning Microscope
- problem here at the moment: intensity
- in future: adaption to NEPOMUC at FRM-II

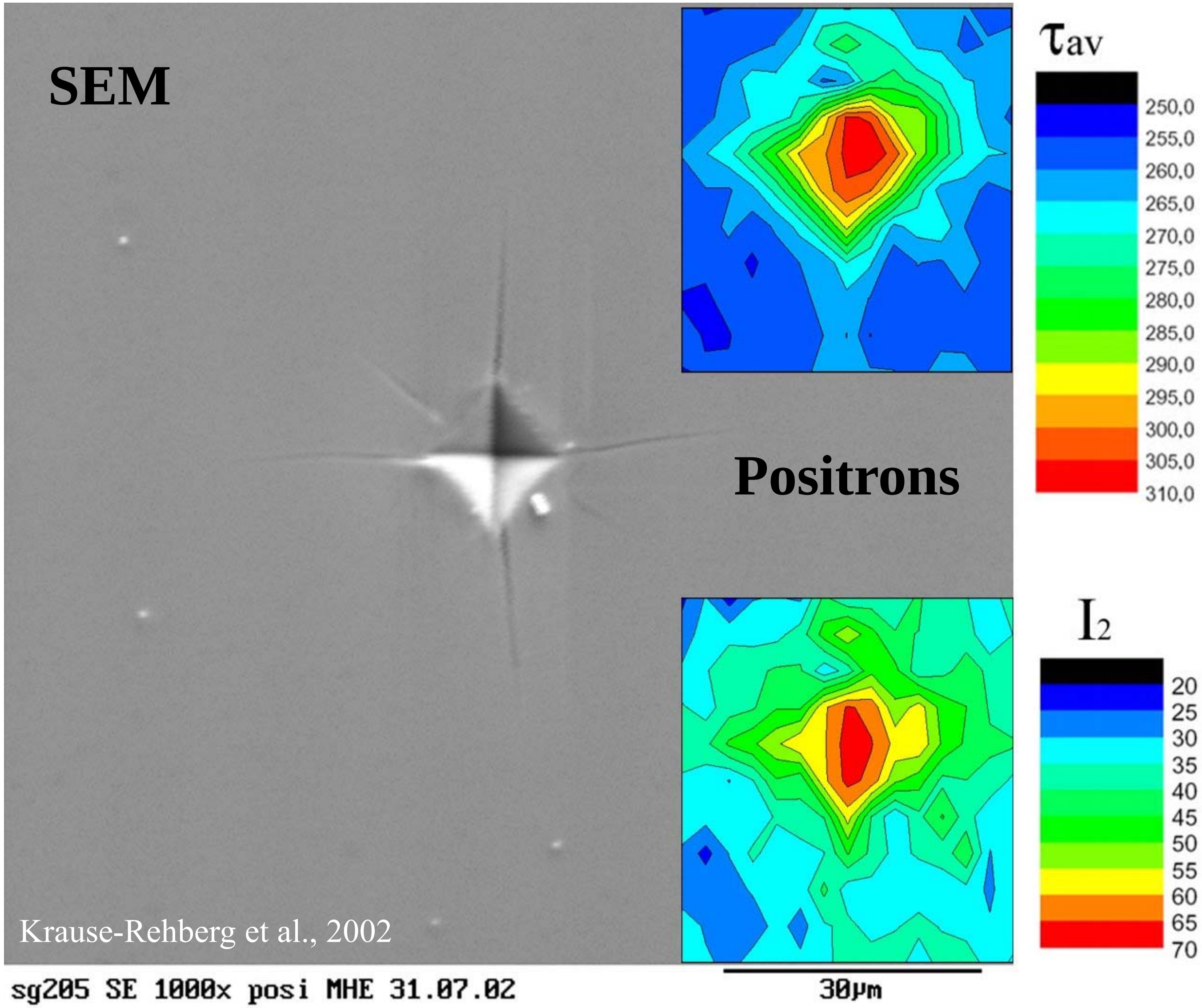

Defects in high-energy self-implanted Si: The Rp/2 effect

- after high-energy (3.5 MeV) self-implantation of Si ($5x10^{15}$ cm^{-2}) and RTA annealing (900°C, 30s): two new gettering zones appear at Rp and Rp/2 (Rp = projected range of Si^+)
- visible by SIMS profiling after intentional Cu contamination

TEM image by P. Werner, MPI Halle

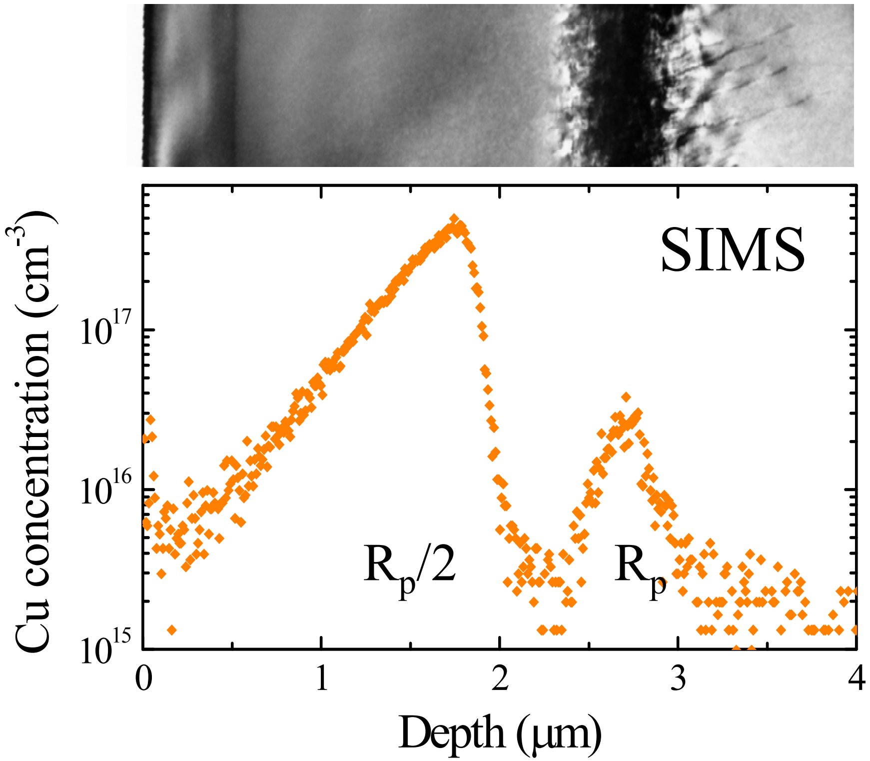

- at R_p: gettering by interstitial-type dislocation loops (formed by excess interstitials during RTA)
- no defects visible by TEM at Rp/2
- What type are these defects?

Investigation of the Rp/2 effect by conventional VEPAS

- the defect layers are expected in a depth of 1.7 mm and 2.8 mm corresponding to $E^+ =$ 18 and 25 keV
- implantation profile too broad to discriminate between the two zones
- simulation of S(E) curve gives the same result for assumed blue and yellow defect profile (solid line in upper panel)
- furthermore: small effect only
- no conclusions about origin of $R_p/2$ effect possible

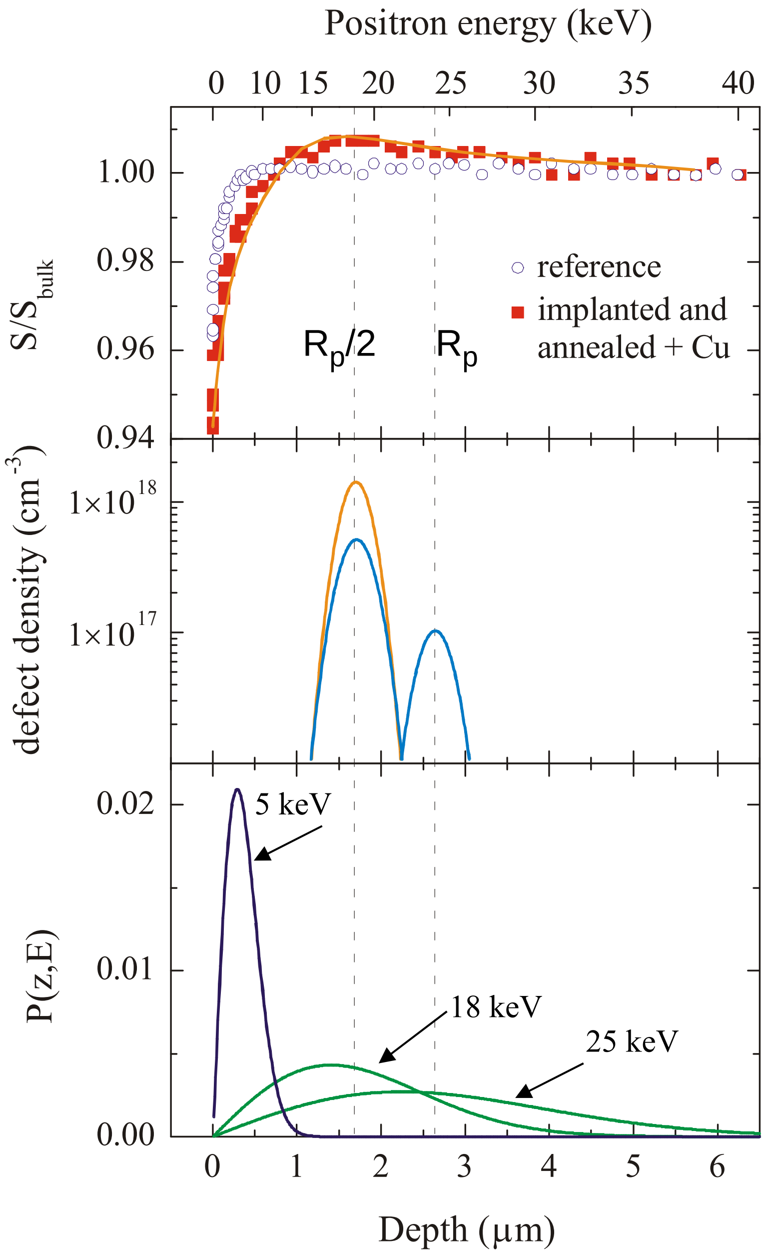

Enhanced depth resolution by using the Positron Microscope

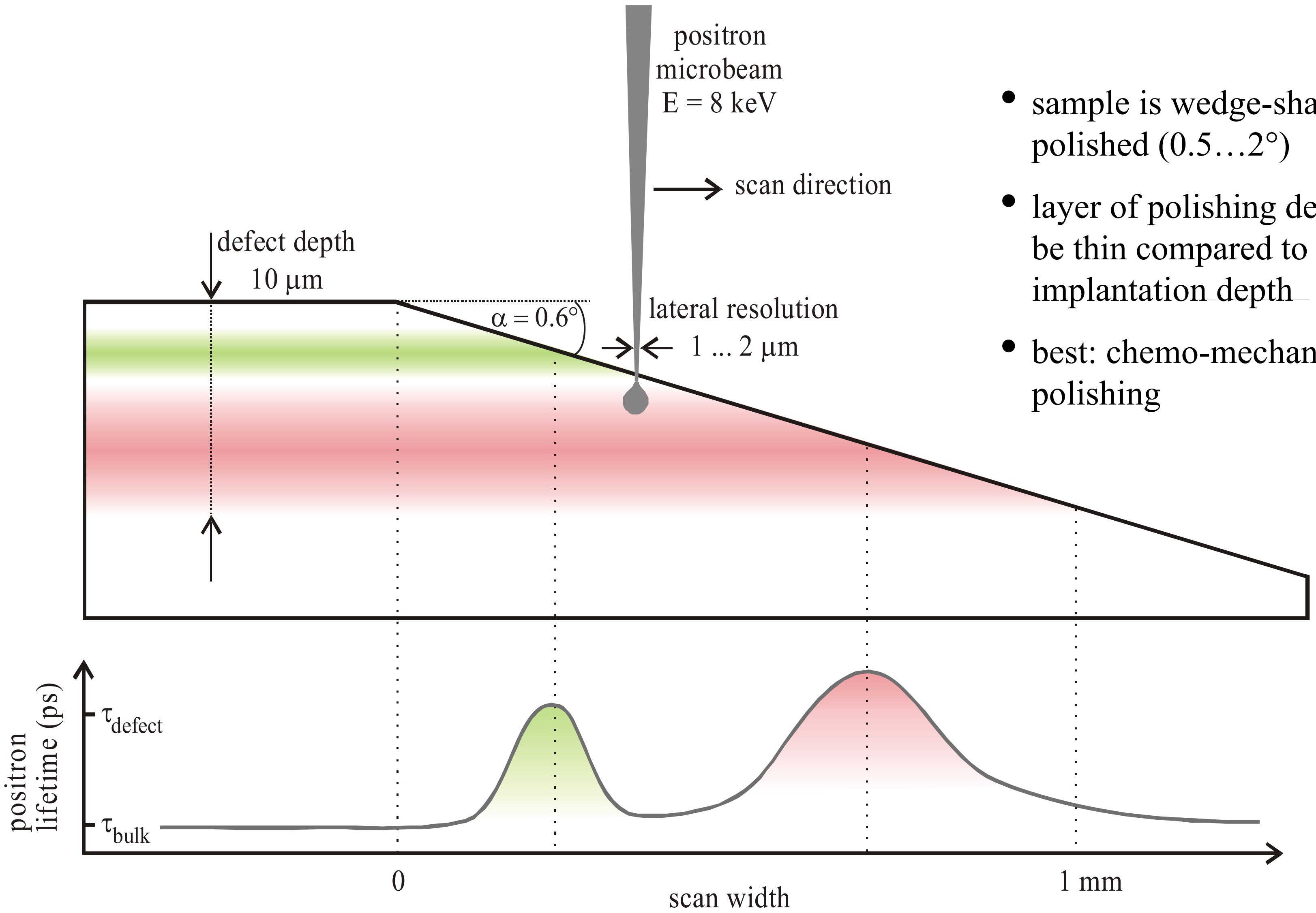

- sample is wedge-shaped polished (0.5…2°)
- layer of polishing defects must be thin compared to e^+ implantation depth
- best: chemo-mechanical polishing

First defect depth profile using Positron Microscopy

- 45 lifetime spectra: scan along wedge
- separation of 11 µm between two measurements corresponds to depth difference of 155 nm (α = 0.81°)
- beam energy of 8 keV: mean penetration depth is about 400 nm; represents optimum depth resolution
- no further improvement possible due to positron diffusion: L_+(Si @ 300K) » 230 nm
- both regions well visible:
  - vacancy clusters with increasing density down to 2 µm ($R_p/2$ region)
  - in R_p region: lifetime τ_2 = 330 ps; corresponds to open volume of a divacancy; must be stabilized or being part of interstitial-type dislocation loops
- excellent agreement with gettered Cu profile

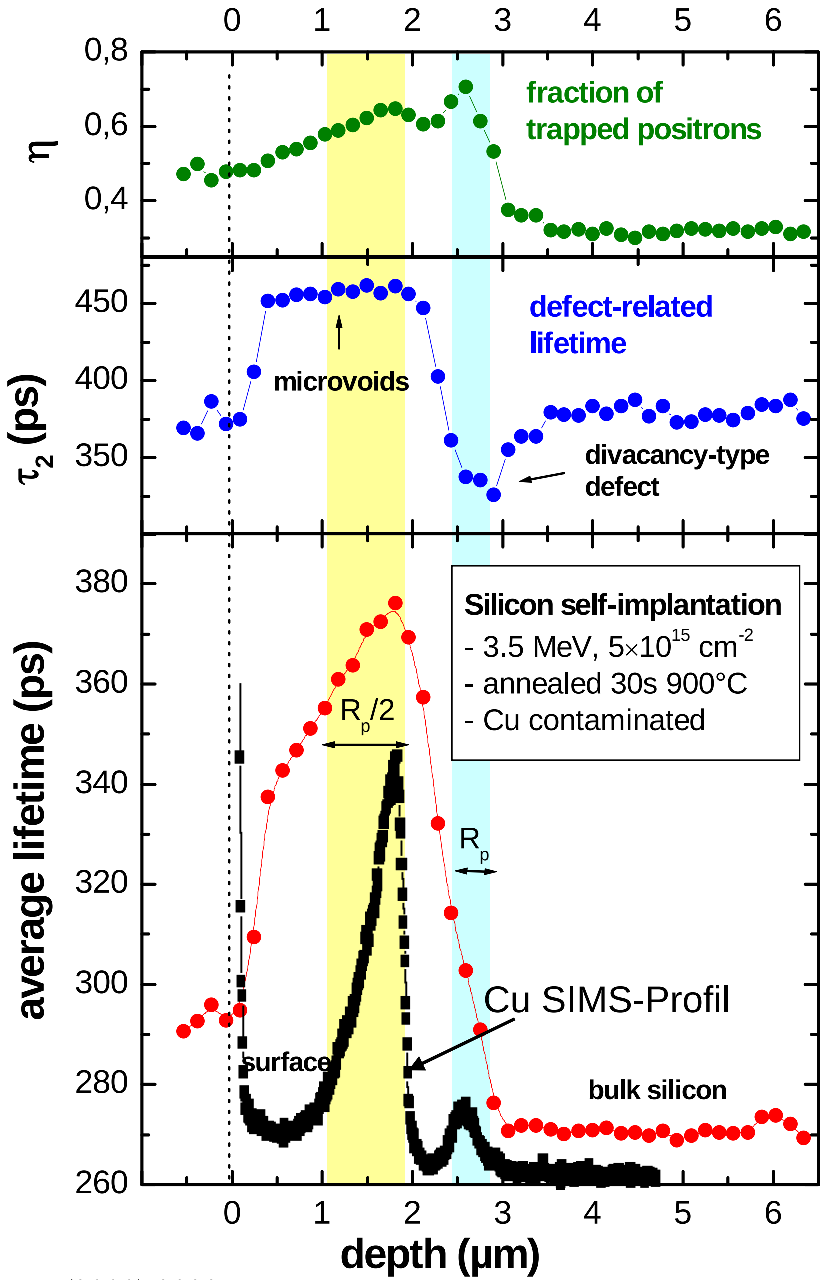

R. Krause-Rehberg et al., Appl. Phys. Lett. 77 (2000) 3932

EPOS = ELBE Positron Source

- ELBE -> electron LINAC (40 MeV and up to 40 kW) in HZDR Research Center Dresden-Rossendorf
- EPOS -> collaboration of Univ. Halle with HZDR
- EPOS will be the combination of a positron lifetime spectrometer, Doppler coincidence, and AMOC
- User-dedicated facility
- main features:
  - high-intensity bunched positron beam (E_+ = 0.5…30 keV)
  - very good time resolution by using the unique primary time structure of ELBE
  - digital multi-detector array
  - fully remote control via internet by user

Ground plan of the ELBE hall

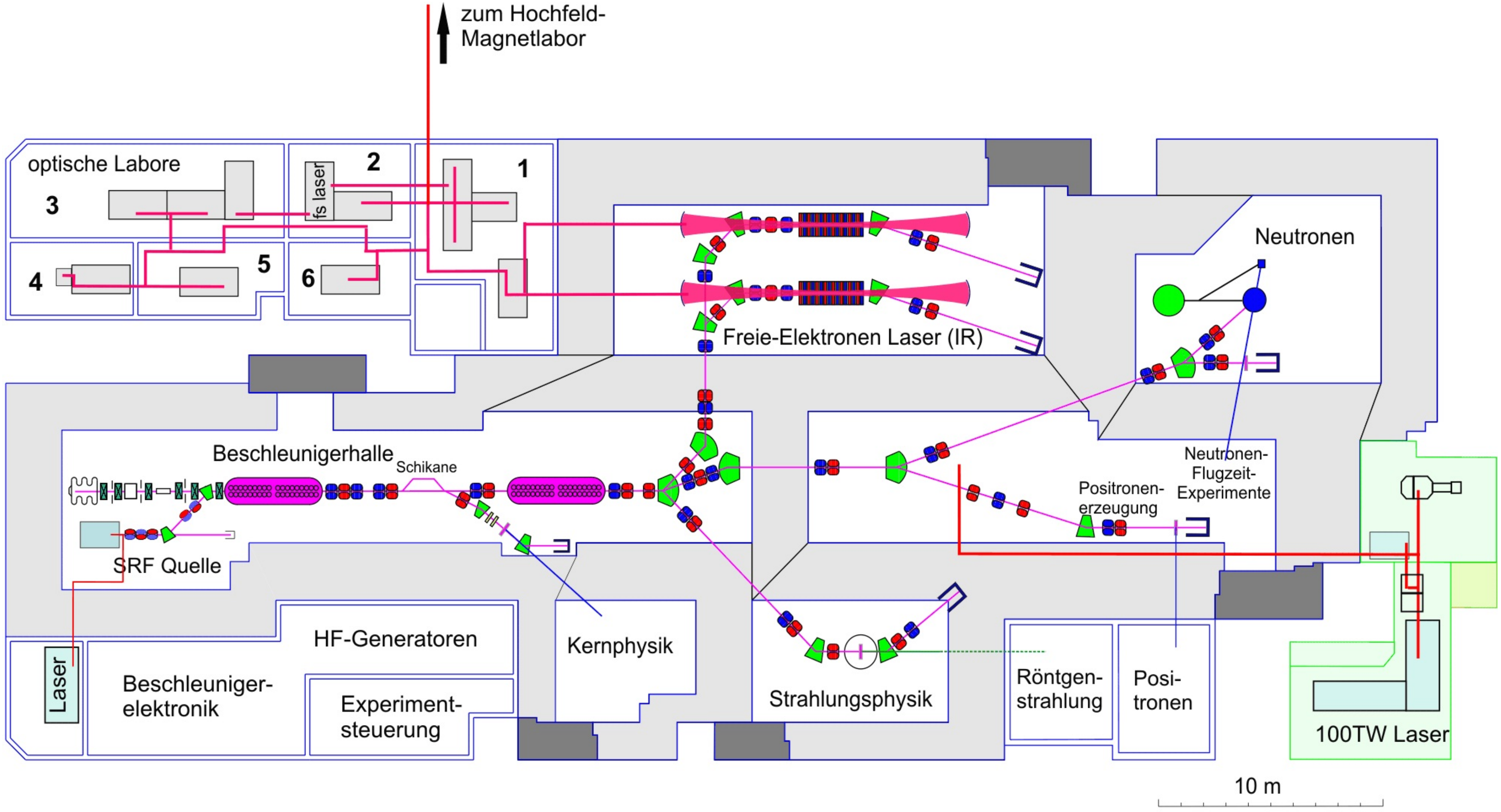

1: Diagnosestation, IR-Imaging und biologische IR Experimente
2: Femtosekundenlaser, THz-Spektroskopie, IR Pump-Probe Experimente
3: Zeitaufgelöste Halbleiter-Spektroskopie, THz-Spektroskopie

4: FTIR, biologische IR Experimente
5: Nahfeld und Pump-Probe IR Experimente
6: Radiochemie und Summenfrequenz-Erzeugung, photothermische Spektroskopie

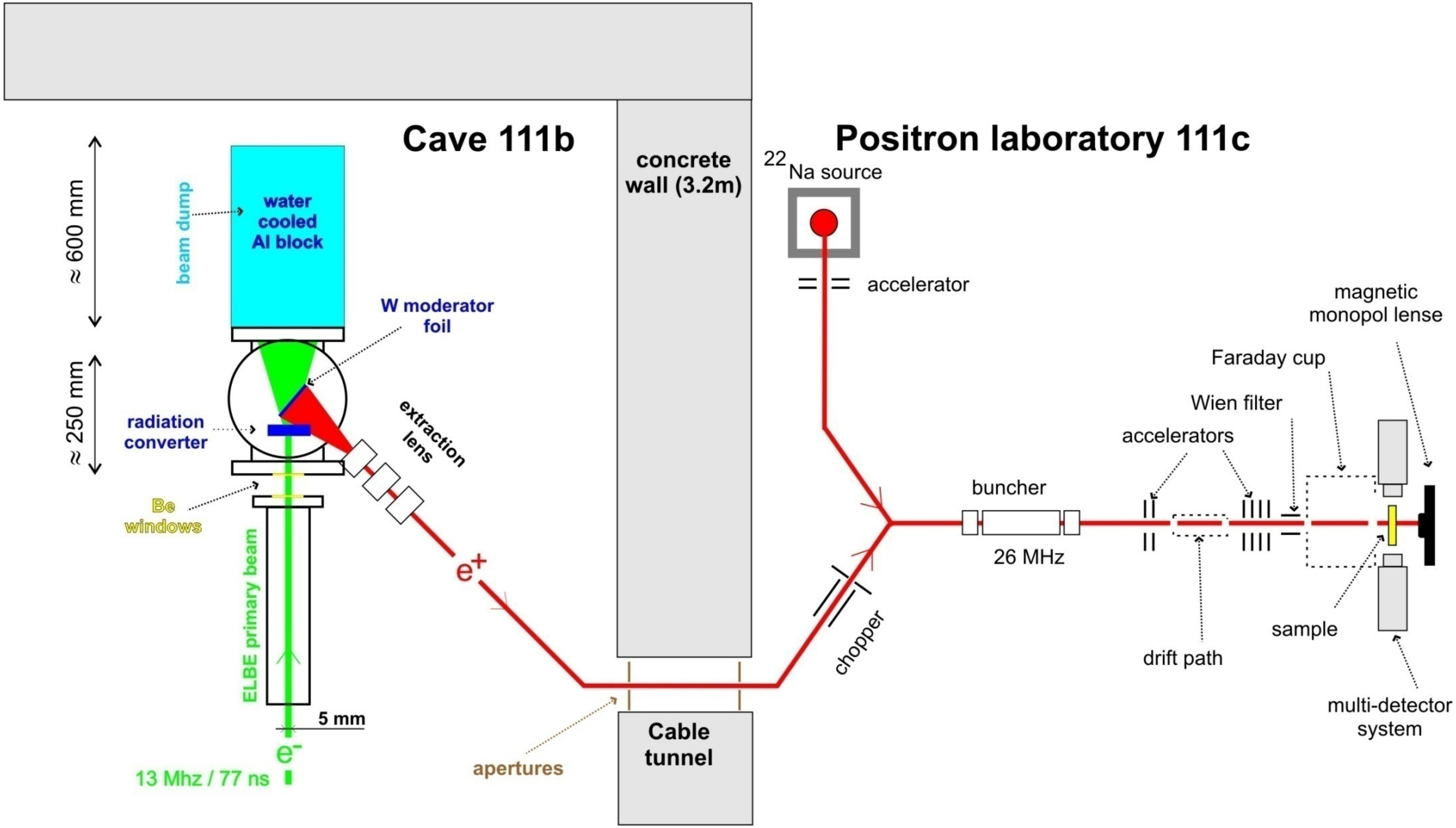

Cave 111b
Positron laboratory 111c
concrete wall (3.2m)
22 Na source
accelerator
≈ 600 mm
≈ 250 mm
beam dump
water cooled Al block
W moderator foil
radiation converter
extraction lens
Be windows
ELBE primary beam
e+
5 mm
e-
13 Mhz / 77 ns
apertures
Cable tunnel
chopper
buncher
26 MHz
accelerators
drift path
Wien filter
Faraday cup
magnetic monopol lense
sample
multi-detector system

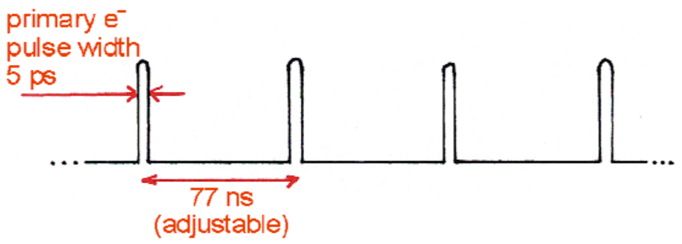

primary e-
pulse width
5 ps
77 ns
(adjustable)

MePS scheme

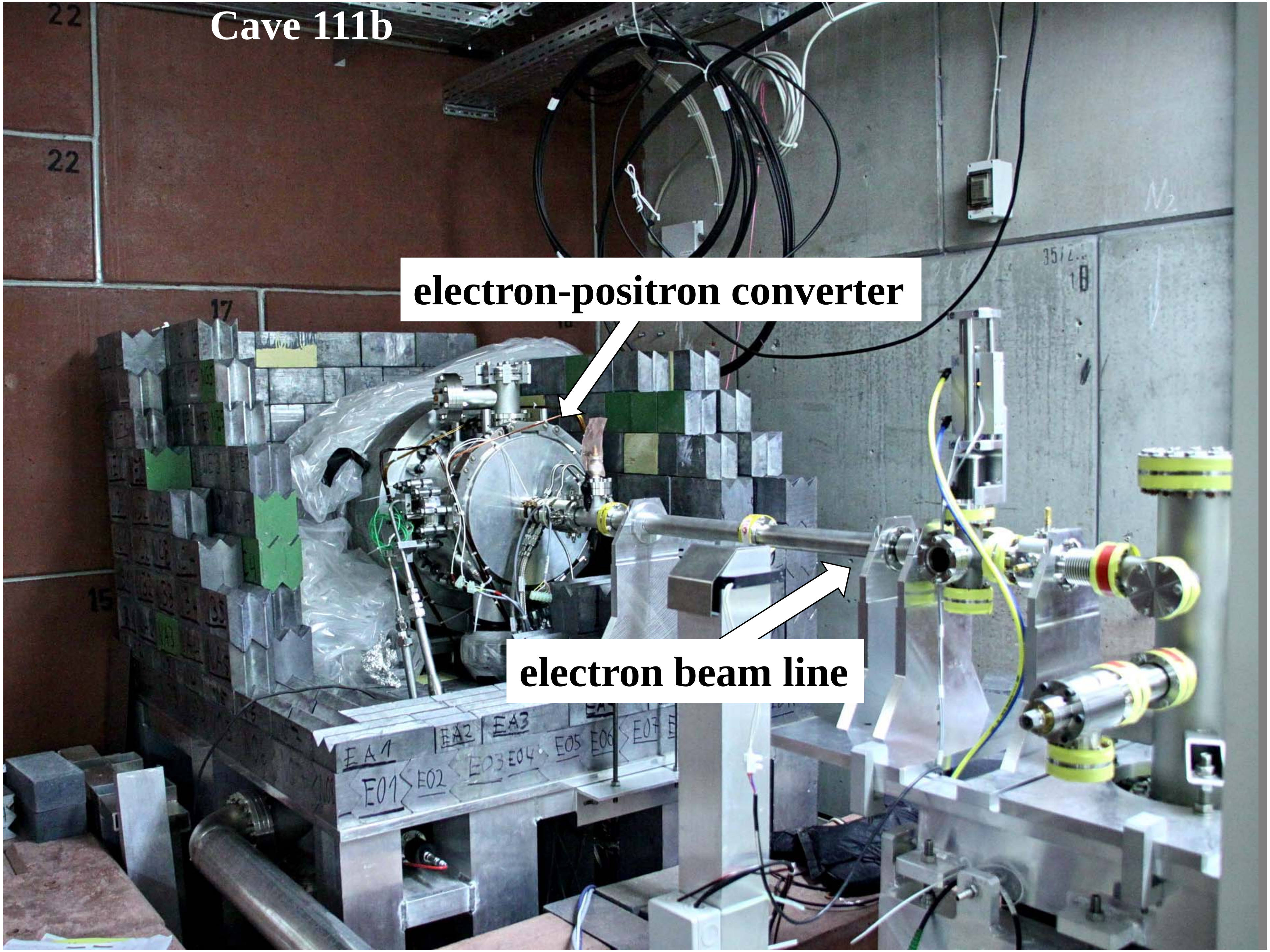
Cave 111b
electron-positron converter
electron beam line

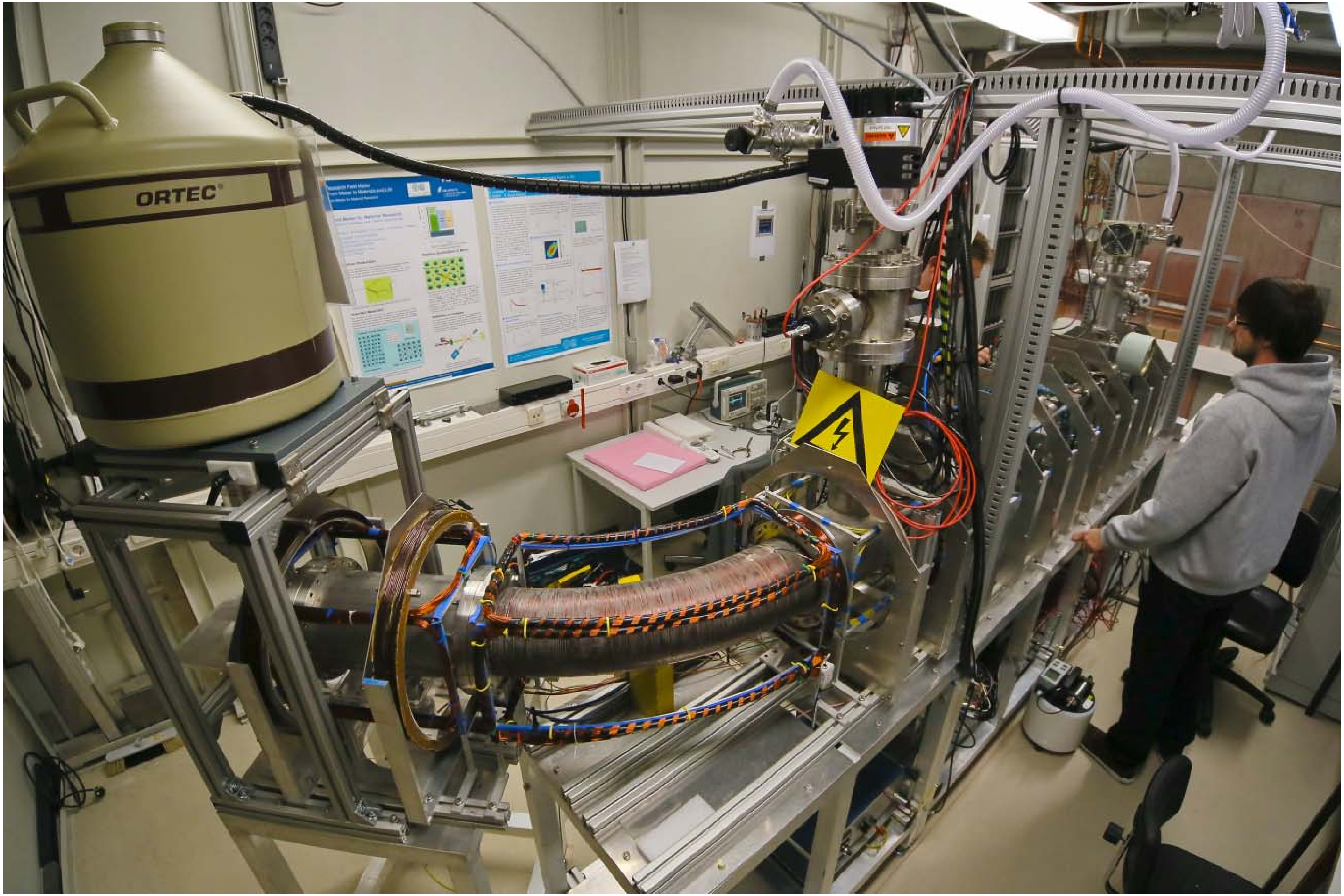
ORTEC®

Beam time in September 2011
First successful application: low-k Layers

- low-k dielectric layers shall replace SiO_2 as isolation in CPU’s
- higher speed possible because τ=RC decreases
- high-quality spectra already without chopper

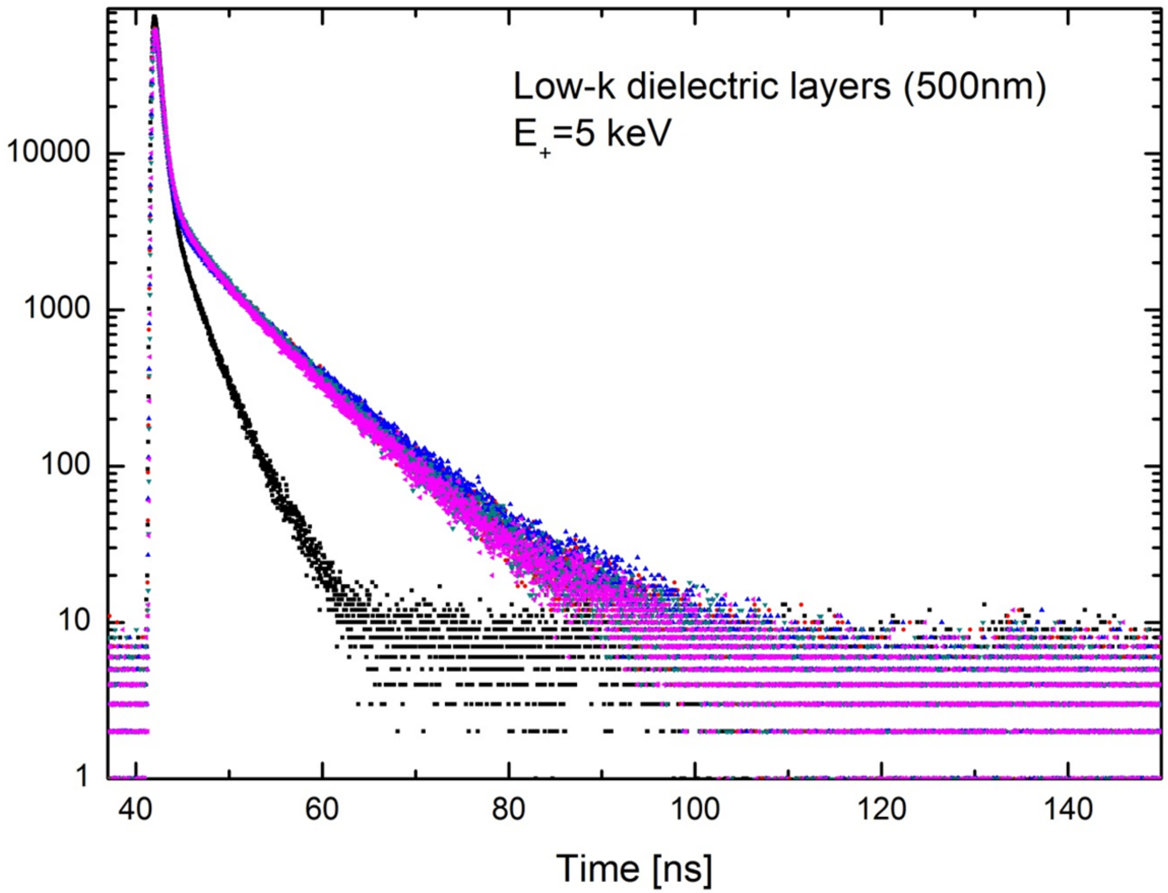

Bremsstrahlung Gamma Source of ELBE (FZ Dresden-Rossendorf)

- Pulsed gamma source using superconductive Linac ELBE
  - repetition frequency 26 MHz (or smaller by factor 2^n) in CW mode!
  - bunch length < 5 ps
  - up to 20 MeV (we used 16 MeV), no activation of samples by γ-n processes was found
  - average electron current 1 mA = 20 kW beam power; electron beam dump outside lab
  - thus gamma background at target position is very low (Ge detectors with 100% efficiency)
- **Ideal for GiPS ! Is now part of EPOS project – user dedicated positron source.**

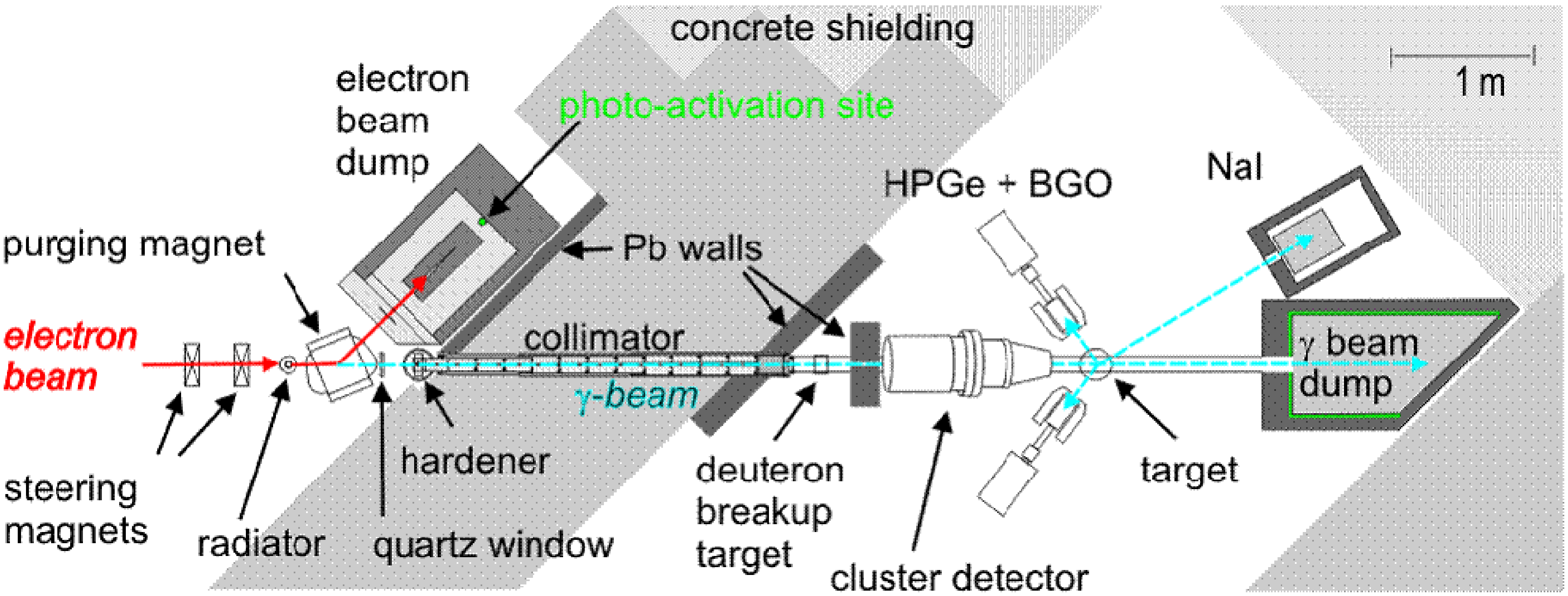

GiPS: Gamma-induced Positron Spectroscopy

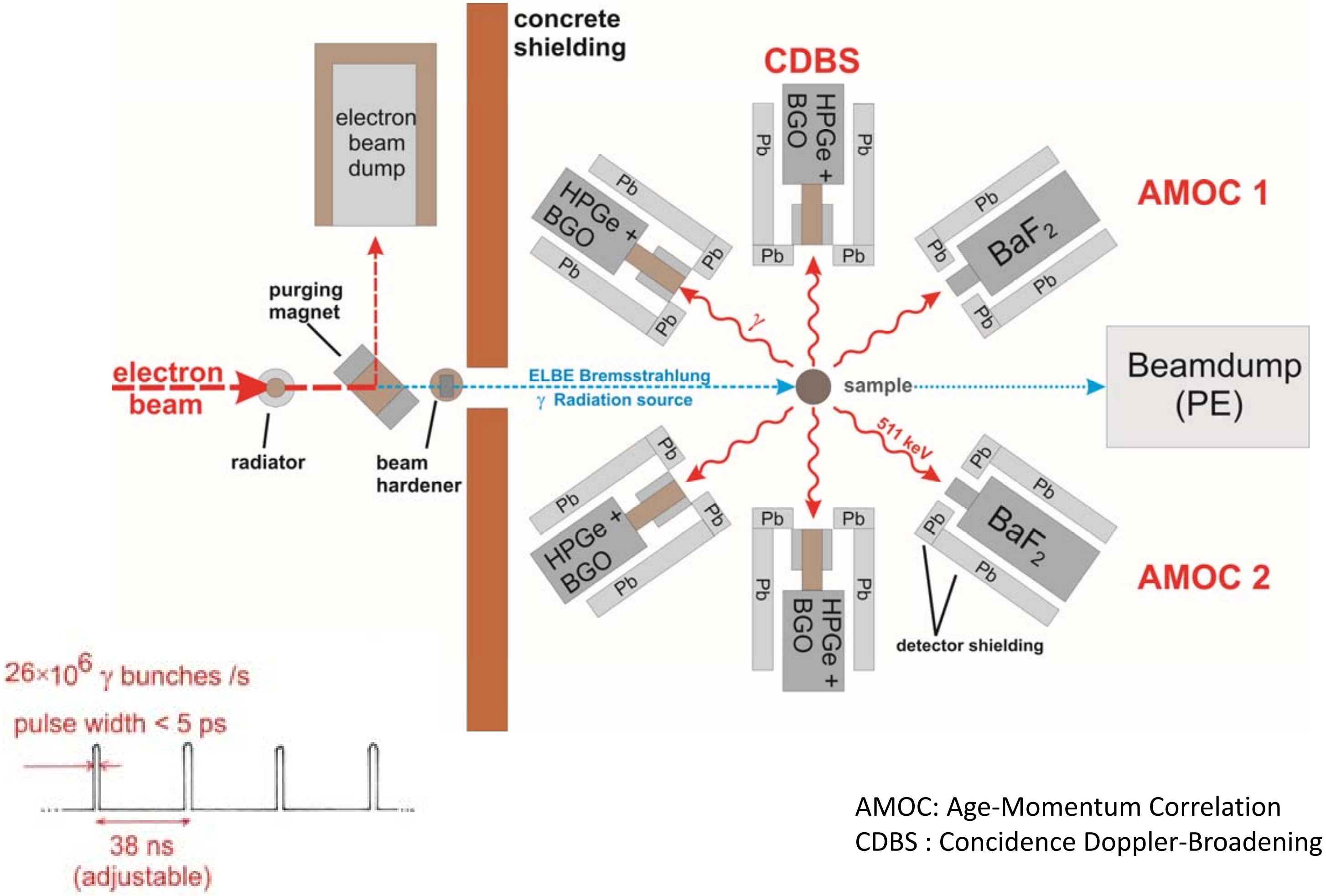

AMOC: Age-Momentum Correlation
CDBS : Concidence Doppler-Broadening Spectroscopy

- 3 coincident setups were used: 2 AMOC and 1 CDBS spectrometer
- only coincident detection ensures high spectra quality

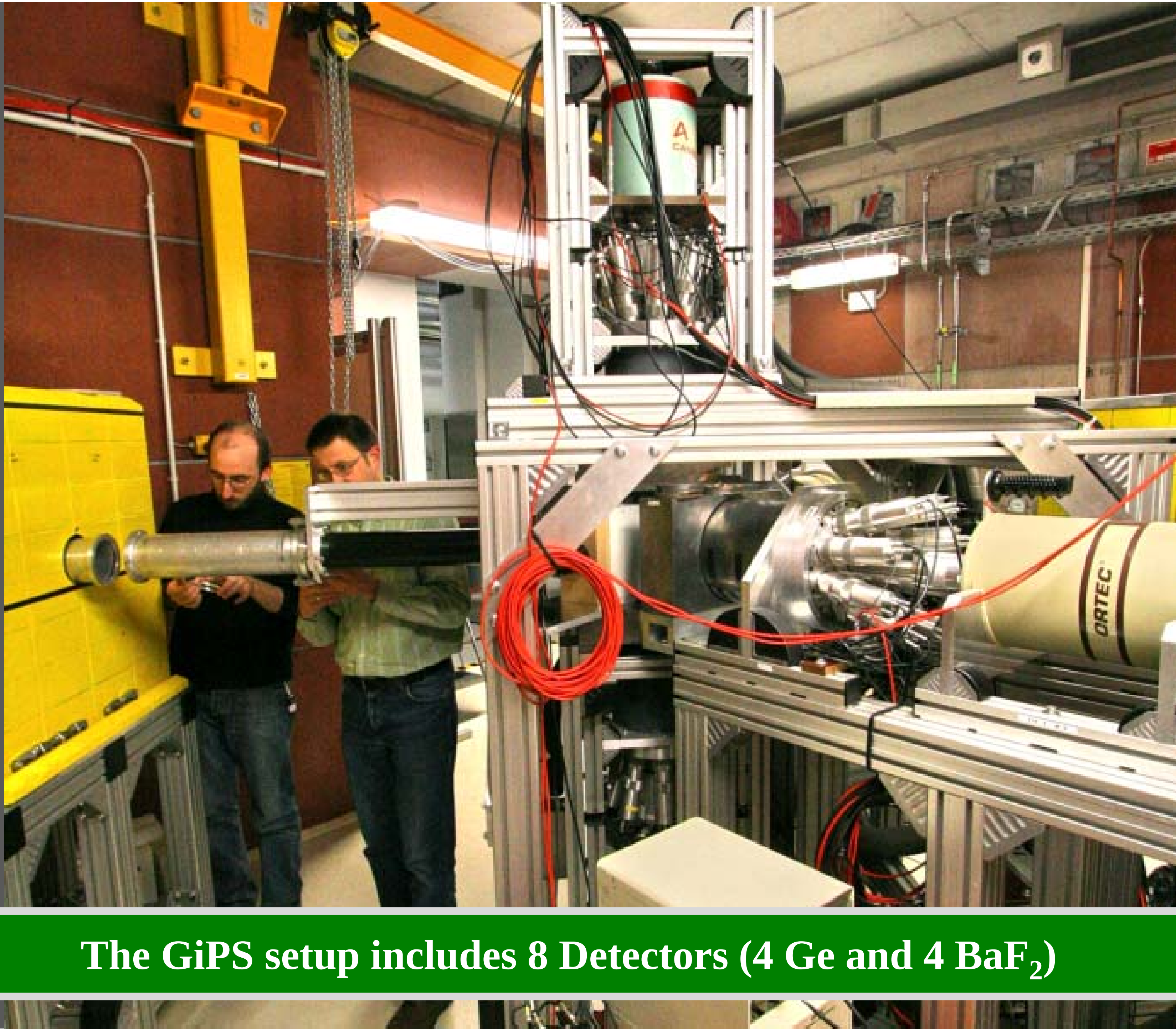

The GiPS setup includes 8 Detectors (4 Ge and 4 BaF_2)

Example: Water at RT

- total count rate in spectrum: $12x10^6$

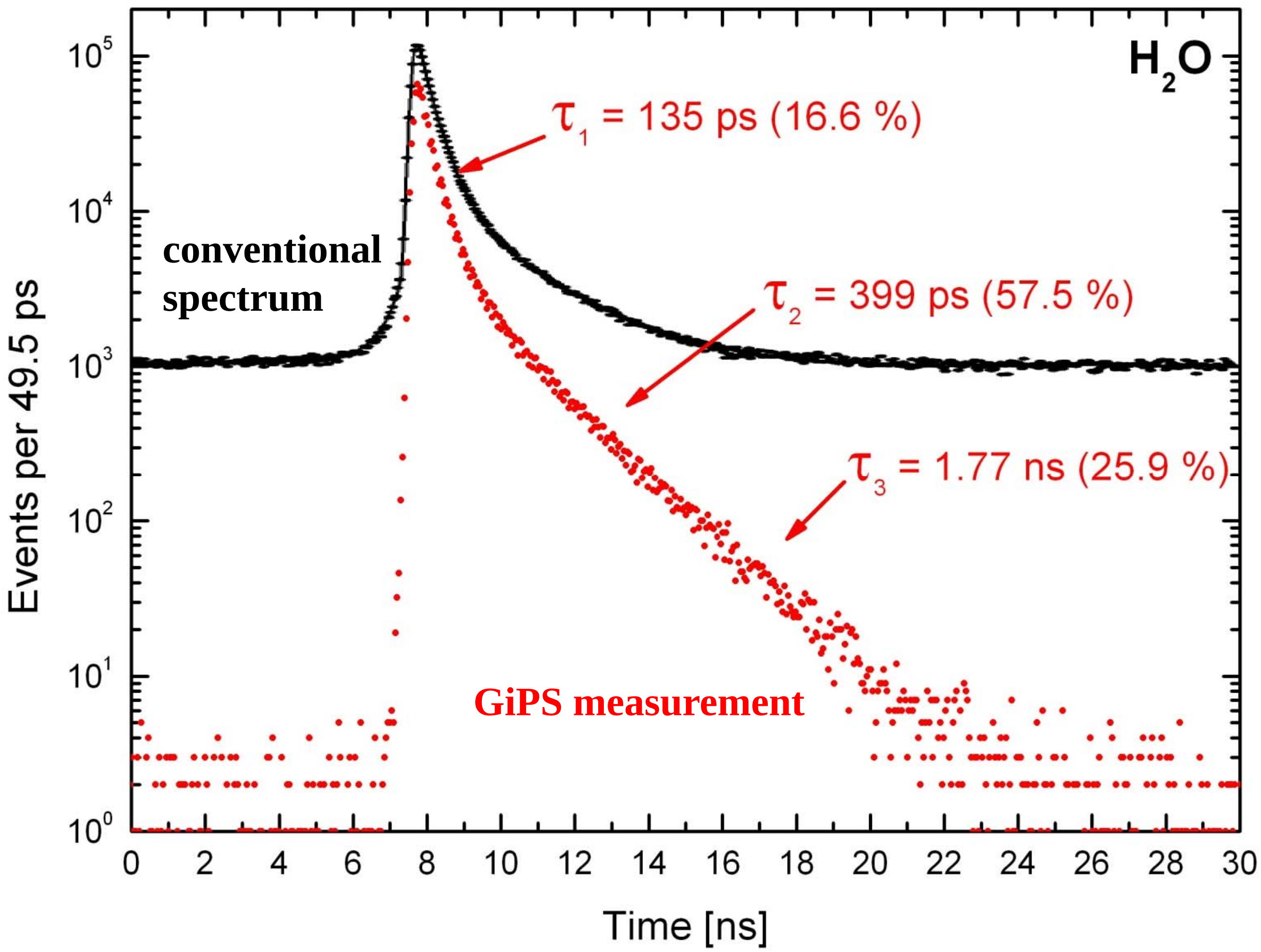

- Black spectrum: conventional measurement by Kotera et al., Phys. Lett. A 345, (2005) 184

Conclusions

- Positrons are a unique tool
  - for characterization of vacancy-type defects in crystalline solids
  - for embedded nano-particles (e.g. small precipitates)
  - for porosimetry (0.2 … 50 nm)
- New facilities become available for user-dedicated operation having
  - better time resolution and spectra quality
  - much higher intensity
  - microscope @ FRM-II: lateral resolution 1 μm

This presentation can be found as pdf-file on our Website:
http://positron.physik.uni-halle.de

reinhard.krause-rehberg@physik.uni-halle.de

Thank you for your attention!

http://positron.physik.uni-halle.de